This article was downloaded by: [Tomsk State University of Control Systems and Radio]
On: 19 February 2013, At: 12:54
Publisher: Taylor & Francis
Informa Ltd Registered in England and Wales Registered Number: 1072954
Registered office: Mortimer House, 37-41 Mortimer Street, London W1T 3JH, UK

Molecular Crystals and Liquid Crystals Incorporating Nonlinear Optics
Publication details, including instructions for authors and subscription information:
http://www.tandfonline.com/loi/gmcl17

Ferroelectric Liquid Crystals

L. A. Beresnev [a], L. M. Blinov [a], M. A. Osipov [a] & S. A. Pikin [a]
[a] Institute of Crystallography, Academy of Sciences USSR, Leninsky pr. 59, Moscow, 117333, USSR
Version of record first published: 20 Apr 2011.

To cite this article: L. A. Beresnev, L. M. Blinov, M. A. Osipov & S. A. Pikin (1988): Ferroelectric Liquid Crystals, Molecular Crystals and Liquid Crystals Incorporating Nonlinear Optics, 158:1, 1-150

To link to this article: http://dx.doi.org/10.1080/00268948808075350

PLEASE SCROLL DOWN FOR ARTICLE

Full terms and conditions of use: http://www.tandfonline.com/page/terms-and-conditions

This article may be used for research, teaching, and private study purposes. Any substantial or systematic reproduction, redistribution, reselling, loan, sub-licensing, systematic supply, or distribution in any form to anyone is expressly forbidden.

The publisher does not give any warranty express or implied or make any representation that the contents will be complete or accurate or up to date. The accuracy of any instructions, formulae, and drug doses should be independently verified with primary sources. The publisher shall not be liable for any loss, actions, claims, proceedings, demand, or costs or

damages whatsoever or howsoever caused arising directly or indirectly in connection with or arising out of the use of this material.

Downloaded by [Tomsk State University of Control Systems and Radio] at 12:54 19 February 2013

Mol. Cryst. Liq. Cryst., 1988, Vol. 158A, pp. 3–150
Photocopying permitted by license only
© 1988 Gordon and Breach Science Publishers S.A.
Printed in the United States of America

Downloaded by [Tomsk State University of Control Systems and Radio] at 12:54 19 February 2013

Ferroelectric Liquid Crystals

L. A. Beresnev, L. M. Blinov, M. A. Osipov, S. A. Pikin

Institute of Crystallography, Academy of Sciences USSR, Leninsky pr. 59, Moscow 117333, USSR

CONTENTS

Page

I. Introduction 3
II. General Phenomenological theory. 6
2.1. Parameters of the phase transition A* – C* and A – C 6
2.2. Invariants of components of electric polarization 8
2.3. Invariants to describe the elastic energy..... 11
2.4. Helical ferroelectrics 15
2.5. The behaviour in an external electric field 19
2.6. Lifshitz point in a liquid crystal ferroelectric..... 26
2.7. The role of the boundary conditions 29
2.8. Free-standing films 33
III. Dipolar ordering in ferroelectric liquid crystals. 36
3.1. Technique for the measurement of the spontaneous polarization 36
3.2. Experimental studies of the dielectric properties 40
3.2.1. Ultra-high frequencies..... 42
3.2.2. High frequencies 42
3.2.3. Middle frequencies. Tilt angle dynamics, soft mode, electroclinic effect..... 43
3.2.4. Low frequencies. The Goldstone mode. Switching the polarization 47
3.3. Chemical classes of ferroelectric liquid crystals... 50
3.4. Ferroelectricity in mixtures 61
3.5. Non-helical liquid-crystalline ferroelectrics 66
3.6. The effect of the steric and dipolar interactions on the value of the spontaneous polarization 67
3.7. Polymorphism of ferroelectric phases 73
3.8. Polymeric liquid crystalline ferroelectrics 74
3.9. The possibility of ferroelectric ordering in living tissues 77

IV. Molecular-statistical theory of ferroelectric liquid crystals 79
4.1. Microscopic origin of spontaneous polarization in liquid crystals 79
4.2. Model potentials of interaction between chiral molecules in smectics C* 81
4.3. The general theory of ferroelectric ordering 84
4.3.1. Free energy of the smectic C* 88
4.3.2. Ferroelectric ordering in smectic C* composed of molecules with steric dipoles 91
4.3.3. Ferroelectric ordering in the system of symmetric molecules 93
4.3.4. Discussion 94
4.4. Ferroelectricity in mixtures 97
4.4.1. Binary mixtures of ferroelectric liquid crystals 98
4.4.2. Achiral smectic C doped with chiral molecules 99
4.4.3. Ferroelectric liquid crystals doped with achiral molecules 100
V. Molecular theory of flexoelectricity and helical twisting in ferroelectric liquid crystals 101
5.1. Introduction 101
5.2. Dipolar and quadrupolar flexoelectricity 104
5.3. Flexoelectric coefficients in the smectic C phase. 107
5.4. Macroscopic helical structure of the ideal smectic C* 109
5.5. Temperature variation of the helical pitch in the smectic C* phase 111
VI. Optical properties of the chiral smectic C* phase. 117
6.1. A mirror-symmetrical smectic C 117
6.2. The ideal helical structure of a smectic C* 121
6.3. Preparation of optically homogeneous samples... 124
6.4. Optical methods for measuring the pitch of the helical structure and the molecular tilt angle..... 126
6.5. Nonlinear optical properties 128
VII. Electro-optical effects. 128
7.1. The Fredericks transition in a smectic C 129
7.2. The chiral smectic C* phase in a weak electric field 130
7.3. The helix unwinding 132
7.4. Switching the director in a strong field 138
VIII. Possibilities for the practical application of ferroelectric liquid crystals 143

Downloaded by [Tomsk State University of Control Systems and Radio] at 12:54 19 February 2013

Downloaded by [Tomsk State University of Control Systems and Radio] at 12:54 19 February 2013

I. INTRODUCTION

The idea either to reveal or to construct a liquid ferroelectric was never abandoned by researchers since the discovery of ferroelectricity in solid crystals at the beginning of this century. In principle, nature does not forbid the existence of ferroelectric liquids. For instance, a centro-symmetric liquid can change its point symmetry from the K_h to $C_{\infty v}$ group with the formation of a uniform ferroelectric phase. A liquid without the inversion center can have a phase transition $K \rightarrow C_\infty$ into the inhomogeneous, helical structure. In both these hypothetical cases the spontaneous polarization, $\mathbf{P}_s$, would play the role of the true order parameter. However, such liquid ferroelectric phases (proper ferroelectrics) have not been discovered as yet.

The reason for such a situation is the absence of dipole moments in atomic liquids and the weakness of the dipolar interaction in molecular liquids. To form a ferroelectric state at temperature T_c the energy of the dipole-dipole interaction p^2/a^3 (p is the dipole moment and a is an average distance between the dipoles) has to be of the order of $k_B T_c$. In dipolar liquids with relatively bulky molecules the energy p^2/a^3 is usually less than $k_B T$ even at the melting temperature. Thus crystallization takes place before the hypothetical phase transition to the ferroelectric state. On the other hand, when the molecules possess very large dipoles, they tend to form dimers with opposite directions of the dipole moments. This effect also prevents the appearance of the spontaneous polarization.

Fortunately there exist quite another way to success proposed originally by R. Meyer in 1975.[1] The idea was to construct a liquid crystal with polar molecular ordering resulting from other, not dipole–dipole, interactions. In this case the order pararmeter can be related to a certain type of molecular orientation and the spontaneous polarization appears as a secondary effect (quasi-proper ferroelectrics). Such a situation takes place, for example, at the transition from the smectic A* (point group D_∞) to the smectic C* (point group C_2) phase in a substance composed of chiral molecules having no mirror planes, Fig. 1. The phenomenon of ferroelectricity in liquid crystals was discovered[1] in the smectic C* phase of the chiral isomer of p-decyloxybenzylidene-p-amino-2-methylbutyl-cynnamate (DOBAMBC).

The appearance of the ferroelectric state is assisted by the formation of an incommensurate structure in the spatial distribution of molecular axes, Fig. 2. If the average molecular orientation is specified by a unit vector $\mathbf{n}$ (the director) its direction would form a helix with an axis along the normal z to the smectic planes. The modulation of the direction $\mathbf{n}(z)$ is analogous to the twist of the director in cho-

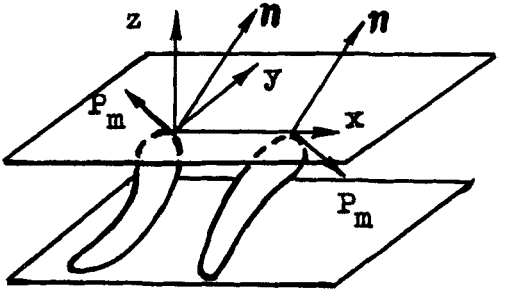

FIGURE 1 Smectic monolayers with point symmetry C_2.

lesteric liquid crystals. In both cases the Lifshitz invariant

$$\lambda\left(n_x \frac{\partial n_y}{\partial z} - n_y \frac{\partial n_x}{\partial z}\right) \tag{1}$$

has a finite value. The situation reminds one of the solid helical ferromagnetics where the macroscopic magnetic moment rotates with a large spatial period.[2]

The spontaneous polarization, $\mathbf{P}_s$, in the ferroelectric phase lies in the smectic layers, in the direction of the C_2 axis perpendicular to the director. Hence, the vector $\mathbf{P}_s$ is also rotated forming the helix with the axis along the normal to the smectic layers. To obtain the non-zero macroscopic polarization the helix has to be unwound by the external field,[3] flow of a liquid crystal[4] or by the interaction with solid surfaces.[5]

Liquid crystal ferroelectrics have much in common with conventional solid ferroelectrics, for example, the temperature behaviour of the spontaneous polarization and dielectric permittivity,[6] Fig. 3, the

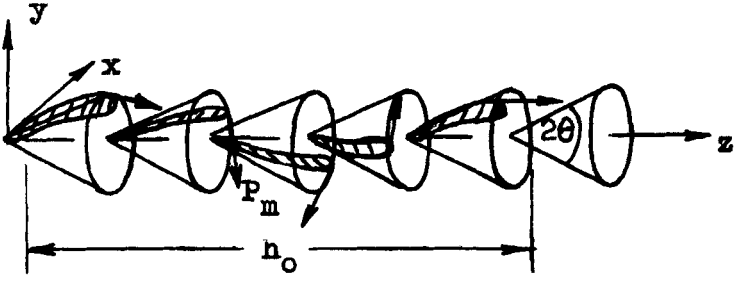

FIGURE 2 Helical structure in the chiral smectic phase C*.

Downloaded by [Tomsk State University of Control Systems and Radio] at 12:54 19 February 2013

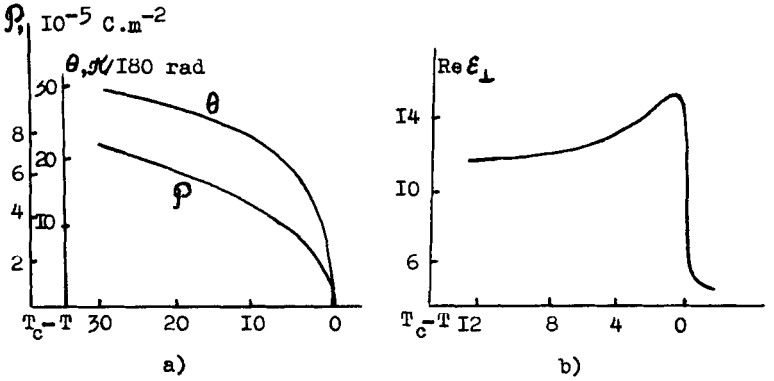

FIGURE 3 Temperature dependence of the spontaneous polarization (a)[6], and the tilt angle (a)[6], and of the dielectric constant (b)[25] in decyloxybenzylideneaminocinnamate (DOBAMBC).

presence of the pyro-electric and piezo-electric (electroclinic) effects.[7–9] At the same time, there are a lot of specific features in the behaviour of ferroelectric liquid crystals. First of all, their electro-optical properties have no solid state analogs. The pitch of the incommensurate helical structure depends anomalously upon temperature,[10–12] Fig. 4. In freely suspended smectic C* films one can observe polarization effects which are characteristic of two-dimensional degenerate systems.[13] Of special interest are multi-component ferroelectric mixtures and ferroelectric liquid crystalline polymers.

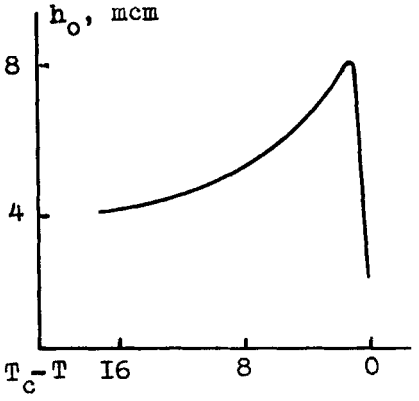

FIGURE 4 Temperature dependence of the helical path in the C* phase of DOBAMBC[11].

Downloaded by [Tomsk State University of Control Systems and Radio] at 12:54 19 February 2013

At present, there is no comprehensive review which would include the variety of information on theory, structure, properties and application of ferroelectric liquid crystals. In the Institute of Crystallography of the USSR Academy of Sciences a group of theoreticians and experimentalists has been working for many years on these substances and the present review is a result of their mutual efforts to shed light upon this problem. The questions included in the review are phenomenological and microscopic theories of ferroelectricity, chemical aspects, optical, electric and electro-optical properties, and some problems of technical applications. We sincerely hope that our work will be useful for a wide circle of researchers in this new fascinating field of science.

Downloaded by [Tomsk State University of Control Systems and Radio] at 12:54 19 February 2013

II. GENERAL PHENOMENOLOGICAL THEORY

2.1. Parameters of the phase transitions A*–C* and A–C

A parameter of the orientational transition is such a combination of physical parameters which could serve to describe a one-dimensional structure of smectic liquid crystals (SLC), the presence of an average molecular orientation $\mathbf{n}$ ($\mathbf{n}^2 = 1$) and the symmetry properties of SLC. One-dimensional crystal order can be described by the density wave $\psi = |\psi| \exp [i(\mathbf{kr} + \alpha)]$, where $|\psi|$ is the amplitude, α—the wave phase, $\mathbf{k}$—the wave vector. The two-component parameter ψ is known to serve both as an order parameter of the phase transition NLC–SLC A, point symmetry $D_{\infty h}$ being preserved, and of the phase transition CLC–SLC A*, point symmetry also being preserved. The magnitude $\mathbf{kr} = kz$ is invariant to symmetry operations in the groups $D_{\infty h}$, D_{∞}, C_{2h}, C_2. The parameter of the A–C transition is to be invariant to the change $\mathbf{n} \rightarrow -\mathbf{n}$ due to the physical identity of the counter direction of the director. Such symmetry properties are characteristic of the two-dimensional symmetry (relating to inversion) representation E_{1g} in the group $D_{\infty h}$. The corresponding parameter of the transition A–C, transformed according to E_{1g}, is two-component and can be written as follows[14]

$$e_{ij1} n_j n_p \frac{\partial^2 \psi}{\partial x_1 \, \partial x_p} \sim (\mathbf{nk})\,[\mathbf{nk}]\,\psi$$

on condition that $\psi = 0$, that is, the density wave being absent, this parameter is transformed to 0. Assuming that in the phase transition

Downloaded by [Tomsk State University of Control Systems and Radio] at 12:54 19 February 2013

described $|\psi| = \text{const}$ and the wave vector $\mathbf{k}$ is parallel to the z axis, the given order parameter, within an accuracy of an unimportant constant factor, is the combination of two components (ξ_1, ξ_2)[15]

$$\xi_1 = n_z n_x, \qquad \xi_2 = n_z n_y \tag{2}$$

A similar order parameter can serve to describe the orientational phase transition A*–C*, even in the case when spontaneous polarization is absent, on condition that molecules have no constant dipole moments. In such cases components (ξ_1, ξ_2) are transformed according to two-dimensional representation E_1 of the group D_∞. It should be noted that components of the polarization vector (P_x, P_y) transform according to the same representation (E_1). Consequently, there must be a linear relation between the components (ξ_1, ξ_2) and the components (P_x, P_y) of the symmetry group D_∞ which is as follows

$$(P_x, P_y) \sim (\xi_2, -\xi_1) \tag{3}$$

and is shown in Fig. 1. According to the expression (3), the components P_x and P_y transform respectively, like ξ_2 and $-\lambda\xi_1$ under the symmetry operations of the group D_∞ (turns through an angle around the C_∞ axis and turns through the angle π around the axes perpendicular to the C_∞ axis). It follows from (3), which is true only for chiral SLC (with no inversion centre) and corresponds to the piezoelectric effect, that in the C* phase of this substance spontaneous polarization is to appear (in case molecules have transverse electric dipole moments) as a result of the final tilt of the molecules through an angle θ which is, in fact, the parameter of the transition A*–C*. At low magnitudes of θ the proportionality $P \sim \theta$ is valid.

It should be noted that the antisymmetry of the two-dimensional representation E_{1u} of the group $D_{\infty h}$ points to the possibility of the transition of SLC A from the nonpolarized to the polarized state accompanied by symmetry lowering $D_{\infty h} \rightarrow C_2$ without any tilt of the molecules. Simultaneously, polarization could be a parameter of the transition and imply the effect of significantly strong dipole–dipole interactions. Till now such a mesophase has not been discovered.

Obviously, analogous to the proportionality of the components (P_x, P_y) in (3), components of the intensity vector of the electric field (E_x, E_y) are to be proportional too. Respectively, the expression (3) describes the effect of the tilt of the molecules in phase A* induced by the external field. As it was mentioned above, this effect was called electroclinic.[9]

Equation (3) belongs to point symmetry group D_∞ and can describe the appearance of the spontaneous polarization both in the phase transition A*–C* and in other phase transformations, for instance, in the first order transition CLC–SLC C*. This transition, to our knowledge, is accompanied by a jump-like change of the tilt angle θ from 0 to the finite magnitude of the order of $\theta \sim \pi/6$. According to (3) the given orientational transition is to be accompanied by the jump-like appearance of spontaneous polarization as shown by experiment.[16] At larger magnitudes of θ in the expression describing spontaneous polarization $P(\theta)$, one should account for larger θ: $P(\theta) \sim \theta(1 + \text{const}\,\theta^2 + \ldots)$. We should point out here that orientational contributions of a higher order to spontaneous polarization can be induced by various physical factors and can differ, for example, in their relaxation properties. To make a correct analysis of the polarization effects of various types, one should study the invariants which enter the expansion for the free energy density and are formed from the components of various order parameters.

2.2. Invariants of components of electric polarization

Piezoeffect (3) testifies to the existence of an invariant in the expression for free-energy density F of chiral SLC with symmetry group D_∞

$$-\mu_p (P_x\xi_2 - P_y\xi_1), \tag{4}$$

where μ_p is the piezoelectric coefficient. Besides (4), F contains usual invariants, quadratic with respect to the components (P_x, P_y) and (ξ_1, ξ_2),

$$a_0 (\xi_1^2 + \xi_2^2) + \frac{1}{2\chi_0} (P_x^2 + P_y^2), \tag{5}$$

where the phenomenological coefficient a_0 is assumed to depend on the temperature T and can vanish at the point T_0 ($a_0(T_0) = 0$), the coefficient $\chi_0 > 0$ and hardly depends on T. These assumptions correspond to the case discussed when the orientational phase transition A*–C* with the order parameter (ξ_1, ξ_2) is taken into account, and when the polarization (P_x, P_y) is not responsible for the given transition. The combination of (4) and (5) is a simple interpretation of the phenomenon discussed and shows that spontaneous polarization occurs even at a weak piezoelectric coupling μ_p in the phase C*

Downloaded by [Tomsk State University of Control Systems and Radio] at 12:54 19 February 2013

Downloaded by [Tomsk State University of Control Systems and Radio] at 12:54 19 February 2013

($\theta \neq 0$). Indeed, minimizing the sum of the invariants (4) and (5) with respect to the polarization (P_x, P_y) and taking into account the smallness of the angle θ, we obtain

$$P = P_p = \chi_0 \mu_p \theta,$$

where the magnitude θ can be deduced by minimizing the functional $F[\theta]$ in the common form.

As it was mentioned above, in the chiral system with symmetry group D_∞ we can observe the effect of space modulation of the orientational order parameter owing to the presence of Lifshitz invariants in F which have the following form for the components (ξ_1, ξ_2) and P_x, P_y)

$$\lambda_0 \left(\xi_1 \frac{\partial \xi_2}{\partial z} - \xi_2 \frac{\partial \xi_1}{\partial z} \right), \lambda_1 \left(P_x \frac{\partial P_y}{\partial z} - P_y \frac{\partial P_x}{\partial z} \right) \tag{6}$$

The account of linear coupling (3) shows that these invariants can be reduced to the one containing an effective chiral parameter λ and at small tilts of the director **n** from the z axis ($n_z^2 \approx 1$) this invariant has the form of (1).

Spontaneous inhomogeneous space distribution **n**(**r**) induces additional contribution to the polarization (the so-called flexoelectric effect) owing to the linear connection

$$(P_x, P_y) \sim \left(\frac{\partial \xi_1}{\partial z}, \frac{\partial \xi_2}{\partial z} \right), \tag{7}$$

which is permitted by the symmetry group D_∞ associated with the invariant in F

$$- \mu_f^0 \left(P_x \frac{\partial \xi_1}{\partial z} + P_y \frac{\partial \xi_2}{\partial z} \right), \tag{8}$$

where μ_f^0 is the flexoelectric coefficient. Note, that the relations (7) and (8) are also permitted by the symmetry group $D_{\infty/h}$ and are connected in no way with the chiral aspect of the system. In principle, orientational distortions can also be characterized by the dependence of the components (ξ_1, ξ_2) on the coordinates x and y. In this case we observe the appearance of the polarization component

$$P_z \sim \left(\frac{\partial \xi_1}{\partial z} + \frac{\partial \xi_2}{\partial y} \right) \tag{9}$$

and the invariant in F

$$P_z\left(\frac{\partial\xi_1}{\partial x}+\frac{\partial\xi_2}{\partial y}\right) \tag{10}$$

There are no other flexoelectric contributions to the polarization which are proportional to the first spatial derivatives of the components of the transition parameter (ξ_1, ξ_2) in the first order in the tilt angle θ.

Flexoelectric effects in SLC A and C can also be caused by the bending of the smectic monolayers which is, in fact, a displacement of the layer u along the crystal axis z. For smooth bendings the invariants in the expression for F should be taken into account[17]

$$P_x\frac{\partial^2 u}{\partial x\partial z}+P_y\frac{\partial^2 u}{\partial y\partial z},\ P_z\left(\frac{\partial^2 u}{\partial x^2}+\frac{\partial^2 u}{\partial y^2}\right),\ P_z\frac{\partial^2 u}{\partial z^2} \tag{11}$$

Under considerably larger shifts of θ and u, F should include invariants of the order $P\theta^2$, $Pu\theta$, etc., which also have additional derivatives with respect to space coordinates. Flexo-electric contributions of a higher order to the polarization of SLC were analysed by Dahl and Lagerwall.[18] For the invariants proportional to $P\theta^2$ and $Pu\theta$ we can take into account scalar values of the type (8), (10) and (11) multiplied by a pseudoscalar[14]

$$\frac{\partial\xi_1}{\partial y}-\frac{\partial\xi_2}{\partial x} \tag{12}$$

and also the scalar value

$$(P_x\xi_2-P_y\xi_1)\left(\frac{\partial\xi_1}{\partial y}-\frac{\partial\xi_2}{\partial x}\right) \tag{13}$$

and besides (12) remains valid only for symmetry group D_∞, whereas (13) is permitted by symmetry groups D_∞ and $D_{\infty h}$. Use of (12) and (13) is necessary in case the order parameters are dependent on the coordinates x and y. As it will be shown, under thermodynamic equilibrium and the absence of an external field, however, the components (ξ_1, ξ_2), (P_x, P_y) cannot change in the smectic plane xy, since the presence of the corresponding gradients would increase free energy.

Downloaded by [Tomsk State University of Control Systems and Radio] at 12:54 19 February 2013

Downloaded by [Tomsk State University of Control Systems and Radio] at 12:54 19 February 2013

Under thermodynamic equilibrium and at a considerably low temperature a certain effect can be caused by invariants of flexo-electric nature of the order $P\theta^3$, in particular, the values

$$\begin{aligned} &-\mu_f^1(\xi_1^2 + \xi_2^2)\left(P_x \frac{\partial \xi_1}{\partial z} + P_y \frac{\partial \xi_2}{\partial z}\right), \\ &\delta\mu_f^1\left(\xi_2 \frac{\partial \xi_1}{\partial z} - \xi_1 \frac{\partial \xi_2}{\partial z}\right)(P_x\xi_2 - P_y\xi_1). \end{aligned} \tag{14}$$

It is clearly shown that the invariant (8) and the first of the invariants (14) contribute to F

$$-(\mu_f^0 + \mu_f^1\theta^2)\left(\frac{1}{2} P_0 \sin(2\theta) \frac{\partial \varphi}{\partial z} - P_1 \cos(2\theta) \frac{\partial \theta}{\partial z}\right),$$

where P_0 is the projection of the polarization vector **P** on the C_2 axis (in the plane xy), P_1 is the projection of the polarization vector **P** on the component of the director **n** in the xy plane and perpendicular to the C_2 axis (Fig. 1). The second invariant in (14) includes only a contribution proportional to the value $\delta\mu_f^1 P_0\theta^3(\partial\varphi/\partial z)$. Thus, the gradients $\partial\varphi/\partial z \neq 0$ and $\partial\theta/\partial z \neq 0$ in the smectic plane give rise to the polarization components

$$P_0 \sim \left(\mu_f\theta \frac{\partial \varphi}{\partial z}\right) \text{ and } P_1 \sim (\mu_f - \delta\mu_f) \frac{\partial \theta}{\partial z},$$

which have the corresponding flexo-electric coefficients μ_f, $\mu_f - \delta\mu_f$ which differ by a value of the order of θ^2:$\delta\mu_f = \delta\mu_f'\theta^2$ at $\theta^2 << 1$. Nearby the phase transition point of the second order $A^* - C^*$ the difference $\delta\mu_f$ is not significant. Far from the transition point in phase C^* the coefficients μ_f and $\mu_f - \delta\mu_f$ can differ considerably, and the magnitude $\delta\mu_f$ can have either sign. Note that the presence of the gradients $\partial\theta/\partial z \neq 0$ together with the gradients $\partial\varphi/\partial x$, $\partial\varphi/\partial y$, $\partial\theta/\partial x$, $\partial\theta/\partial y$ is not energetically favourable, though a homogeneous electric field can induce heterogeneous distribution of $\theta(z)$.

2.3. Invariants to describe the elastic energy

The invariants of the second order with respect to the derivatives of the components of the transition parameter (ξ_1, ξ_2) contributing

to the elastic free energy of SLC C and C* have the form

$$\frac{1}{2}\left\{K^0\left[\left(\frac{\partial\xi_1}{\partial z}\right)^2+\left(\frac{\partial\xi_2}{\partial z}\right)^2\right]+K'\left(\frac{\partial\xi_1}{\partial x}+\frac{\partial\xi_2}{\partial y}\right)^2+K''\left(\frac{\partial\xi_1}{\partial y}-\frac{\partial\xi_2}{\partial x}\right)^2\right.$$
$$\bar{K}\left[\left(\frac{\partial\xi_1}{\partial x}\right)^2+\left(\frac{\partial\xi_2}{\partial x}\right)^2+\left(\frac{\partial\xi_1}{\partial y}\right)^2+\left(\frac{\partial\xi_2}{\partial y}\right)^2\right]$$
$$+K'''\left(\xi_1\frac{\partial\xi_2}{\partial z}-\xi_2\frac{\partial\xi_1}{\partial z}\right)\left(\frac{\partial\xi_1}{\partial y}-\frac{\partial\xi_2}{\partial x}\right), \quad (15)$$

where K^0, K', K'', $\bar{K}$, K''' are the elastic moduli. The latter of the invariants (15) is proportional to the value of θ^3 and appears effective when far from the transition point T_c. Within the temperature region lower than T_c the components proportional to the constants K', K'', $\bar{K}$, K''' can be very effective as well as the component proportional to the constant K^0. In this case the fluctuations of the polar angle θ can be neglected and the components mentioned appear to be squared combinations of derivatives of the azimuthal angle φ.[19] Nearby T_c these components are the values of a higher order of the infinitesimal parameter θ if compared to the first member in (15) proportional to the value $\theta^2 q_0^2$. The invariant containing the coefficient K''' reflects the possibility of heterogeneous distribution of the azimuthal angle in the chiral smectic C* along the x and y axes. Nearby the transition point, however, the polar angle being small, the heterogeneity of this kind is not beneficial energetically. Let us take, for instance, the model equality of the constants $K^0 = 2K' = 2K'' = 2\bar{K} = K'''$ and the appearance of the heterogeneity $\varphi_1(x, z) = \varphi - \varphi_0(z)$ where $|\partial\varphi_1/\partial x| << |\partial\varphi_0/\partial z| = |q|$. The minimization of the functional of the free energy with respect to the magnitude φ_1 gives the equation of the following form

$$\frac{\partial^2\varphi_1}{\partial z^2}+\frac{\partial^2\varphi_1}{\partial x^2}-2\theta\cos(q_0 z)\frac{\partial^2\varphi_1}{\partial x\partial z}=0.$$

The substitution of $\varphi_1(x, z) = \tilde{\varphi}(z)\exp(-px)$ gives the following form of the equation for the function $\tilde{\varphi}(z)$:

$$\frac{d^2\tilde{\varphi}}{dz^2}+2\theta\,\mathrm{p}\cos(qz)\frac{d\tilde{\varphi}}{dz}+p^2\tilde{\varphi}=0.$$

The solution of $\tilde{\varphi}(z)$ in the form

$$\tilde{\varphi}(z)=u(z)\exp\left(-\frac{\theta p}{q}\sin(qz)\right),$$

Downloaded by [Tomsk State University of Control Systems and Radio] at 12:54 19 February 2013

will give, at $\theta^2 << 1$ the equation for the function $u(z)$

$$\frac{d^2u}{dz^2} + (p^2 - qp\theta \sin(qz))u = 0$$

or—the Mathieu equation, in case the argument $qz = 2t + \frac{\pi}{2}$ is substituted,

$$\frac{d^2u}{dt^2} + \left(\frac{4p^2}{q^2} - \frac{4p\theta}{q}\cos(2t)\right)u = 0 \tag{16}$$

As it is known, the general solution of (16) at $|p\theta/q| << 1$ has the following form

$$u(t) = A \sum_{k=-\infty}^{\infty} C_{2k} e^{2i(p/q+k)t} + B \sum_{k=-\infty}^{\infty} C_{2k} e^{-2i(p/q-k)t}$$

where A and B are arbitrary constants, the coefficients C_{2k} are approximately (at $p^2 << q^2$) given by the expressions

$$C_{\pm 2}/C_0 \approx -(p\theta/2q),\ C_{\pm 4}/C_0 \approx (p\theta/4q)^2 \ldots$$

Thus, the function searched for $\varphi_1(x, z)$ in this case is

$$\varphi_1(x, z) \approx C_0 \exp\left(-px - \frac{\theta p}{q}\sin(qz)\right)\left(1 - \frac{p\theta}{q}\cos\left(qz - \frac{\pi}{2}\right)\right)$$

$$\cdot \left[A \exp\left(ipz - i\frac{\pi p}{2q}\right) + B \exp\left(-ipz + i\frac{\pi p}{2q}\right)\right]$$

$$\approx e^{-px}\left(1 - \frac{2p\theta}{q}\sin(qz)\right)(\tilde{A}\cos(pz) + \tilde{B}\sin(pz)) \tag{17}$$

The amplitudes $\tilde{A}$ and $\tilde{B}$ and the characteristic scale p^{-1} of the heterogeneity in the distribution of the azimuthal angle are determined by the substitution of the function (17) in the equation for the free energy density (15), by integrating the expression obtained with respect to the liquid crystal volume and by minimizing this functional for $\tilde{A}$, $\tilde{B}$ and p. As it follows from (17) the derivative $\partial\varphi_1/\partial z$ contains the characteristic contributions $p\theta \cos(qz)$, $p \cos(pz)$ and $p \sin(pz)$. Substituting the function $\varphi_1(x, z)$ into the last term of equation (15) in the functional for the free energy we observe terms of the order

Downloaded by [Tomsk State University of Control Systems and Radio] at 12:54 19 February 2013

$p^2\theta^4 \cos^2(qz)$ and $p^2\theta^3 \cos(qz)$ containing also squared amplitude combinations $\tilde{A}$ and $\tilde{B}$. The integration with respect to the coordinate z gives the magnitude of the order $p^2\theta^4$, simultaneously the first four components of equation (15) have a positive sign and the integration results in the magnitude of the order $p^2\theta^2$. Thus, the contribution of the heterogeneity of the azimuthal angle to the free energy is positive, at least at small polar angles θ, in other words this kind of heterogeneity ($p \neq 0$) is indeed not energetically favourable.

The contribution to the elastic energy due to the change of the distance between the monolayers ($\partial u/\partial z \neq 0$) and by the bending of the layers, under condition that $\partial^2 u/\partial x^2 \neq 0$, $\partial^2 u/\partial y^2 \neq 0$, $\partial^2 u/\partial x \partial y \neq 0$ can be obtained with the help of the following invariants (and corresponding coefficients):

$$\left(\frac{\partial u}{\partial z}\right)^2, \left(\frac{\partial^2 u}{\partial x \partial z}\right)^2 + \left(\frac{\partial^2 u}{\partial y \partial z}\right)^2, \left(\frac{\partial^2 u}{\partial x^2} + \frac{\partial^2 u}{\partial y^2}\right)^2, \quad 4\left(\frac{\partial^2 u}{\partial x \partial y}\right)^2 + \left(\frac{\partial^2 u}{\partial x^2} - \frac{\partial^2 u}{\partial y^2}\right)^2 \tag{18}$$

In addition, the equation may have mixed scalar invariants (for the symmetry groups $D_{\infty h}$ and D_∞)

$$\left(\frac{\partial \xi_1}{\partial x} + \frac{\partial \xi_2}{\partial y}\right)\left(\frac{\partial^2 u}{\partial x^2} + \frac{\partial^2 u}{\partial y^2}\right), \left(\frac{\partial^2 u}{\partial x \partial z} \cdot \frac{\partial \xi_1}{\partial z} + \frac{\partial^2 u}{\partial y \partial z} \cdot \frac{\partial \xi_2}{\partial z}\right), \tag{19}$$

and also pseudo-scalar invariants (for the symmetry group D_∞), for example,

$$\frac{\partial u}{\partial z}\left(\frac{\partial \xi_1}{\partial y} - \frac{\partial \xi_2}{\partial x}\right), (\xi_1^2 - \xi_2^2)\frac{\partial^2 u}{\partial x \partial y} + \xi_1 \xi_2 \left(\frac{\partial^2 u}{\partial x^2} - \frac{\partial^2 u}{\partial y^2}\right) \tag{20}$$

The invariants in (18)–(20) are analogous to the values analysed by the Orsay group.[20]

We shall not dwell further upon the bending of the monolayers and the distance variations between them. Owing to the account of these distortions according to (18) and (19)–(20), which are a result of orientational deformations, the elastic constants K', K'', $\bar{K}$, K''' are reevaluated. The invariants of a higher order with respect to the components (P_x, P_y) will not be taken into account either, and also those with respect to the derivatives from these components and

Downloaded by [Tomsk State University of Control Systems and Radio] at 12:54 19 February 2013

corresponding mixed invariants, since these effects will not change the results and will contribute to the effectiveness of the already known phenomenological coefficients. Generally speaking, a considerably strong interaction of the polarization components, of the orientational transition parameter and the shift of the layers can cause the sign to change to "$-$" for the coefficient for θ^4 in $F(\theta^2)$, which, in turn, causes a phase transition of the first order.

Downloaded by [Tomsk State University of Control Systems and Radio] at 12:54 19 February 2013

2.4. Helical ferroelectrics

Assuming the polar angle θ to be small and taking into account all the remarks made concerning the absence of spontaneous deformations $(\partial\xi_1/\partial x) + (\partial\xi_2/\partial y)$ . . . and the renormalization of phenomenological coefficients, we write the free energy density of the smectic phase A^* in the form (see invariants (4)–(6), (8), (14), (15))

$$
\begin{aligned}
F = {} & a_0(\xi_1^2 + \xi_2^2) + b_0(\xi_1^2 + \xi_2^2)^2 + \frac{1}{2}\mathrm{K}^\circ \\
& \cdot\left[\left(\frac{\partial\xi_1}{\partial z}\right)^2 + \left(\frac{\partial\xi_2}{\partial z}\right)^2\right] + \lambda_0\left(\xi_1\frac{\partial\xi_2}{\partial z} - \xi_2\frac{\partial\xi_1}{\partial z}\right) \\
& + \frac{1}{2\chi_0}(\mathrm{P}_x^2 + \mathrm{P}_y^2) + \mu_p(\xi_1\mathrm{P}_y - \xi_2\mathrm{P}_x) \\
& - \mu_f^0\left(\mathrm{P}_x\frac{\partial\xi_1}{\partial z} + \mathrm{P}_y\frac{\partial\xi_2}{\partial z}\right) + \lambda_0'(\xi_1^2 + \xi_2^2)\left(\xi_1\frac{\partial\xi_2}{\partial z} - \xi_2\frac{\partial\xi_1}{\partial z}\right) \\
& - \mu_f'(\xi_1^2 + \xi_2^2)\left(\mathrm{P}_x\frac{\partial\xi_1}{\partial z} + \mathrm{P}_y\frac{\partial\xi_2}{\partial z}\right) \\
& - \delta\mu_f'\left(\xi_1\frac{\partial\xi_2}{\partial z} - \xi_2\frac{\partial\xi_1}{\partial z}\right)(\xi_1\mathrm{P}_y - \xi_2\mathrm{P}_x),
\end{aligned}
\tag{21}
$$

where $a = a_0'(\mathrm{T} - \mathrm{T}_0)$, $a_0' > 0$, $b_0 > 0$, $\mathrm{K}^\circ > 0$, $\chi_0 > 0$.

The variation of the expression (21) with respect to the polarization components

$$\mathrm{P}_x = \mathrm{P}\sin\varphi(z),\ \mathrm{P}_y = -\mathrm{P}\cos\varphi(z) \tag{22}$$

permits one to obtain at $\theta = \text{const} << 1$

$$P = \chi_0\left(\mu_p - \mu_f \frac{\partial\varphi}{\partial z}\right), \tag{23}$$

$$F = a\theta^2 + b\theta^4 + \frac{1}{2}K\theta^2\left(\frac{d\varphi}{dz} - q_0\right)^2,$$

$$a = a_0 - \frac{1}{2}\chi_0\mu_p^2 - \frac{(\lambda_0 + \chi_0\mu_p\mu_f^0)^2}{2K},$$

$$q_0 = -\frac{\lambda + \chi_0\mu_p\mu_f}{K}, \qquad \lambda = \lambda_0 + \lambda'\theta^2, \tag{24}$$

$$\mu_f = \mu_f^0 + (\mu_f' + \delta\mu_f')\theta^2, \qquad K = K^\circ - \chi_0\mu_f^{02}$$

As it follows from (24), the minimal free energy is characterized by the distribution of the azimuthal angle

$$\varphi(z) = \varphi_0(z) = q_0 z,\ q_0 = q_c + q'\theta^2 + \ldots,$$

$$q_c = -\frac{\lambda_0 + \chi_0\mu_p\mu_f^0}{K} \tag{25}$$

and the helical distribution of the polarization with the amplitude

$$P_s = \chi_0|\mu_p - \mu_f q_0|\theta. \tag{26}$$

The equations (24) and (25) include revalued effective coefficients a, b, K, λ', q', and the phenomenological dependence $q_0 = q_0(\theta^2)$,[14,21,22] i.e. temperature dependence of the spiral pitch $h_0(T) = 2\pi/q_0(\theta^2)$ is determined by the value $q' = -[\lambda' + \chi_0\mu_p(\mu_f' + \delta\mu_f')]/K$. The value $q_c = q_0(T_c)$ at the phase transition temperature T_c is determined from

$$T_c = T_0 + \frac{1}{2a_0^1}(\chi_0\mu_p^2 + Kq_c^2)$$

Below the point T_c in phase C* the finite tilt angle of the director is

$$\theta = \theta_0 = \left(-\frac{a}{2b}\right)^{1/2}$$

Downloaded by [Tomsk State University of Control Systems and Radio] at 12:54 19 February 2013

Downloaded by [Tomsk State University of Control Systems and Radio] at 12:54 19 February 2013

It is to be noted that incommensurate and polarized structures are induced owing to two Lifshitz invariants in (21), which are characterized by different physical effects. In case the dominant role is also played by piezo- and flexoelectric effects (3) and (7), the following equations can be obtained from (25) by neglecting the contribution of the invariant (6) $q_0 \sim -\chi_0\mu_p\mu_f/K$ and $P_s \sim \chi_0|\mu_p|\theta$. In another extreme case, the flexoelectric effect being small (7), helical twisting is determined by the invariant (6), and $q_0 \sim -\lambda/K$ and $P_s \sim \chi_0|\mu_p|\theta$. Under condition

$$\lambda + \chi_0\mu_p\mu_f = 0 \tag{27}$$

the Lifshitz invariants mentioned above are counterbalanced, allowing for the existence of a macroscopic ferroelectric state at $q_0 = 0$. This appears possible in mixtures, whose various components make various contributions to the cholesteric twisting and polarization effects.

The expression (26) shows that in the first approximation $P_s \sim \theta$. Taking into account the terms of a higher order in (21) with respect to the tilt angle θ, we obtain an expansion of $P_s(\theta)$ and a small correction to (26) of the order of θ^3. Small corrections such as these induced by the same piezo-electric effect (4) are of little interest since they can be characterized by the same relaxation times as the main contribution. Additional small contributions to the spontaneous polarization $P_s(\theta)$ can be singled out if they are due to various molecular mechanisms and are characterized by different relaxation times.[23] For instance, an additional contribution P_t to the polarization P_s can result from the development of the degree of order with respect to some additional degree of freedom possessed by the molecules, in particular, with respect to the orientation of the transverse molecular axis. In the last case the order parameter for transverse axes $Q_t \neq 0$.

The ordering of short molecular axes is to occur lower than the point of the phase transition A*–C* as a secondary phenomenon and to have its own relaxation time. The parameters of this ordering are the components (η_1, η_2) formed by square combinations of projections of the cross director $\mathbf{n}'$:

$$\eta_1 = Q_t(n_x'^2 - n_y'^2), \qquad \eta_2 = 2Q_t n_x' n_y',$$

where $n_x' = -\sin\varphi$, $n_y' = \cos\varphi$. The components (η_1, η_2) are transformed with respect to irreducible vector representation E_2 of the symmetry group D_∞. Since the components (ξ_1, ξ_2) are the proper parameter of the transition A*–C*, and the components (P_x, P_y)

transform as $(\xi_2, -\xi_1)$, the expression for F has an invariant

$$\mu_t[(P_y\xi_1 + P_x\xi_2)\eta_1 + (P_y\xi_2 - P_x\xi_1)\eta_2] \approx \mu_t P\theta Q_t \tag{28}$$

where μ_t is a phenomenological parameter.

The qualitative dependence $Q_t(\theta)$ can be determined from the correction to the free energy

$$\delta F(Q_t)$$

$$= \frac{1}{2\chi_t}(\eta_1^2 + \eta_2^2) + g[\eta_1(\xi_1^2 - \xi_2^2) + 2\eta_2\xi_1\xi_2] \approx -g\theta^2 Q_t + \frac{1}{2\chi_t}Q_t^2,$$

where g and $\chi_t > 0$ are phenomenological constants. Minimizing $\delta F(Q_t)$ with respect to the parameter Q_t, we find

$$Q_t = g\chi_t\theta^2 \tag{29}$$

Taking into account (5), (28) and (29) one can see that the additional contribution P_t to the spontaneous polarization of phase C* is to be proportional

$$P_t \sim \mu_t\chi_0\chi_t g\theta^3, \tag{30}$$

in other words, the component of the polarization P_s can be described by both its relaxation time, corresponding to rotation of the molecules around their long axes, and its cubic dependence on the tilt angle of the molecules, θ.

Pozhidaev et al.[23] (1983) used the pyroelectric effect to observe the temperature dependence of the "fast" component of the pyroelectric response, the relaxation time being less than 10^{-8} s. The substance DOBAMBC and thermo-laser impulses, $2 \cdot 10^{-8}$ s long, were used during the experiment. The temperature dependence of the "fast" component of the pyroresponse, reproducing laser impulse, was used to determine, by integration, the temperature dependence of the corresponding component of the spontaneous polarization which appeared proportional to the cubic power of the angle of the molecular tilt. Equation (30) agrees well with this observation. As it follows from the experiment, the coefficient in (30) is strongly dependent on the magnitude of the dipole moment of the molecules, and the increase of the dipole moment gives a sharp increase of this coefficient.

Downloaded by [Tomsk State University of Control Systems and Radio] at 12:54 19 February 2013

This fact points to a strong dependence of the "fast" component of the polarization P_t on the polar structure of chiral molecules.

Downloaded by [Tomsk State University of Control Systems and Radio] at 12:54 19 February 2013

2.5. The behaviour in an external electric field

The analysis of the behaviour of chiral SLC in the external field **E** demands that the term $-\mathbf{PE}$ should be added to (21). Variation of the functional $F - \mathbf{PE}$ with respect to the values **P**, θ and φ gives the necessary equations for the functions $\theta(\mathbf{r})$ and $\varphi(\mathbf{r})$. Under the effect of the external field the incommensurate structure of phase C* gets distorted, the distortions $\theta(\mathbf{r}) - \theta_0$ and $\varphi(\mathbf{r}) - \varphi_0(z)$ being insignificant in weak fields. These distortions are due to the spiral untwisting of dipole moments and the increase of the tilt angle θ in strong fields. In weak fields, considerably weaker than the value of E_c at which the full untwisting of the spiral occurs, the disturbances of the director orientation can be divided into asimuthal $\varphi - \varphi_0$ (at the homogeneous distribution of $\theta = \theta_0$) and polar $\theta - \theta_0$ (at an undisturbed pitch of the helix $h_0 = 2\pi/q_0$).

We shall assume that the electric field **E** has an orientation in the smectic plane xy, that is $E_z = 0$. Under this condition the effects induced by the polarization component P_z and orientational distortions in the plane xy can be neglected, and the values θ and φ can be taken for the functions of the coordinate z. In other words this phenomenon is a linear response of the system to the external field. The value of the dielectric susceptibility should have a correction $\delta\chi = \chi - \chi_0$ due to the orientational distortions mentioned above, moreover, both asimuthal and polar deformations make their contribution to the value $\delta\chi$ owing to the piezoeffect, while macroscopic polarization of the medium can be due to the flexoeffect only under the modulated polar deformation.

Assuming that the field **E** is parallel to the axis y, varying the sum of the expressions in (21) and $-\mathbf{PE}$ with respect to the values P_x, P_y, and also $\theta(z)$ and $\varphi(z)$, we obtain the following results:

$$P_x = \chi_0\left(\mu_p - \mu_f \frac{d\varphi}{dz}\right)\theta \sin\varphi + \chi_0(\mu_f - \delta\mu_f)\frac{d\theta}{dz}\cos\varphi,$$

$$P_y = \chi_0 E - \chi_0\left(\mu_p - \mu_f \frac{d\varphi}{dz}\right)\theta \cos\varphi + \chi_0(\mu_f - \delta\mu_f)\frac{d\theta}{dz}\sin\varphi \tag{31}$$

where the functions $\theta(z) = \theta_0 + \theta_1(z)$ and $\varphi(z)$ satisfy the following equations

$$K\theta_0 \frac{d^2\varphi}{dz^2} + \chi_0\mu_p E \sin\varphi = 0,$$
$$K^0 \frac{d^2\theta_1}{dz^2} + 4a\theta_1 - \chi_0 E\left(\mu_p - \delta\mu_f \frac{d\varphi}{dz}\right)\cos\varphi = 0 \tag{32}$$

on condition that $E << E_c$, $|\theta_1| << \theta_0$.

The first of the equations in (32) describes the distortion of the helix in the electric field if $\varphi(z) = \varphi_0(z)$ at $E = 0$. This problem seems analogous to the one concerning the cholesteric spiral.[24] Making use of the known solution, we find[25]

$$E_c = \frac{\pi^2}{16}\frac{Kq_0^2\theta_0}{\chi_0\mu_p} \tag{33}$$

In weak electric fields ($E << E_c$) the periodic solution $\theta_1(z)$ has the following form

$$\theta_1(z) = \frac{\chi_0 E(\mu_p - \delta\mu_f q_0)\cos(q_0 z)}{4a - K^0 q_0^2} \tag{34}$$

and the function $\varphi(z)$ is described by the following expression

$$\varphi(z) = q_0 z + \frac{\chi_0\mu_p E}{Kq_0^2\theta_0}\sin(q_0 z) \tag{35}$$

Using (31), (34) and (35) we obtain the macroscopic average value of the polarization P along the y axis in phase C* [14]

$$P = (\chi_0 + \delta\chi)\,E,$$
$$\delta\chi_c = \frac{1}{2}\chi_0^2\left[\frac{\mu_p^2}{Kq_0^2} + \frac{(\mu_p - q_0\delta\mu_f)^2}{K^0 q_0^2 - 4a}\right] \tag{36}$$

In phase A^*, that is at $T > T_c$, the structure of SLC is homogeneous ($q = d\varphi/dz = 0$), if the electric field is absent. Owing to this, we

Downloaded by [Tomsk State University of Control Systems and Radio] at 12:54 19 February 2013

obtain[15] in the linear approximation with respect to the field E using (23) and (24) where the component $-\mathbf{PE}$ is added to F

$$\delta\chi_A = \frac{\chi_0^2\mu_p^2}{2a + Kq_c^2},$$
$$\theta_1 \equiv \theta = \frac{\chi_0\mu_p}{2a + Kq_c^2}\,\mathrm{E}, \qquad \varphi = \begin{cases} 0, & \mu_p < 0 \\ \pi, & \mu_p > 0 \end{cases}, \tag{37}$$

Thus, in phase A* the value $\delta\chi$ is determined only by the piezoelectric coefficient μ_p, since there is no macroscopic twisting of the molecular orientation, and, consequently, no flexoeffect. It should be stressed that dielectric susceptibility becomes infinite at the point T_c, that is at $a = 0$, since the low-temperature phase is modulated, and, consequently, it is only the response of the system to the external field, modulated correspondingly, that can be infinitely large. At $a >> Kq_c^2$ the expression (37) reminds one of the Curie–Weiss law because in a situation like this the radius of the correlation $r_c \sim (K/a)^{1/2}$ is much smaller than the pitch of the spiral $h_c = 2\pi/q_c$ in the fluctuation region (of the radius r_c), i.e., the medium has homogeneous orientations.

It should be noted that equation (36) is valid at $E << E_c$. According to (33) the critical value of E_c is transformed to 0 at the transition point T_c. Therefore the inequality $E << E_c$ is violated at the point T_c and equation (36) is no longer valid; instead, equation (37) should be used which proves to be valid within the temperature region $T - T_c > -1°\mathrm{K}$.

The experimental measurements of the dielectric permeability[25,26] show that the value $\delta\chi_A \sim (\chi_0\mu_p)^2/Kq_c^2$ is much smaller than the value $\delta\chi_c$, if the field E is much smaller than the field of untwisting E_c, and v.v., $\delta\chi_A \approx \delta\chi_C$, if the helix in phase C^* is untwisted by a strong field. The corresponding estimates give $(\chi_0\mu_p)^2 << Kq_c^2$. The anomalous increase of the dielectric permeability in phase C^* of a perfect large sample (i.e., of samples having about 100 mcm in thickness with no structure defects) can be accounted for by the flexoelectric contribution to the value $\delta\chi_C$ in weak fields [see (36)]. At the transition point T_c this contribution transforms to 0, it can be, however, considerable at lower temperatures; the value $\delta\mu_f$ is noted to increase. Glogarova et al.[26] pointed to another factor contributing to the increase of $\delta\chi_C$, in particular, the disturbance of the defective (disclinating) structure in phase C^* by the field.

Downloaded by [Tomsk State University of Control Systems and Radio] at 12:54 19 February 2013

Downloaded by [Tomsk State University of Control Systems and Radio] at 12:54 19 February 2013

The study of dielectric properties is usually carried out in an alternating electric field. In this case the dispersion of the dielectric permeability and corresponding relaxation processes, typical of a chiral system, should be taken into account. Relaxation phenomena can be described phenomenologically, by adding to the right hand side of (32) terms containing the derivatives with respect to the time t of the functions $\varphi(z, t)$ and $\theta(z, t)$, in particular, $\gamma_\varphi\ \theta_0\ \partial\varphi/\partial t$ and $\gamma_1\ \partial\theta_1/\partial t$ where γ_1 and γ_φ are the viscosity coefficients, in the general case $\gamma_1 \neq \gamma_\varphi$. As it can be seen from the solution of such equations, there are, at least, two characteristic relaxation times in phase C*, τ_φ and τ_θ;

$$\tau_\varphi = \frac{\gamma_\varphi}{Kq_0^2}, \qquad \tau_{\theta|C} = \frac{\gamma_1}{K^0 q_0^2 - 4a},$$

and only one relaxation time in phase A^*

$$\tau_{\theta|A} = \frac{\gamma_1}{2a + Kq_c^2}$$

The relaxation time, τ_φ, characterizes deterioration of azimuthal disturbances $\varphi - \varphi_0$ at a constant value of the polar angle $\theta = \theta_0$, i.e. the reconstruction process of the helix. The time τ_θ serves to describe a relaxation of the disturbances of the polar angle θ_1, the pitch of the helix being unchanged $h = h_0$. The relaxation time τ_φ in phase A* is absent, since the orientational structure here is homogeneous.

Taking into account (31) and the linear dependence between weak orientational disturbances and macroscopic polarization, we easily obtain quantitatively the dispersion of dielectric susceptibility, and the real parts of the correction are

$$\delta\chi_C(\omega) = \frac{\chi_0^2}{2}\left[\frac{\mu_p^2 K q_0^2}{(Kq_0^2)^2 + (\gamma_\varphi\omega)^2} + \frac{(\mu_p - \delta\mu_f q_0)^2(K^0 q_0^2 - 4a)}{(K^0 q_0^2 - 4a)^2 + (\gamma_1\omega)^2}\right],$$

$$\delta\chi_A(\omega) = \frac{\chi_0^2\mu_p^2(2a + Kq_c^2)}{(2a + Kq_c^2)^2 + (\gamma_1\omega)^2} \tag{38}$$

Blinc[27–29] and Blinc and Zeks[30] analyzed dynamic aspects of ferroelectric phenomena by comparing the orientational fluctuations in chiral systems and soft and Goldstone modes in the usual solid fer-

Downloaded by [Tomsk State University of Control Systems and Radio] at 12:54 19 February 2013

roelectrics. "Goldstone mode" is used here for azimuthal disturbance of the director orientation and the polarization, restoring the symmetry of the high temperature phase A*, while a "soft mode" is used for synphase fluctuations of the polar angle and the polarization of the low-temperature C* phase. These modes can be energetically described by reciprocal values of the corresponding relaxation times (of the type τ_φ^{-1} and τ_θ^{-1}). The phase transition A*–C* can be imagined as a sort of "condensation" of the above mentioned soft mode. The "frequencies" of such fluctuation modes at the zero value of the wave vector remain finite at the transition point.[30]

The temperature dependence of the dielectric permeability $\epsilon(\omega) = \epsilon_\infty + 4\pi\delta\chi(\omega)$, shown in Fig. 3b, is experimentally proved to have a characteristic maximum at low frequencies and temperature, which is some degrees lower than the transition temperature. Such behaviour can be qualitatively accounted for by the expressions (36)–(38).[25] Also the pitch of the spiral $h_0(T)$ (Fig. 4) is experimentally proved to have nonmonotonic temperature dependence. The strong dependence of $h_0(T)$ within a narrow temperature interval can hardly be accounted for by a phenomenological approach.[21] Indeed, the expansion of the (25) type in terms of increasing θ^2 implies the assumption that the coefficients in the terms of the expansion from θ^2 and θ^4 should be anomalously large (about 10^2 times as large as $h_0(T_c)$). This anomaly can be accounted for by using the molecular-statistical approach which deals with the anomalous temperature dependence of flexoelectric coefficients.[21]

It follows from (24) and (36) that the maxima of the temperature dependencies of $\epsilon(T)$ and $h_0(T)$ correspond, generally speaking, to temperatures which do not coincide with the transition point T_c. Levstik et al.[22] proved this phenomenon experimentally.

It should be stressed that the temperature dependence of $\delta\chi(T)$ outside the narrow region of the C* phase, mentioned above, can be determined by both the absolute values and the signs of the values μ_p and $\delta\mu_f q_0$, according to the expression (36). Since $\delta\mu_f \sim \theta^2 \sim (T_c - T)$, we can expect both an increase and a decrease of the function $\delta\chi(T)$ at the lower temperatures. Levstik et al.[22] observed a slowly increasing dependence $\delta\chi(T)$ on decreasing temperature in a liquid crystal mixture.

The problem of assigning values to the material constants μ_p, μ_f, $\delta\mu_f$ has been much discussed in the literature.[25,31–33] It was Ostrovsky et al.[25] who first estimated these values and showed that $\mu_p \sim \mu_f p$ under certain assumptions concerning the values of other material constants. Durand and Martinet-Lagarde[31] concluded that $\mu_p >> \mu_f q$, assuming that even under the influence of the flexoeffect the polar

angle θ remains a homogeneous function of the coordinates within the electric field. This assumption is, however, not true. Beresnev *et al.*[32] found that $\mu_p >> \mu_f q$, basing their conclusion on the data on the minimum of the electro-optic modulation amplitude in a mixture at some concentration of the components, assuming that this minimum corresponds to the zero value of the complete polarization of the mixture. This assumption is not true either. Let's analyze in more detail the experiments by Beresnev et al.[32] who studied the diffraction of polarized light on a periodic structure of chiral smectic C* under the effect of an external electric field.

Since the helix becomes distorted by the external field, the intensities of the passing and diffracted waves change their values according to the piezo- and flexocoefficients. The dielectric permeability tensor of phase C* contains the following terms[55]

$$\epsilon_{ij} = \epsilon_1\delta_{ij} + \epsilon_2 l_i l_j + \epsilon_3 n_i n_j + \epsilon_4(n_i l_j + l_i n_j)(\mathbf{nl})$$

where $\mathbf{l}$ is a unit vector of the normal to the layers of the smectic. Within linearity with respect to θ in the expansion of the tensor $\hat{\epsilon}$ into a Fourier series

$$\hat{\epsilon} = \sum_{n=-\infty}^{\infty} \hat{\epsilon}_n \exp(inqz)$$

the only terms (as far as optical frequencies are concerned) differing from the zero, the field being absent, are as follows:

$$\hat{\epsilon}_0 = \begin{pmatrix} \epsilon_1 & 0 & 0 \\ 0 & \epsilon_1 & 0 \\ 0 & 0 & \epsilon_{33} \end{pmatrix} \qquad \hat{\epsilon}_1 = \hat{\epsilon}^*_{-1} = \frac{\epsilon_a\theta_0}{2}\begin{pmatrix} 0 & 0 & 1 \\ 0 & 0 & -i \\ 1 & -i & 0 \end{pmatrix},$$

where $\epsilon_{33} = \epsilon_1 + \epsilon_2 + \epsilon_3 + 2\epsilon_4$, $\epsilon_a = \epsilon_3 + \epsilon_4$. Under the effect of a constant field E the corrections to $\hat{\epsilon}_n$, taking account of (34) and (35), have the form

$$\hat{\epsilon}'_0 = \epsilon_a \frac{U - G\theta_0}{2} E \begin{pmatrix} 0 & 0 & 1 \\ 0 & 0 & 0 \\ 1 & 0 & 0 \end{pmatrix}$$

$$\hat{\epsilon}'_2 = \epsilon_a \frac{U + G\theta_0}{4} E \begin{pmatrix} 0 & 0 & 1 \\ 0 & 0 & i \\ 1 & i & 0 \end{pmatrix},$$

Downloaded by [Tomsk State University of Control Systems and Radio] at 12:54 19 February 2013

where

$$G = \frac{\chi_0 \mu_p}{K q_0^2 \theta_0}, \qquad U = \frac{\chi_0(\mu_p - \delta\mu_f q_0)}{4a - K^0 q_0^2}.$$

Thus, within the external field a second diffraction order appears, while the zero and the first orders become dependent on the field.

Beresnev et al.[32] studied the intensity of the direct beam whose amplitude is

$$A_0 = \frac{\epsilon_1 - \epsilon_{33}}{2} \sin 2\psi - \frac{\epsilon_a(U - G\theta_0)}{2} E \cos 2\psi,$$

where ψ is the angle between the axis of the polaroid and that of the spiral. The intensity of the zero diffraction maximum in the kinetic approximation is, correspondingly, as follows

$$|A_0|^2 \approx I_0\left(\sin^2 2\psi - \frac{2\epsilon_a}{\epsilon_1 - \epsilon_{33}} \overline{\theta \cos \varphi} \sin 4\psi\right),$$

where the upper bar serves to denote averaging with respect to the coordinate z and, consequently, the linear part of the intensity is proportional[55]

$$\delta|A_0|^2 \sim |\epsilon_a (U - G\theta_0)| E.$$

The temperature and concentration dependence of the relation $\delta|A_0|^2/A_0^2$, as well as the concentration dependence of the parameter μ_p were measured experimentally, and were discovered to transform to zero at certain values of the concentration of the mixtures used. At $T > T_c$ the ratio $\delta|A_0|^2/A_0^2$ is negligible no matter what concentration is used, and therefore $\epsilon_a(\chi_0\mu_p/Kq_0^2)$ can be neglected. Thus, to account for the observed complex temperature dependence of $\delta|A_0|^2/A_0^2$ one should assume that the difference $\delta\mu_f$ as a part of U is of importance. It is also obvious that $\delta|A_0|^2 \neq 0$, if $P_s = 0$ (see eq. (26)).

It should be noted that, generally speaking, the main axis of the dielectric ellipsoid does not coincide with the direction of the director **n**. As it can be seen from simple calculations, at the fixed angle θ the main axis of the dielectric ellipsoid is found in the plane given by the vectors **n** and **l** and makes up the following angle[55]

$$\frac{(\epsilon_3 + \epsilon_4)\theta}{\epsilon_2 + \epsilon_3 + 2\epsilon_4}$$

Downloaded by [Tomsk State University of Control Systems and Radio] at 12:54 19 February 2013

with respect to the direction **l**; owing to this the second term the magnitude of $|A_0|^2$ contains a corresponding factor. Consequently, the optical axis of phase C* does not coincide with the direction **n** either. In the case when one of the axes (1′) coincides with the director **n** and the other (2′) is in the plane (**n**, **l**), the tensor $\hat{\epsilon}$ can not be diagonal: $\epsilon_{1'2'} \approx (\epsilon_2 + \epsilon_4)\theta$. Here the differences of the diagonal components $\epsilon_{1'1'}$; $\epsilon_{2'2'}$ and of the corresponding primary values ϵ_{11}, ϵ_{22} are proportional to $(\epsilon_{1'1'} - \epsilon_{11}) \sim \theta^2$ and $(\epsilon_{2'2'} - \epsilon_{22}) \sim \theta^2$ with coefficients which depend on the constants ϵ_2, ϵ_3, ϵ_4. Thus, in principle one may determine the constants of the dielectric tensor at a given value of the angle θ.

As to the relation of the parameters $\mu_f q_0/\mu_p$ and $\delta\mu_f q_0/\mu_p$, recent experimental data[32] offer the following estimates at several temperatures:

$T_c - T$	0.7	2.7	4
$\mu_f q_0/\mu_p$	5	4	5
$\delta\mu_f q_0/\mu_p$	35	64	82

Thus, one can observe a marked increase to a relatively large value $\delta\mu_f q_0/\mu_p$ within the interval $0.7\ \mathrm{K} < T_c - T < 4\ \mathrm{K}$.

2.6. Lifshitz point in a liquid crystal ferroelectric

The so-called Lifshitz point[35] was observed by Musevich et al.[34] in a substance DOBAMBC in the phase diagram in the following variables: external field-temperature, and it is, in other words, a triple point between the phases A*, C* and the phase C_h^* completely untwisted by the external field (Fig. 5). In this situation either the

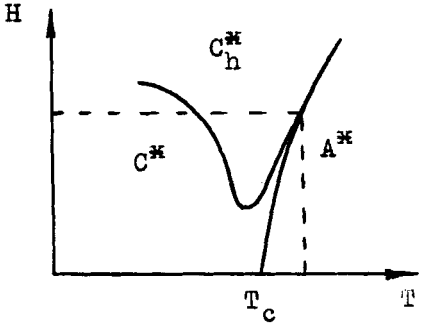

FIGURE 5 Lifshitz point as a triple point between the chiral smectic A* phase, the helical smectic C* phase and the untwisted chiral smectic C_h^* phase.

Downloaded by [Tomsk State University of Control Systems and Radio] at 12:54 19 February 2013

magnetic or the electric field can serve as the external field. It should be noted here that unlike the linear interaction with respect to **E**, the effect of the magnetic field **H** upon the orientational helix is quadratic with respect to **H** and is due to the diamagnetic anisotropy of a liquid crystal χ_a. The corresponding contribution to the magnetic energy has the following value

$$F_H = -\frac{1}{2}\chi_a (\mathbf{H}\cdot\mathbf{n})^2 \tag{39}$$

Adding (39) to (24) and assuming that the field **H** is oriented along the x axis, we obtain the expression for small values of the angle

$$F = a\theta^2 + b\theta^4 + \frac{1}{2}K\theta^2\left(\frac{d\varphi}{dz} - q_0\right)^2 - \frac{1}{2}\chi_a H^2\theta^2\cos^2\varphi,$$

whose minimization with respect to φ gives the following equation

$$\frac{d^2\varphi}{dz^2} = \frac{\chi_a H^2}{2\mathrm{K}}\sin 2\varphi \tag{40}$$

As is well known[24] the solution of the non-linear equation (40), corresponding to the minimum of the free energy, describes the so-called phase solitons whose number becomes zero at a critical value of the field $\mathrm{H} = \mathrm{H}_c = (\pi/2)(\mathrm{K}/\chi_a)^{1/2}q_0$. At $H \geq H_c$ a complete untwisting of the spiral can be observed, i.e. within this region of the H values the C* phase can set in if $\mathrm{T} < \mathrm{T}_c$. Since the wave number q_0 depends on the temperature and the K and χ_a values do not, the dependence $H_c(\mathrm{T})$ must be analogous to the dependence $q_0(\mathrm{T})$ which is observed experimentally (see Fig. 5). In this case the value $H_c(\mathrm{T}_0)$ is finite, since $q_0(\mathrm{T}_c) = q_c$.

Analogous phenomena can be observed in the electric field. However, due to the linear dependence (4) between polarizational and orientational degrees of freedom, the corresponding formulas change their forms. The formula (33) may have the following form

$$\mathrm{T}_c(\mathrm{E}) = \mathrm{T}_c - \frac{2b}{a'}\left(\frac{16\chi_0\mu_p}{\pi^2\mathrm{K}q_0^2}\right)^2\mathrm{E}^2,$$

where the critical temperature $\mathrm{T}_c(\mathrm{E})$ is a transition point from a homogeneous state (the C_h^* phase) to a heterogeneous state (the C*

Downloaded by [Tomsk State University of Control Systems and Radio] at 12:54 19 February 2013

phase), the value of the field being constant. In case the temperature dependence $q_0(T)$ is neglected the equation $(T_c - T_c(E)) \sim E^2$ is to be valid[35] which can be confirmed by experiment.[12]

Such structural transformations in weak fields are phase transitions of the second order. However, in strong fields the nature of the transition becomes different.[36] Indeed, the energy of the homogeneous state (with $\theta \approx (\chi_0\mu_p E/4b_0)^{1/3}$)

$$F^*_{Ch} \approx a_0\theta^2 + b_0\theta^4 - \chi_0\mu_p F\theta \approx -3b_0\left(\frac{\chi_0\mu_p E}{4b_0}\right)^{4/3}$$

being compared to the energy of the heterogeneous structure (with $\theta \approx \theta_0 = (-a/2b)^{1/2}$)

$$F^*_C \approx \frac{a^2}{4b}$$

shows that in a strong field, i.e. at $E >> (b/\chi_0\mu_p)\ \theta_0^3$, a transition of the first order occurs at the point

$$a^* \sim b\left(\frac{\chi_0\mu_p E}{b}\right)^{2/3}$$

accompanied by a corresponding jump of the tilt angle, which is

$$(\theta_{C^*} - \theta_{Ch^*}) \sim \left(\frac{\chi_0\mu_p E}{b}\right)^{1/3}$$

At a certain intermediate value of the field $E = E_{tc}$,

$$E_{tc} \sim \frac{(Kq_0^2)^{3/2}}{b^{1/2}\chi_0\mu_p},$$

there is a tricritical point $T_{tc} = T_c(E_{tc})$, on the curve $T_c(E)$ at which the first order phase transition is transformed into one of the second order.

The dependence of the critical field E on temperature according to (33) can be, mainly, determined by the proportionality $E_c(T) \sim \theta_0(T)/h_0^2(T)$. Far from the phase transition point T_c where $h_0(T)$ is a weak function, the temperature dependence of the untwisting field is mainly determined by the temperature dependence of the tilt angle

Downloaded by [Tomsk State University of Control Systems and Radio] at 12:54 19 February 2013

$\theta_0(T)$. Within the narrow temperature region (2°K) near the transition point, where the pitch of the spiral changes anomalously non-monotonically (see Fig. 4), the function $E_c(T)$ must have a local minimum corresponding to the local maximum of the function $h_0(T)$. At the very point T_c the field of untwisting E_c vanishes owing to the zero value of the tilt angle θ_0. Such behaviour of $E_c(T)$ was experimentally observed[12] as is shown in Fig. 6. Thus, the phase diagram of the variables (T, E) points to a possible appearance of a certain reentrant phase C* at temperatures near T_c within a certain region of the values of the field E analogous to the behaviour of the system in an external magnetic field (cf. Fig. 5).

2.7. The role of the boundary conditions

The surface layer of the C* phase has a considerable effect on the orientational distribution of the director and the phase transition A*–C*, especially when the samples are not thick. One of the first models of the interaction of a SLC C* with a solid surface was the one shown in Fig. 7.[14,37] It was assumed that the layer of the C* phase has the thickness d and the strong anchoring between molecules and the solid surface where the angle $\theta = 0$; the azimuthal angle φ is fixed in the plane xy, the value of the coordinate z along the spiral axis being fixed. In this situation the term $1/2\ g\ (\partial\theta/\partial y)^2$ from (15) should be taken account of in (21), since it corresponds to the energy of elastic distortions in a subsurface layer, and for simplicity it was assumed that $g = K' + \tilde{K} = K'' + \tilde{K}$.

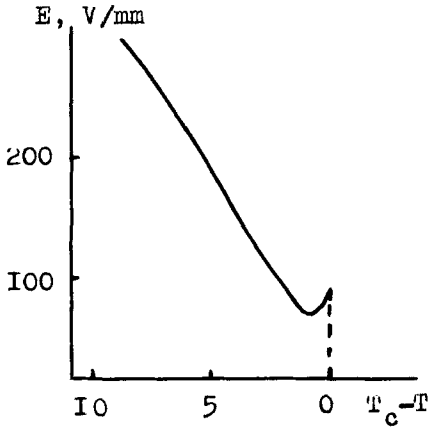

FIGURE 6 Temperature dependence of the critical electric field in DOBAMBC[12].

Downloaded by [Tomsk State University of Control Systems and Radio] at 12:54 19 February 2013

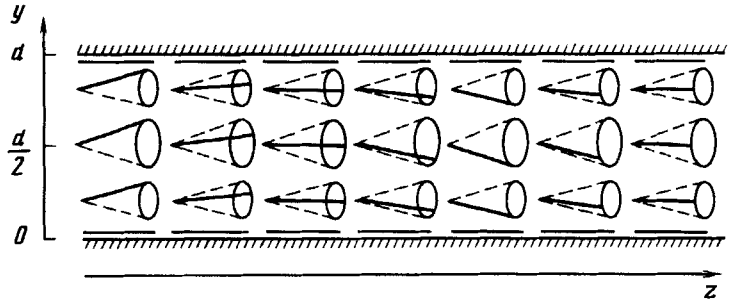

FIGURE 7 Geometry of the C* layer for strong planar anchoring conditions.

Outside the field the minimum value of F has a corresponding function $\varphi_0(z) = q_0 z$ at any value of y and the function $\theta(y)$ which agrees with the equation

$$g\frac{d^2\theta}{dy^2} - 2a\theta - 4b\theta^3 = 0 \tag{41}$$

if $\theta(0) = \theta(d) = 0$. The value of the angle θ in the centre of the layer at $y = d/2$ is

$$\theta_m \approx \theta_0\left[1 - 4\exp\left(-d\sqrt{\frac{|a|}{g}}\right)\right],$$

if $g << |a|d^2$. These results are valid for comparatively thick samples and for the temperatures not very close to the transition point. Assuming that $|a| \sim 10^3\ n/m^2$ and $g \sim 10^{-10}$ n (for DOBAMBC), we obtain that the deviation $\theta_m - \theta_0$ becomes noticeable when the thickness of the sample is about 1 mcm at $|T - T_c| < 1°K$.

The solution of equation (41) in the general case is as follows

$$\left(-\frac{2a}{g}\right)^{1/2} y = \left(1 + \frac{b\theta_m^2}{a}\right)^{-1/2} \int_{\arcsin(\theta_s/\theta_m)}^{\arcsin(\theta/\theta_m)} \frac{du}{\sqrt{1 - k^2\sin^2 u}} \tag{42}$$

where $k^2 = -\lambda b\theta_m^2(b\theta_m^2 + a)^{-1}$, $\theta_m = \theta(d/2)$, the magnitude θ_s is the value of the angle θ on the boundaries, $\theta_s = \{\theta(0), \theta(d)\}$, and $\theta(y)$ obeys the equation (at $y = 0$ and $y = d$)

$$W\theta_s = \pm g\frac{d\theta}{dy}.$$

Downloaded by [Tomsk State University of Control Systems and Radio] at 12:54 19 February 2013

Here W is the effective anchoring energy, the signs $\mp$ correspond to the values $y = d$ and $y = 0$. At $W >> (g\,|a|)^{1/2}$ the magnitude $\theta_s \approx (\sqrt{2g|a|}/|W|)\theta_m$ for $y = 0$, and from (42) it follows that at $y = d/2$

$$\left(\frac{-\lambda a}{2g}\right)^{1/2} d = \frac{\pi}{2} - \frac{(2g|a|)^{1/2}}{|W|}$$

or

$$T_c(d, W) - T_c^* \approx -\frac{\pi^2 g}{2a'} \frac{1}{\left(d + \dfrac{2g}{|W|}\right)^2}, \tag{43}$$

where T_c^* is the transition point at $d \to \infty$ or $W \to 0$.

It can be seen from (43) that at large values of the anchoring energy W, $|W|d >> g$, there appears a strong dependence of the transition point shift on the thickness of the layer: $|T_c - T_c^*| \sim d^{-2}$; when the anchoring is weak, $|W|d << g$, the transition point is shifted very little and hardly depends on the thickness of the layer. The experimental data[37] show that strong anchoring gives the predicted dependence $T_c(d)$ (Fig. 8). Note that a similar dependence $T_c(d)$ is observed when the effective elastic constant g is small.

The effective value of the constant g can depend considerably on the presence of other degrees of freedom, for example, the defor-

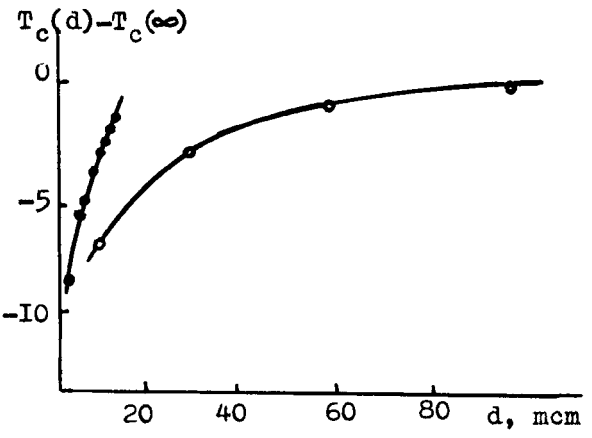

FIGURE 8 Dependence of the phase transition temperature T_c on the layer thickness d: ○—strong anchoring conditions,[37] ○—weak anchoring conditions.[12]

Downloaded by [Tomsk State University of Control Systems and Radio] at 12:54 19 February 2013

mation $\partial u/\partial z$ (see (20)), the heterogeneity of the azimuthal orientation $\partial\varphi/\partial x$ (see (15)), etc. In the case of a "suppressed" SLC C*, i.e. at $\partial u/\partial z = 0$, $\partial^2 u/\partial x^2 = 0$, etc., which occurs under rigid boundary conditions, the constant g must be larger if compared to the case of free development of such deformations. In the case of free conditions such deformations can be found by minimizing the free energy, for example, in (18)–(20) and (15). Here, the magnitudes $\partial u/\partial z$ and $\partial^2 u/\partial z^2$ turn out to be proportional to the magnitude $\partial\theta/\partial y$ which causes the renormalization of the coefficient before $(\partial\theta/\partial y)^2$, while the effective value of the constant g decreases. Such a case is possible under free boundary conditions, in particular, for the orientation of the helix axis and rigid planar orientation of the director. According to[12] the dependence $T_c(d)$ under such boundary conditions includes a larger derivative $\partial T_c/\partial d \sim W^3/g^2$ for a thinner layer (Fig. 8), this can be accounted for by a low value of the effective constant g.

It was assumed above that the constant dipole moments of the molecules do not affect the orientational boundary conditions. One can imagine a situation where transverse molecular dipoles have a strong interaction with a solid surface, being rigidly directed, for example, from the surface. Glogarova et al.[26] showed that under such conditions in the layer of the C* phase there appear disclinations localized near the surface. Fig. 9 shows a model according to which the director in the plane of the surface makes an angle θ_0 with the axis of the helix, and the asimuthal angles of the director on the opposite surfaces differ by the value π, in case the directions of the dipole moments on these surfaces are mutually opposite. Such bound-

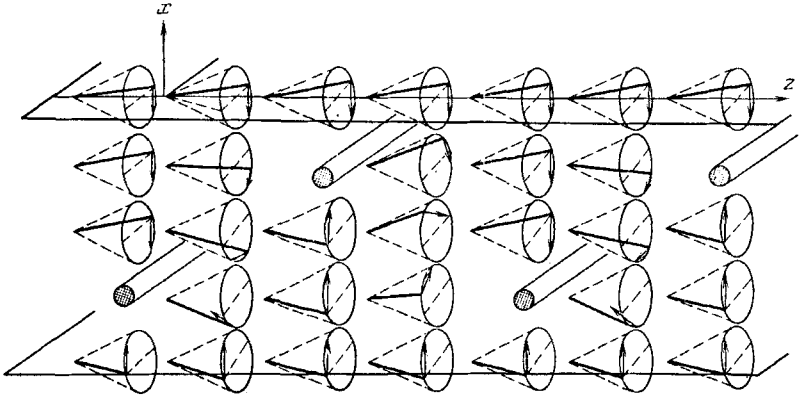

FIGURE 9 Planar helical structure with equivalent boundary conditions: surface dipole moments antiparallel, +2 and −2 twist disclinations exist.[26]

Downloaded by [Tomsk State University of Control Systems and Radio] at 12:54 19 February 2013

ary conditions can, evidently, be possible if the solid surface is isotropic, i.e. it does not have a direction which could be energetically advantageous as far as the long molecular axes are concerned, the position of the smectic monolayers being fixed. Also, at all temperatures $T < T_c$ the polar angle θ is constant throughout the sample ($\theta = \theta_0$), whereas the azimuthal angle φ has a heterogeneous distribution $\varphi(y,z)$. The developing twist disclinations have the indices $+2\pi$ and -2π.

It should also be noted that the disclinations mentioned above are characterized by a peculiar distribution of the electric dipoles (see Fig. 9). In the dipole distribution near the surfaces similar singularities should set in the case of rigid anchoring (Fig. 7). And near each of the surfaces one can observe the formation of periodic systems of polarization peculiarities with the period h_0 along the z axis, moreover, such diffraction patterns are displaced from one another by $h_0/2$.

2.8. Free-standing films

As for small thickness a question arises concerning the ferroelectric properties of the film in the C^* phase with free boundaries. For the first time this case was realized in the experiment carried out by Young et al.[13] who studied the properties of the films several smectic layers thick. It is natural that in such a situation there is a plane system of two-dimensional rotators ($\xi_1(\mathbf{r})$, $\xi_2(\mathbf{r})$), and this system is degenerate with the anisotropy of smectic layers being absent. Similar plane systems (superfluid liquid, superconductors, ferromagnetics, etc.) possess peculiar properties. As is known, they may have a phase transition at a certain temperature $\tilde{T}_c$, however, the low-temperature phase has no macroscopic spontaneous moment (ξ_1^0, ξ_2^0), since the components $\xi_\alpha(\mathbf{r})$ diffusively change their values from one point to another in the xy plane. The latter condition corresponds to the logarithmic divergence of the mean square fluctuation of the azimuthal angle $\langle\delta\varphi^2(\mathbf{r})\rangle$, and the equation for it can be easily obtained from (21).

Along with this, below the point $\tilde{T}_c$ there is a value of the critical index Δ_ξ which is different from zero and which describes the gradual decrease of the correlation $\langle\xi_\alpha(\mathbf{r})\xi_\beta(\mathbf{r}')\rangle$ when long distances are concerned

$$\langle\xi_\alpha(\mathbf{r})\xi_\beta(\mathbf{r}')\rangle \sim \langle\cos(\varphi(\mathbf{r}) - \varphi(\mathbf{r}'))\rangle \sim |\mathbf{r} - \mathbf{r}'|^{-2\Delta_\xi}. \tag{44}$$

Downloaded by [Tomsk State University of Control Systems and Radio] at 12:54 19 February 2013

The index $\Delta_\xi = (T/4\pi K l)$, where K is the modulus of elasticity and l is the thickness of the thin film, depends here on temperature and can be estimated for various models.[41] Nelson and Pelcovits[42] showed that renormalized elastic constants of the layer within the long-wave region, together with an account of the fluctuations, equal one effective constant K. Pelcovits and Galperin[43] analysed, in particular, the model of the phase transition in a two-dimensional smectic layer, according to which in the high-temperature phase there appear separate disclinations ("curls"), and in the low-temperature phase disclinations of the opposite sign are twinned. The energy of the individual disclination with the $\pm 2\pi$ strength (without spiral twisting) is $U_d = (T/4\ \Delta_\xi)\ \ln\ (R/l)$, and the entropy of the curl is $S_d = 2\ln\ (R/l)$, where R is the radius of the curl. Thus, the change of the thermodynamic potential due to the separate curl is

$$\delta\Phi_d = U_d - TS_d = T\left(\frac{1}{4\Delta_\xi} - 2\right)\ln\frac{R}{l}$$

and becomes negative at $\Delta_\xi > 1/8$, i.e. $\Delta_\xi(\tilde{T}_c) = 1/8$.

Expression (44) shows that in a plane system like this below the transition point $\tilde{T}_c$ there is no definite correlation radius. Above the transition point the correlations decrease exponentially. The susceptibility of the system $\chi(E)$ at $T < \tilde{T}_c$ becomes infinite at the external field **E** tending to zero as confirmed by the non-linear dependence of the average moment on the external field[44]

$$\langle \xi_\alpha \rangle = \xi_\alpha^0 \sim E_\alpha^{\Delta_\xi/(2-\Delta_\xi)}$$

This type of phase transition may take place in the smectic layer only when the piezoelectric link is absent, for example in the non-chiral C phase. In the chiral C_h^* phase (untwisted) owing to the piezoeffect the plane system is somewhat different in its properties. Primarily the chiral system differs in the following: its orientational fluctuations are to be suppressed as they are accompanied by polarization fluctuations which give rise to strong Coulomb interaction of the polarization charges impeding the development of these fluctuations.[13] If the energy parameter of such Coulomb (dipole-dipole) interaction is $u \sim (\mu_p l)^2$, the macroscopic polarization **P** and the finite average ξ_α^0 may exist owing to the piezoelectric effect in a thin film. Obviously, these values are small since u is small. This case reminds one of the effect of weak anisotropy in a plane ferromagnetic.[44] Since the main

Downloaded by [Tomsk State University of Control Systems and Radio] at 12:54 19 February 2013

interaction v, responsible for the transition A–C, is much greater than the interaction u, the following estimates can be made[14]

$$\xi_\alpha^0 \sim \left(\frac{u}{v}\right)^{\Delta_\xi/(1-2\Delta_\xi)}, \quad P_\alpha \sim \mu_p \xi_\alpha^0, \quad r_c \sim \left(\frac{u}{v}\right)^{-1(1-2\Delta_\xi)}, \qquad \chi \sim \left(\frac{u}{v}\right)^{-(2-2\Delta_\xi)/(1-2\Delta_\xi)} \tag{45}$$

At $u \to 0$ the averages ξ_α^0 and P_α turn to zero and the correlation radius r_c and the susceptibility χ become infinite.

With the increase of the number of monolayers in a film N the transition temperature $\tilde{T}_c$ acquires its "volume" value T_c, and relations (45) are substituted for the temperature dependencies discussed above. So far there is no detailed experimental investigation of the critical behaviour of plane ferroelectrics. The data obtained till now[13] point to high susceptibility of thin films of the C_h^* phase below the transition point $\tilde{T}_c$. The difference between $\tilde{T}_c$ and T_c goes up to the value of the temperature region within which the C^* phase exists, which indicates a significant interaction of the monolayers.

Heinekamp *et al.*[45] proved theoretically and experimentally that the temperatures $\tilde{T}_c(N)$ and T_c may not coincide when the thickness is large, in case on the surface of the film, i.e. in the boundary monolayers, there is an order parameter ξ_α^0 different from zero (at $\tilde{T}_c(2) > T_c$). To prove this the authors used a model of the monolayer system in which every layer has its own order parameter θ_i, and took into account the interaction of the nearest monolayers $\theta_i\theta_{i+1}$ in developing the free energy as a series in powers of θ_i, including the sixth one. According to the experiment, in the free-standing bi-layered film of DOBAMBC the transition temperature $\tilde{T}_c(2)$ is considerably higher than the transition temperature T_c in a sample of large thickness, which indicates a significant effect of the free boundary conditions. The increase of the number of layers N is accompanied by the decrease of the ferroelectric transition temperature. Near the transition point in a bi-layered film within the interval 0,5 K the average angle of the director tilt (the parameter of the transition ξ_α^0) turns to zero in a jump-like manner, which is altogether different from the temperature dependence predicted by the mean field theory. Such a behaviour may be due to the anisotropic dipole–dipole interaction (see (45)).

Downloaded by [Tomsk State University of Control Systems and Radio] at 12:54 19 February 2013

III. DIPOLAR ORDERING IN FERROELECTRIC LIQUID CRYSTALS

3.1. Technique for the measurement of the spontaneous polarization

There are some classical methods for the measurements of the P_s value in solid ferroelectrics (capacitive,[6,56,57] pyroelectric[7,8,58] etc.) which may be useful for the investigation of liquid crystalline ferroelectrics as well. In addition, one can use several techniques specific to liquid crystals. For example, it is possible to measure an a.c. piezoelectric voltage induced by a shear flow of the liquid crystal.[4,59] The spontaneous polarization can also be calculated from the analysis of experimental data on light scattering by freely suspended smectic C* films with a thickness of several molecular layers.[60]

The well known technique for measuring P_s uses the observation of transient currents i. For the square-wave form of the applied voltage U the current $i = i_R + i_C + i_P$ includes the conductive term $i_R = U/R$, the capacitive term $i_C = CdU/dt$ and the term $i_P = dP_s/dt$ which is due to the polarization switching (C and R are the capacity and resistance of a liquid crystal layer).

Here, the principal problem is the extraction of the i_P term from the total current. For example, currents i_C and i_R may be compensated for by a Souyer-Tower circuit[61,62] with a sine-form voltage. The corresponding dependencies of i_P and the spontaneous polarization (in the form of a hysteresis loop) on an external voltage are shown in Fig. 10.[63] The term i_P may also be separated using the voltage pulses of a special form[64] and subsequent processing oscillograms. In particular, the capacitive term i_C depends on time exponentially[65] or linearly[66] for the square-wave and triangular pulses, respectively, Fig. 11.

The compensation for the conductive term i_R is especially difficult

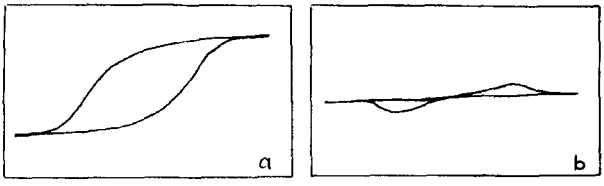

FIGURE 10 Typical hysteresis loops for polarization (a) and switching current (b) for a ferroelectric liquid crystal; frequency = 40 Hz (from Ref. 63).

Downloaded by [Tomsk State University of Control Systems and Radio] at 12:54 19 February 2013

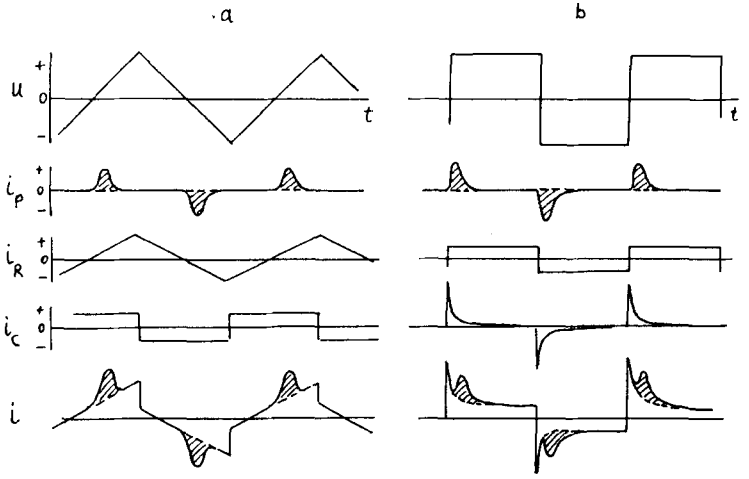

FIGURE 11 Current oscillograms in an a.c. field of the triangular form (a) and the rectangular form (b). Currents: switching (i_p), ohmic (i_R) and capacitive (i_C). The hatched area of the pulses reduced to unit surface of the cell is equal to $2P_s$.

as it depends upon the amplitude and the duration of the pulses, temperature, etc.[64]

When the transient current technique is used the voltage is chosen high enough to unwind completely the helical structure of a ferroelectric liquid crystal. Thus, the measured value of P_s does not include the flexo-electric contribution which just results from a non-uniform structure. The other limitation of the technique discussed is the problem with too low frequencies which are necessary for switching the polarization in relatively viscous substances. The frequency of the external voltage must be lower than the inverse of the relaxation time for the director depending on sample thickness, anchoring energy, defects, etc. For example, to study the polarization of low temperature phases (others than the smectic C* one) one has to use frequencies up to tenths of herz[67] even for fields as high as tens of $kVcm^{-1}$.[68]

The high strength of the electric field enhances the polarization to be measured by a value P_E due to the electroclinic effect.[9] The latter value is usually not taken into account. However, its contribution becomes appreciable near the C*–A* phase transition where the dielectric susceptibility increases critically. Therefore, the critical index β for the temperature dependence of the measured polarization

$$P_s \sim (T_c - T)^{\beta}$$

Downloaded by [Tomsk State University of Control Systems and Radio] at 12:54 19 February 2013

becomes markedly decreased. For example, the values of $\beta \approx 0.4$ or even less,[6,57,69,70] obtained from the transient current technique, can be accounted for by the field-induced term without any references to the fluctuating nature of the phase transition[17] (note, $\beta = 0.5$ for the mean-field model).

Now, let us discuss the pyro-electric method. The first observations of the pyroelectric effect in ferroelectric liquid crystals were made using permanent heating of a sample at a given rate.[7] This technique is rather qualitative and allows only rough estimates of the pyro-electric coefficient to be made at several temperature points (DOBAMBC).

More precise measurements of the magnitude and the temperature behaviour of the spontaneous polarization can be made using a pulsed pyroelectric technique. In such studies[8,58] a liquid crystal layer was heated by light pulses of a Nd-glass laser ($\lambda = 1.06\ \mu$) operating either in the free running or the Q-switching regime. In the first case, the pulse duration (100 μS) is longer than the relaxation time τ_θ for the tilt of the director θ (soft mode) and such a regime may be considered as a steady-state regime. In the second case, the giant pulse with duration ~10 nS allows the relaxation time τ_θ to be measured directly from the exponential decay of the pulsed pyro-electric signal.[71] For the high rate of heating by laser pulses rather small values of the pyroelectric coefficient, $\gamma \leq 10^{-12}\ \mathrm{C \cdot cm^{-2} \cdot K^{-1}}$ may be measured with high temperature resolution (the total laser heating of a sample is of the order of 0.02–0.05 K). The method is especially sensitive in the vicinity of the C*–A* transition where the pyro-coefficient $\gamma = dP_s/dT$ passes through a maximum. The value of the spontaneous polarization $P_s(T)$ is calculated by integration of $\gamma(T)$ over temperature

$$P_s(T) = \int_{T_{CA}}^{T} \gamma\,(T)dT$$

Generally, the pyro-electric coefficient is measured in the field-on condition in order to deal with the uniform untwisted structure of a ferroelectric liquid crystal. Therefore, it consists of two terms, the equilibrium $\gamma_0(T)$ and the field-induced, or electro-clinic $\gamma_e(T)$ ones:

$$\gamma(T,E) = \gamma_0(T) + \gamma_e(T) = \gamma_0 + \frac{\partial\gamma}{\partial E} E \tag{46}$$

Downloaded by [Tomsk State University of Control Systems and Radio] at 12:54 19 February 2013

The equilibrium part $\gamma_0(T)$ and the corresponding equilibrium value of $P_s(T)$ may be calculated from the extrapolation of the series of curves $\gamma(T,E)$ to zero field, Fig. 12. The critical index for P_s ought to be determined only after such an extrapolation and its corrected value usually corresponds to the mean-field model.[72]

Of particular interest is an isobestic point in the set of curves in Fig. 12. It is the point which defines the phase transition temperature $T_{C^*A^*}$. This fact could be understood from the following consideration. The dielectric susceptibility χ_θ for the tilt of the director (soft mode) is maximum at $T_{C^*A^*}$. At the same time there is a thermodynamic equality.[72]

$$\frac{\partial\chi}{\partial T} \equiv \frac{\partial}{\partial T}\left(\frac{\partial P}{\partial E}\right) \equiv \frac{\partial}{\partial E}\left(\frac{\partial P}{\partial T}\right) \equiv \frac{\partial\gamma}{\partial E} \tag{47}$$

which results in $\partial\chi/\partial T = \partial\gamma/\partial E = 0$ at $T_{C^*A^*}$. The appearance of the isobestic point ($\partial\gamma/\partial E = 0$) allows the phase transition point and critical index β for P_s to be found with high accuracy.

Moreover, the susceptibility χ_θ may be calculated by integration of $\partial\chi_\theta/\partial T$ over temperature, Fig. 13, and this value may be used for subsequent calculations of the elastic modulus

$$K_\theta = \frac{\alpha^2}{\chi_\theta} = \frac{P_s^2}{\theta^2\chi_\theta} \tag{48}$$

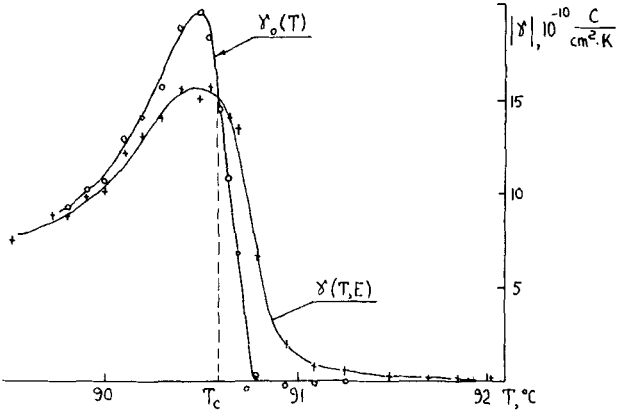

FIGURE 12 Temperature behaviour of the pyroelectric coefficient γ (T, E) in the electric field E = 1.5 10^4 V·cm^{-1} (+) and the zero-field pyro-coefficient (0) for DOBAMBC.

Downloaded by [Tomsk State University of Control Systems and Radio] at 12:54 19 February 2013

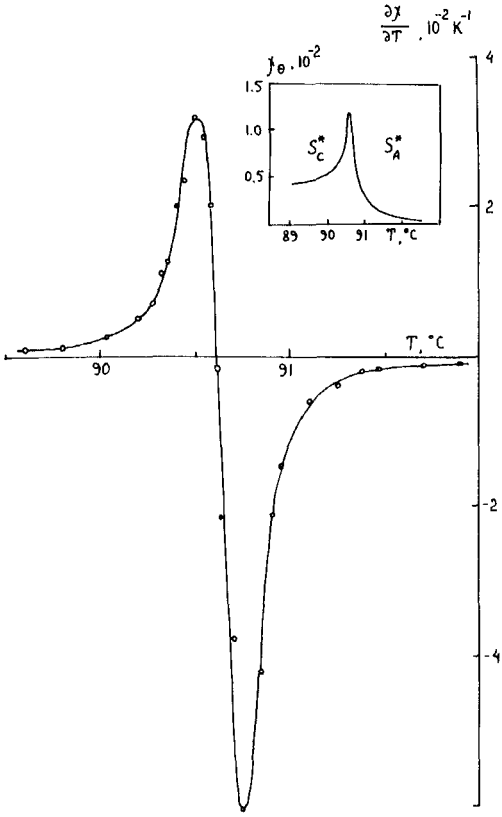

FIGURE 13 Temperature behaviour of the dielectric susceptibility χ_θ and its temperature derivative $\partial\chi_\theta/\partial T$ obtained by a pyroelectric technique for DOBAMBC at $E >> E_c$.

and the twist-viscosity coefficient

$$\gamma_1^\theta = \tau_\theta K_\theta \tag{49}$$

for the tilt of the director (for details see Ref. 72).

3.2. Experimental studies of the dielectric properties

The response of liquid crystalline ferroelectrics to an external electric field is more complicated than that of the conventional solid ferroelectrics since it involves not only collective intermolecular modes but also the molecular and intramolecular modes as well. As com-

Downloaded by [Tomsk State University of Control Systems and Radio] at 12:54 19 February 2013

pared with non-ferroelectric liquid crystals, where the dielectric properties are due mainly to the quadratic interaction of the electric field with the anisotropy of the dielectric permittivity ($\epsilon_a E^2$), in ferroelectric liquid crystals the additional linear term $P_s E$ appears for the interaction of the field with the spontaneous polarization. The latter dominates at weak fields and low frequencies (e.g. for $P_s = 10^{-4} C \cdot m^{-2}$ and $\epsilon_a = 10$, $P_s E > \epsilon_a E^2$ at field strength $0 < E < 10^5$ V · m^{-1}). For example, the linear term manifests itself in a strong (up to several times) increase of the dielectric permittivity at low frequencies ($f \leqq 10^3$Hz).

In this part we review the dielectric behaviour of ferroelectric liquid crystals over a wide frequency range and discuss the various mechanisms of their field response. The discussion will be illustrated mainly by experimental data obtained for the "classical" liquid crystalline ferroelectric *D* (or *L*)-2-methylbutyl ester of the 4-cetyloxybenzylidene-4′-aminocinnamic acid (DOBAMBC).

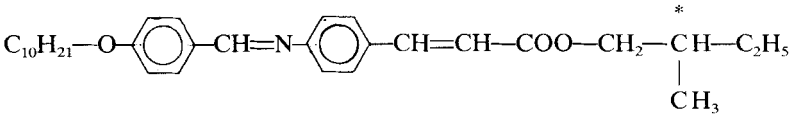

The frequency dependence of the real part of the dielectric permittivity $\epsilon'(f)$ of DOBAMBC is shown in Fig. 14. The curve is a

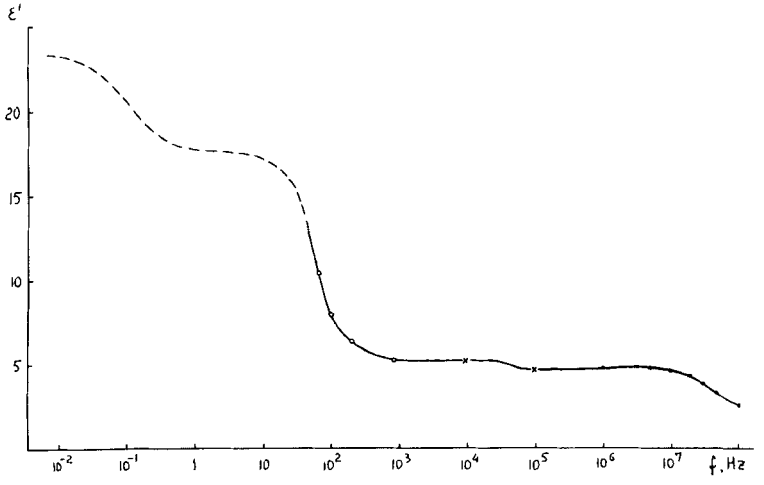

FIGURE 14 The generalized frequency dependence of the dielectric permittivity ε' for the helical structure of the ferroelectric smectic C* phase of DOBAMBC.

Downloaded by [Tomsk State University of Control Systems and Radio] at 12:54 19 February 2013

combination of various experimental results obtained under weak field conditions $E << E_c$, where E_c is a critical field for unwinding the helical structure of the smectic C^* phase. The several frequency domains of the $\epsilon'(f)$ dispersion seen in Fig. 14 will be discussed separately.

3.2.1. Ultra-high frequencies For frequencies $f > 10^8$ Hz all intermolecular motions are frozen and the value of ϵ includes only the electronic contribution and some intramolecular modes. The value $\epsilon \approx 2.5$ is found for $f > 100$ MHz.[73]

3.2.2. High frequencies In the range $f \approx 1$–50 MHz the main contribution to the ϵ-value results from the rotation of molecules around their long axes. For weak fields $E << E_c$ when the helical structure exists the average perpendicular dielectric permittivity $\langle\epsilon_\perp\rangle$ is nearly equal to the component $\epsilon_\perp$ for the smectic A phase.[74,75] At the strong field limit $E > E_c$, when the helix is unwound, the component $\epsilon_\perp$ becomes anisotropic in the plane perpendicular to the director. Of two new perpendicular components ϵ_3 and ϵ_2, Fig. 15, the former, which is perpendicular to the symmetry plane, is higher than that which lies in this plane, i.e. $\epsilon_3 > \epsilon_2$ and $\epsilon_3 > \langle\epsilon_\perp\rangle$. In the achiral smectic C phase such an anisotropy[75] results from the hinderance of the molecular rotation around the long axes which is described by the order parameter $\langle\cos 2\psi\rangle$ where ψ is an azimuthal angle of a transverse molecular axis. The chirality eliminates the two-fold

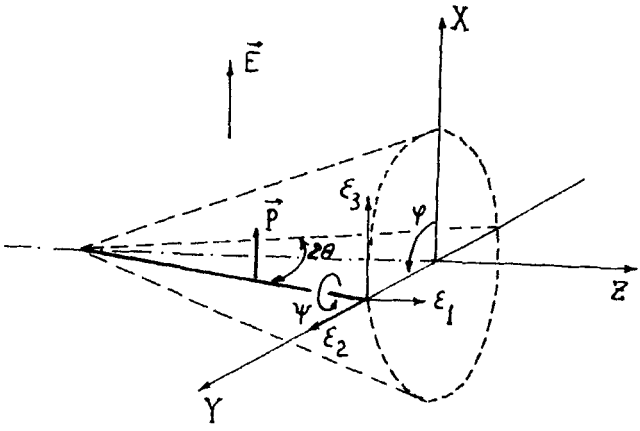

FIGURE 15 A molecule in the smectic C phase in the planar orientation. zy—electrode plane, xy—smectic layer plane, θ—molecular tilt angle with respect to the normal z, φ—azimuthal angle, ϵ_i (i = 1.2.3) components of the dielectric tensor.

Downloaded by [Tomsk State University of Control Systems and Radio] at 12:54 19 February 2013

degeneracy and results in the appearance of polar ordering described by the order parameter $\langle \cos \psi \rangle$.[76] According to[77] the difference $\epsilon_3 - \langle \epsilon_\perp \rangle$ increases linearly with increasing tilt of the long molecular axes θ, Fig. 16, and this difference remains positive within the frequency range 1–50 MHz.[73]

Of special interest is the temperature behaviour of the value $\epsilon_3 - \langle \epsilon_\perp \rangle$ for ferroelectric mixtures composed of achiral smectic C matrices and chiral additives with large dipole moments in chiral moieties. In such systems, in contrast to[77] one may anticipate a strong nonlinear dependence of $\epsilon_3 - \langle \epsilon_\perp \rangle$ on the tilt angle due to the dipole-induced dipole interactions. Such interactions appear to be responsible for the additional contribution to the spontaneous polarization of these mixtures[23] which is cubic in θ and very fast (relaxation times are less than 10^{-8}S).

3.2.3. Middle frequencies. Tilt angle dynamics, soft mode, electroclinic effect. The frequency range 10^3–10^5 Hz is especially remarkable because of the contribution of the molecular tilts and their rotation around short axes to the longitudinal component of the dielectric permittivity. (e.g., for DOBAMBC $\epsilon_\parallel \approx 6$–$7$ at $f = 20$ Hz[78]). The corresponding relaxation times lie in the microsecond range.[58]

It is this molecular mode, i.e., the tilt of the long molecular axes or, in other words, their turn over the short axes, results in the phase transition from the smectic A to the smectic C phase. Such a lowering of symmetry is assisted by the hinderance of molecular rotation around

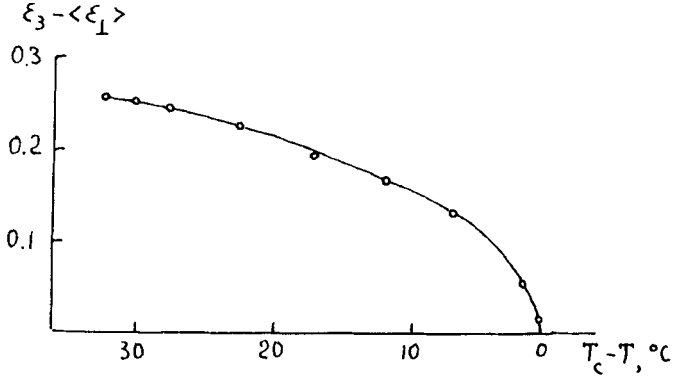

FIGURE 16 Temperature dependence of the difference between the field-on, $E = 2 \div 5$ kV · cm$^{-1} > E_c$ (ϵ_3) and the field-off ($\langle \epsilon_\perp \rangle$) values of the dielectric permittivity (DOBAMBC, $f = 1.5$ MHz, the amplitude of the measuring field 17 V · cm^{-1}, the experimental geometry is shown in Fig. 15).

Downloaded by [Tomsk State University of Control Systems and Radio] at 12:54 19 February 2013

the long axes and the appearance of the non-zero value of the average perpendicular dipole moment, that is, the spontaneous polarization.

The dynamics of the tilt angle and the spontaneous polarization, in the simplest case of the absence of the helical structure, obey the Landau-Khalatnikov equations[27]:

$$\frac{\partial\theta}{\partial t} = -\Gamma_1 \frac{\partial F}{\partial\theta}; \qquad \frac{\partial P}{\partial t} = -\Gamma_2 \frac{\partial F}{\partial P} \tag{50}$$

Here, the decay constant $\Gamma_1 = 1/\gamma_1$, where γ_1 is the twist viscosity coefficient, and the free energy is expanded in the series:

$$F = F_A + a(T)\theta^2 + b\theta^4 + \frac{1}{2\chi_\perp} P^2 - \mu_p \cdot \theta \cdot P \tag{51}$$

One of the solutions of (50) corresponds to the in-phase fluctuations of θ and P. It is the soft mode which is responsible for the appearance of the ferroelectric order at $T = T_c$. For $\Gamma_2 >> \Gamma_1$, near the phase transitions one gets

$$\tau_A = \frac{\gamma_1}{2a'(T - T_c)} \tag{52}$$

for the smectic A phase, and

$$\tau_c = \frac{\gamma_1}{4a'(T_c - T)} \tag{53}$$

for the smectic C* (or C) phase.

For the helical structure equations (52, 53) are true in the vicinity of T_c excluding an extremely narrow interval, ΔT, where the correlation length of the tilt angle fluctuations is comparable with the pitch of the helix $h_0 = 2\pi/q_0$ at the transition point.[79] At the very point T_c in contrast with (52, 53) the soft mode has a finite relaxation time $\tau_A = \tau_{C^*} = \tau_0 = \gamma_1/Kq_0^2$.

In experiments the dynamics of the tilt angle near the C* – A phase transition in DOBAMBC was investigated by two different techniques, namely, using either the pyroelectric or the electroclinic effect. In the first case, one measures the angle θ indirectly by observing the relaxation of the electric polarization (or its temperature derivative, that is the pyroelectric coefficient $\gamma = dP/dT$) caused by

Downloaded by [Tomsk State University of Control Systems and Radio] at 12:54 19 February 2013

a heat pulse. This technique was applied to the smectic C* phase and allowed the relaxation time τ_c to be found[71] (see left part of Fig. 17 for $T < T_c$ and compare with eq. (53)).

The other technique uses the field-induced change of the tilt angle $\theta(E)$ of the director in the smectic A phase.[9,80] The electric field E has to be directed along the smectic planes, say, in the y-direction (z – is the normal to layers). If molecules have the transverse dipole moments, $d_\perp$, the field will orient them in the y-direction proportionally to the factor $\exp(d_\perp E/k_B T)$ where k_B is the Boltzman constant. For achiral molecules the yz-plane would remain a mirror plane even in the field-on condition. However, for chiral molecules the mirror symmetry is lost and the $+x$ and $-x$ directions become non-equivalent. As a result the director is tilted in the xz-plane (see insert in Fig. 18). This electroclinic effect is an inverse of the change in the polarization due to the molecular tilt. From the temperature dependencies of $\theta(E)$ of DOBAMBC shown in Fig. 18 for different frequencies[9,80] one can calculate the temperature behaviour of the relaxation time τ_A (T) for the smectic A phase (the right curve in Fig. 17).

Thus, the critical increase in the relaxation time τ_θ for the molecular tilt has been observed for both sides of the C* – A phase transition. However, the accuracy of the measurements[9,71,80] is not sufficient for the calculations of the corresponding critical exponent. The estimates show that the critical exponent ω in the dependence $\tau_\theta \sim |T_c - T|^\omega$ is close to 1 predicted by the mean-field theory when $|T_c - T|$ exceeds

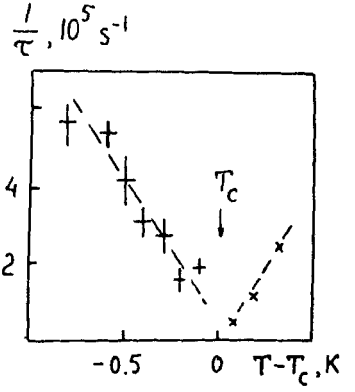

FIGURE 17 Soft modes in the smectic C* and smectic A phases of DOBAMBC. Left part ($T < T_c$) is obtained from the dynamics of the pyroelectric response (Ref. 71); right part ($T > T_c$)—from data on the electroclinic effect (Ref. 9).

Downloaded by [Tomsk State University of Control Systems and Radio] at 12:54 19 February 2013

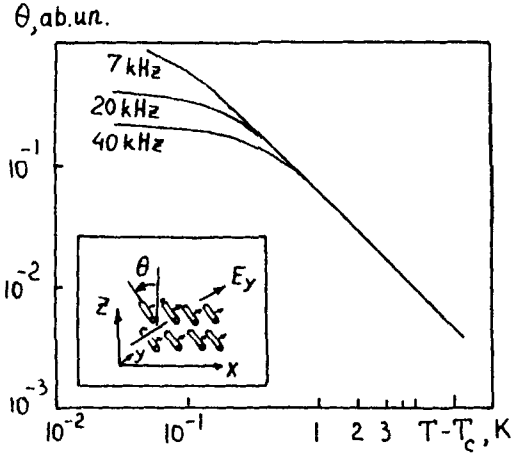

FIGURE 18 Field-induced tilt of the director in the smectic A phase as function of the temperature for various frequencies (from Ref. 9). Inset: geometry of the experiment.

the value of the order of 0.1 K characteristic of the non-ferroelectric C-A transition.[81] In the close vicinity of T_c the exponent may be enhanced up to the value $\omega \approx 1.3$ typical of the helium analogy.[81]

The same exponents ($\omega = 1$ for the mean-field model and $\omega = 1.3$ for the helium analogy) are predicted for the temperature behaviour of the susceptibility χ_θ near the second order $C^* \leftrightarrow A$ phase transition. In the smectic A phase an estimation of ω was made from the curves $\theta(T)$, Fig. 18 for the electroclinic effect. The value $\omega = 1.1$ obtained in[9,80] agree neither with the mean-field nor with the helium (scaling) model. In our opinion, the reason for the discrepancy lies in the optical technique for measuring the electric response. The electric susceptibility is due to the dipolar parts of the molecules which are located near their flexible chiral tails (in the case of DOBAMBC, e.g.) while the optical response is due mainly to the easily polarizable rigid skeletons of the molecules.[82] There is no rigid and temperature independent coupling between the two moieties and the value of the critical exponent has to be corrected to take this temperature dependence into account.

The pyroelectric technique[72] based on the measurements of the field derivative of the pyro-coefficient $\partial\gamma/\partial E$ according to the equality (47) is free of the shortage mentioned above. In this case the dielectric susceptibility is measured in an electric way. In addition, the technique is of a differential type that is, one measures not χ_θ but the

Downloaded by [Tomsk State University of Control Systems and Radio] at 12:54 19 February 2013

derivative $\partial\chi_\theta/\partial T$ which is insensitive to other background components of the permittivity.

The temperature dependence of the derivative $\partial\chi_\theta/\partial T$ for the unwound helical structure ($E >> E_c$) of DOBAMBC is shown in Fig. 13. In the range $0.15 < T_c - T < 1.5$ K the dependence obeys the equation $|\partial\chi/\partial T| = \sigma|T_c - T|^{-\delta}$ where $\delta = 2.0 \pm 0.1$ both in the A and C* phases and the coefficient σ for the A-phase is two times more than that for the C*-phase. Such a behaviour corresponds to the Currie-Weiss law for the susceptibility χ_θ and, therefore, the Landau expansion (51) is true. From (51), it follows (for $E >> E_c$):

$$\chi^{-1} = \begin{cases} \alpha^2[a'(T - T_c)], & T > T_c \\ \alpha^2[2a'(T_c - T)], & T < T_c \end{cases} \tag{54}$$

These equations allow the elastic modulus for the tilt of the director a' to be calculated when the coefficient α coupling the tilt angle and the spontaneous polarization, $P_s = \alpha\theta$, is known from independent experiments. For DOBAMBC the value of $a' \simeq 5 \cdot 10^4 J \cdot m^{-3}K^{-1}$ obtained in Ref. 72 agrees with the independent data of Refs. 83, 84. The insert of Fig. 13 illustrates the temperature dependence of susceptibility χ_θ obtained by integrating the curve $\partial\chi_\theta/\partial T$.

Thus, the soft mode susceptibility has the Curie–Weiss behaviours in the vicinity of the second order A – C* phase transition. However, in contrast with solid ferroelectrics, the anomaly in the susceptibility at T_c is small ($\chi_\theta \approx 10^{-2}$) even against rather small background value of $\chi \approx 0.3$[78] in both the smectic A and C* phases. This is the consequence of the improper nature of ferroelectricity in liquid crystals. Because of this smallness the anomaly predicted theoretically[27,35,85] is hardly detected by other traditional (capacitance) methods.[78,86,87]

3.2.4. Low frequencies. The Goldstone mode. Switching the polarization. There are a lot of papers which contain rather contradictory information on the temperature behaviour of the low-frequency dielectric permittivity of ferroelectric liquid crystals.[11,25,26,38,56,57,78,87–90,92,93] Recently, however, an important thing became clear. As a matter of fact, most of the investigators did not pay sufficient attention to distinguishing polar cases of strong and weak fields. As a result, the effects of the distortion of a helix as well as fluctuation effects in uniform samples with compensated helical structure or stabilized by solid surfaces are usually masked by other effects caused by a field-induced change in the direction of spontaneous polarization coupled with the director.

Downloaded by [Tomsk State University of Control Systems and Radio] at 12:54 19 February 2013

Downloaded by [Tomsk State University of Control Systems and Radio] at 12:54 19 February 2013

Let us try to clarify the question. The theory of §2.5 for the case of low frequencies and weak electric field, $E << E_c$ predicts the dielectric response including the polar (angle θ) and azimuthal (angle φ) distortions, see formulae (34–36). The criterion of weak field means that the field does not change the equilibrium character of the initial orientation of the director but only adds infinitesimal values $\delta\theta$ and $\delta\varphi$ to angles θ and φ. In fact, the field must be smaller not only than the critical field E_c of unwinding the helix but also smaller than any other field which is capable to distort the director. For instance, it may be a field resulting in a motion of defects or switching the vector P_s of spontaneous polarization. The latter effect is of paramount importance as switching polarization needs extremely low voltages (sometimes it is an effect analogous to the Fredericks transition with a threshold field E_f but, in the case of a inhomogeneous initial orientation the effect has no threshold and the condition of a weak field cannot be satisfied in principle). At present, we do not know of any reliable experiment where the Goldstone mode in the helical smectic C* structure would be observed. What we mean by the Goldstone mode is as follows. In the achiral smectic C phase this mode is referred to the motion of the director along the conical surface around the normal to the smectic layers, the angle θ being constant. This mode restores a symmetry of the smectic A phase. In the chiral smectic C* phase the same mode is also accompanied by a process of twisting and untwisting the helix. In particular, the process of the restoring of the helix distorted by an external field is described by this relaxational mode. Thus, we speak of the same restoring mode in two senses.

The theory (§2.5) of the dielectric susceptibility corresponding to the Goldstone mode in the uniform case ($q = 0$) predicts qualitatively the curve $\chi_c(T)$ without any anomaly in the vicinity of the phase transition T_{C^*A}, Fig. 19. The value of χ_c is finite at the transition temperature and the exact temperature behaviour in the C* phase depends on parameters μ_f, μ_p, h, etc. This curve, in principle, can be obtained experimentally only for the ideal structure (without defects) weakly distored by the external field.

Now, let us consider the uniform structure of the chiral smectic C* untwisted, say, by solid boundaries or by a compensation of right and left components, but not by an external field. The external field is again small, $E << E_{th}$, where E_{th} corresponds to any process of reorientation of the director. In this case, one should observe the susceptibility curve corresponding to the soft mode, curve χ_s in Fig. 19. In a thermodynamic limit, $E = 0$, this curve diverges at the

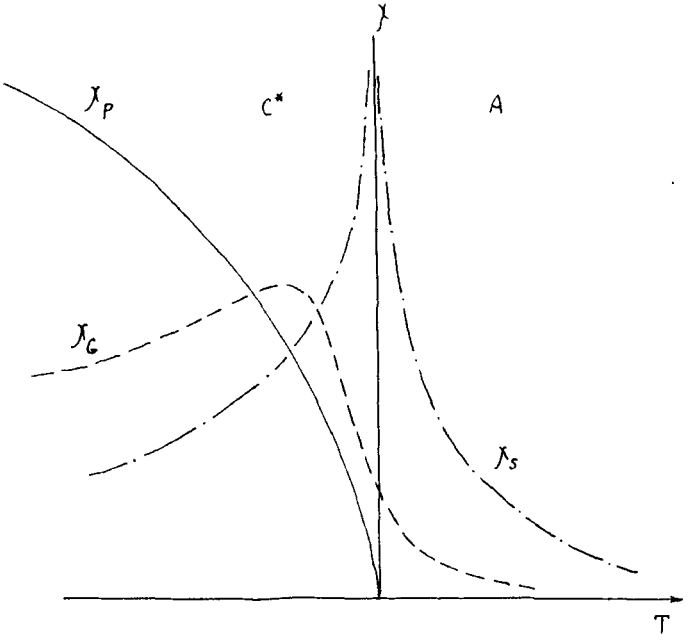

FIGURE 19 Qualitative temperature behaviour of the low frequency dielectric susceptibility for the chiral (χ_G) and the uniform (χ_s) structures in the weak field limit and the apparent susceptibility (χ_P) in the strong field spontaneous switching polarization.

transition point. This curve is to be compared with the experimental curve $\chi_s(T)$, obtained under conditions of a rather high d.c. field, $E >> E_c$, Fig. 19.

If the same uniform structure is placed in a a.c. field which is high enough to switch the direction of spontaneous polarization, strong displacement currents caused by this switching are observed. These currents make a contribution to the observed (apparent) value of the dielectric susceptibility. This component is proportional to the value of the spontaneous polarization in the C* phase and vanishes at the phase transition point T_{C^*A}, curve χ_p in Fig. 19.

Thus, we come to conclusion that new dielectric measurements with precisely fixed experimental conditions are necessary. Recently we managed to measure separately the temperature curve $\chi_p(T)$ using the field dependence of the pyro-electric coefficient, Fig. 19.[93] The curve $\chi_p(T)$ is similar to the curve $P_s(T)$. Such experiments correspond to characteristic times of switching of the order of minutes, that is to frequencies 10^{-3}–10^{-4} Hz (near to the limit $\omega \rightarrow 0$).

Downloaded by [Tomsk State University of Control Systems and Radio] at 12:54 19 February 2013

The calculated values of the dielectric permittivity, $\epsilon = 1 + 4\pi\chi_p$, for DOBAMBC according to[93] are considerably higher than those obtained at frequencies of the order of tens of herz.[11,26,56,57,78,87,90,92] We think that such frequencies are not small enough to provide a steady-state regime for the measurement of ϵ in inhomogeneous samples. In this case, the dynamics of spontaneous polarization is limited by the motion of defects and the frequency dispersion of permittivity is expected at frequencies below 10 Hz, (Fig. 14, dashed line).

The hysteresis loops in the field dependences of dielectric permittivity, Fig. 20 can also be accounted for by the creation and annihilation of defects.[26,92]

3.3 Chemical classes of ferroelectric liquid crystals

According to the simple symmetry considerations of R. Meyer[1] and strict theoretical group analysis[94] the appearance of spontaneous polarization is possible in any system having a lamellar structure and consisting of tilted chiral and dipolar rod-like elements.

Fig. 21 demonstrates a model for dipolar ordering in the chiral

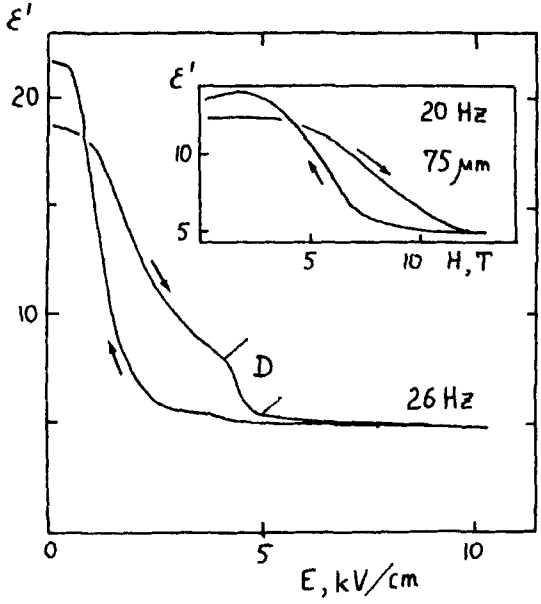

FIGURE 20 Hysteresis curves for the low frequency dielectric permittivity ε′ of DOBAMBC in electric and magnetic (insert) fields. D is the region where disclinations disappear with increasing E.

Downloaded by [Tomsk State University of Control Systems and Radio] at 12:54 19 February 2013

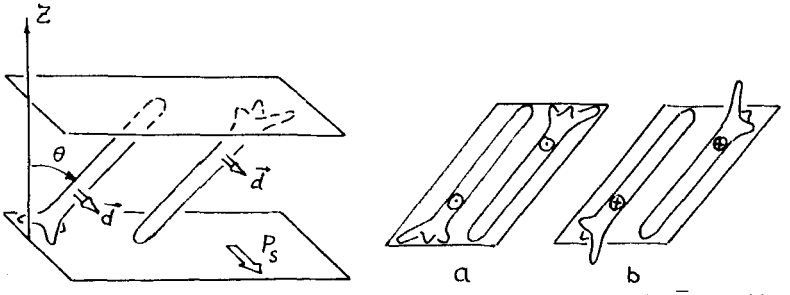

FIGURE 21 A model for the ordering of transverse molecular dipoles $\bar{d}$ in a chiral tilted smectic. Position (a) is more preferable for the molecules than (b).

smectic C* phase. This model is rather similar to that with "ferroelectric fishes" mentioned in the de Gennes book.[17] The chirality results from a tripod at the molecular end, the three legs of which have different length and form a single (e.g. right) triple of vectors. In such a model transverse dipolar moments are not compensated for since the monoclinic surrounding makes the molecular position (a) more preferrable than (b). Thus, there appears an asymmetry in the hindered rotations of the molecules around their long axes and, as a result, a non-zero average dipolar moment perpendicular to the plane of the molecular tilt.

At the present time, the majority of syntesized ferroelectric liquid crystals consist of molecules which meet simultaneously all the requirements necessary and sufficient for the appearance of spontaneous polarization. The conventional way to construct a liquid crystalline ferroelectric is as follows: one looks at an achiral tilted smectic phase, e.g. smectic C, and tries to syntesize a chiral analog of the compound. In many cases the chirality is due to the asymmetric carbon atom in the optically active residue of isopentyl alcohol

$$R^* = -CH_2-\underset{\underset{CH_3}{|}}{\overset{\overset{H}{|}}{C^*}}-C_2H_5$$

The temperature range of the chiral smectic C* phase (asterisk means chirality) does not markedly differ from that of the C-phase of the achiral analog. It may be seen from the comparison of the homologous series of 4-alkoxybenzylidene-4′-amino-pentylcinnamate

Downloaded by [Tomsk State University of Control Systems and Radio] at 12:54 19 February 2013

(I) and its optically active isomers (I*)

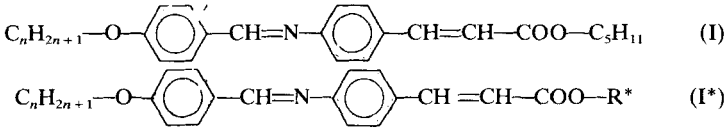

A classical compound DOBAMBC also belongs to the second series (n = 10).

There have been syntesized this way tens of single-component ferroelectric liquid crystals from various chemical classes. Table I summarizes the corresponding data on molecular structure, temperature ranges of the C*-phase and the spontaneous polarization. The additional data may be found in.[95]

All the compounds whose chirality is due to the isopentyl moiety R* have a P_s value not exceeding 10^{-8}C · cm^{-2}. There are two reasons for this effect.

First, the hinderance of the rotation of the molecules around their long axes is rather weak, presumably for some steric reasons. This fact is confirmed by direct measurements[114] of the order parameter for short molecular axes ⟨cos ψ⟩, where ψ is an azimuthal angle of the molecular rotation around the long axes, Fig. 23.

Second, there is rather free internal rotation of the dipolar group with respect to the chiral fragment. Indeed, the further the dipolar moment is removed from the chiral fragment the less is the P_s value, see Table II.

As it is easily seen, the dipolar group —COO— in substance No 1 from Table II is weakly coupled with the assymetric carbon atom due to the almost free relative rotation of the benzene rings in the biphenyl moiety. In this case the spontaneous polarization is negli-

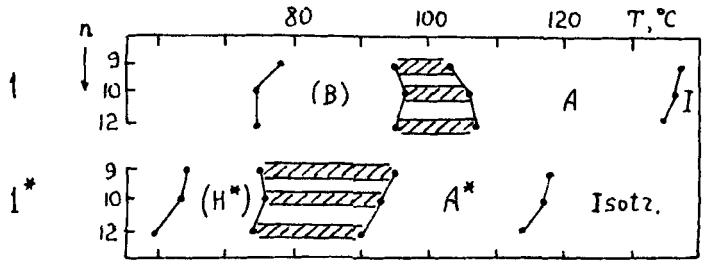

FIGURE 22 Temperature ranges of existence of liquid crystalline phases for chiral compounds (1*) and their achiral counterparts (1) with homolog number n. The symbols Is, A, B, H mean the isotropic and different smectic phases (the parenthezis show monotropic ones). The ranges of the smectic C and C* phases are hatched.

Downloaded by [Tomsk State University of Control Systems and Radio] at 12:54 19 February 2013

Downloaded by [Tomsk State University of Control Systems and Radio] at 12:54 19 February 2013

TABLE I

Single-component ferroelectric liquid crystals.

No.	Structural formula	n	Range of C* phase, grad.†	P_s, 10^{-9} C·cm^{-2}	Ref.
1	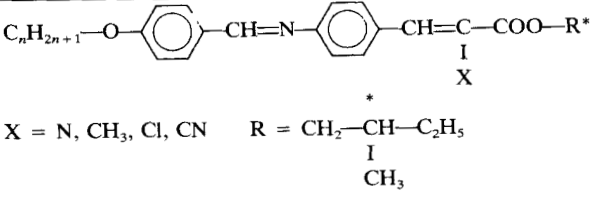	5 ÷ 14	40–95	0.2 ÷ 10	6, 56, 95–98, 100
2	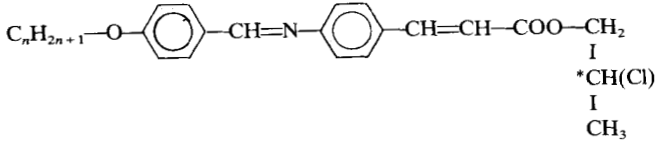	5 ÷ 10	66–87	10–15	59, 97, 101, 102
3	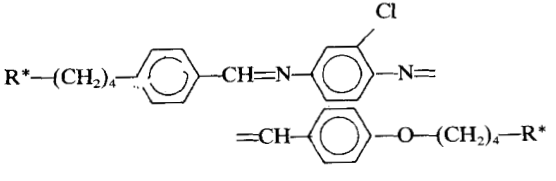		(20) 35–93		103

Downloaded by [Tomsk State University of Control Systems and Radio] at 12:54 19 February 2013

TABLE I (*continued*)

No.	Structural formula	n	Range of C* phase, grad.†	P_s, 10^{-9} C·cm^{-2}	Ref.
4	C_nH_{2n+1}—O—⟨○⟩—CH=CH—COO—⟨○⟩—O—R*	7	(84)		
		8	87–79		
		9	80–93		
		10	(63) 81–94		104
		11	(62) 80–94		
		12	(63) 79–95		
		13	(65) 76–94		
		14	(66) 74–94		
5	C_nH_{2n+1}—O—⟨○⟩—CH=CH—COO—⟨○⟩—COO—R*	7	(46–63)		
		8	(30–68)		
		9	(19–67)		104
		10	(17) 60–71		
		11	(30) 56–73		
		12	(9) 54–72		
6	C_nH_{2n+1}—O—⟨○⟩—CH=N—⟨○⟩—CH=CH—COO—CH*(C$_2$H$_5$)—CH$_3$	6	(80–98)		106
		6	(88)		107
		8	(85)		107
		10	(61) 82–90	18	105, 106
		10	68–83		107
		14	(58) 69–84		106
7	C_nH_{2n+1}—O—⟨○⟩—CH=N—⟨○⟩—CH=CH—COO—CH*(C$_3$H$_7$)—CH$_3$	8	76–82		106
		10	73–83	42	105, 106
		14	63–79		106

Downloaded by [Tomsk State University of Control Systems and Radio] at 12:54 19 February 2013

8	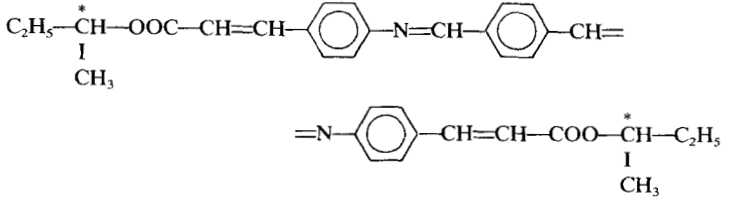		154–222		107
9	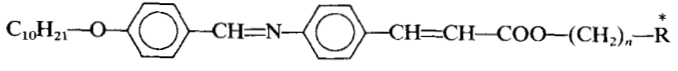	0	(63) 76–92	4–10	6, 56,
		1	83–108		57, 97,
		2	80–107		98
		3	91–117		
		4	88–115		
10	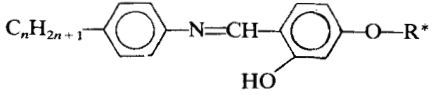	7	43–56	3	108
		8	33–55	2, 6	108
		8	(20) 36–50		103
		9	30–54	2, 3	108
		10	47–54	1, 5	108
11	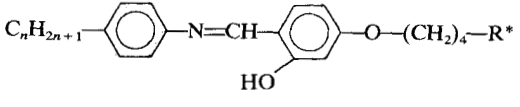	4	(20) 35–62		103
		8	(−40) 12–97		103
		8	(16) 20–86		109
		10	(17) 25–87		109
		12	(20) 35–93		103
		12	(26) 37–86		109

Downloaded by [Tomsk State University of Control Systems and Radio] at 12:54 19 February 2013

TABLE I (*continued*)

No.	Structural formula	n	Range of C* phase, grad.†	P_s, 10^{-9} C·cm^{-2}	Ref.
12	C_nH_{2n+1}—O—⟨⟩—COO—⟨⟩—O—R*	8	(22–42)	3.8	110
		9	(22) 41–47	3.0	110
		9	46–57	1.7	108
		10	(28) 45–49	2.1	110
		10	49–54	1.2	108
		10	44–50		111
		11	(48)		111
		12	(34–46)	1.0	110
		12	49–52		111
13	C_nH_{2n+1}—O—⟨⟩—COO—⟨⟩—O—$(CH_2)_2$—R*	8	49–61		
		9	41–66		111
		10	(30) 35–70		
		11	50–72		
		12	45–75		
		10	30–70	<2	53
14	C_nH_{2n-1}—O—⟨⟩—COO—⟨⟩—O—$(CH_2)_4$—R*	7	54–63		
		8	50–66		111
		9	49–67		
		10	53–69		
15	C_8H_{17}—O—⟨⟩—COO—⟨⟩—COO—R*		(26–32)		104
16	C_6H_{13}—O—⟨⟩—OOC—⟨⟩—OOC—⟨⟩—O—$(CH_2)_n$—R*	0	(55–70)		104
		2	(52) 79–115		

Downloaded by [Tomsk State University of Control Systems and Radio] at 12:54 19 February 2013

17	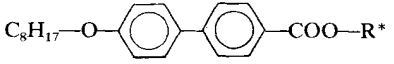		(35–44)		104
18	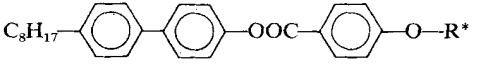		(92) 104–121		104
19	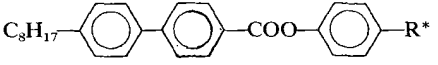		70–87	3	112
20	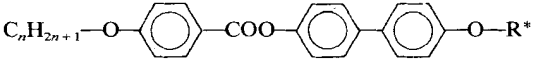	7 8 9 16	(76) 99–125 (74) 88–131 (82) 99–135 90–132	~1	59
21	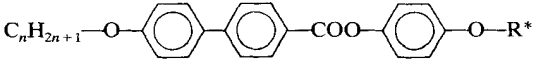	6 7 8 9 10	(89) 106–116 106–150 (97) 99–157 99–152	~1	110
22	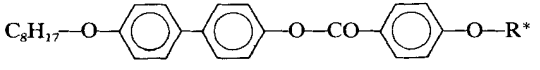		(128)	~1	110
23	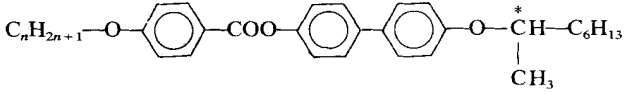	7 8 11	(54) 76–91 (67) 70–101 (66) 67–109	57 55 59	110 110 110
24	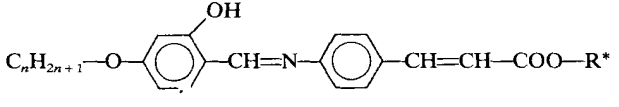	6 10 14 18	(86) 96–106 (72) 88–114 76–95 64–76	2.5 2.0 1.2	106

Downloaded by [Tomsk State University of Control Systems and Radio] at 12:54 19 February 2013

TABLE I (*continued*)

No.	Structural formula	n	Range of C* phase, grad.†	P_s, 10^{-9} C·cm^{-2}	Ref.
25	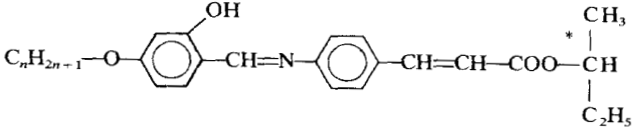	10 14	(108–118) (101–111)		106
26	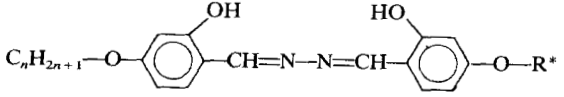	7 8 9 10 12 14 16 18	111–135 106–134 108–134 108–133 110–132 111–129 112–126 112–122		113
27	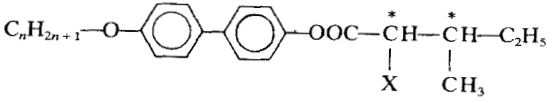 X—halogen		35–55	220	47

Downloaded by [Tomsk State University of Control Systems and Radio] at 12:54 19 February 2013

28 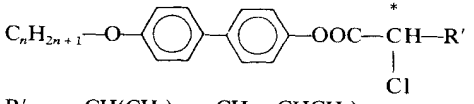

$R' = -CH(CH_3)_2, -CH_2-CHCH_3)_2, -CH(CH_3)(C_2H_5)$

300 48

29 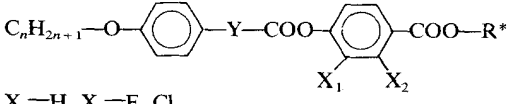

$X_1{=}H, X_2{=}F, Cl$
$X_1{=}F, Cl, X_2{=}H$ $Y{=}-, -CH{=}CH-$

49

30 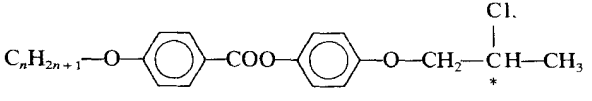

50

31 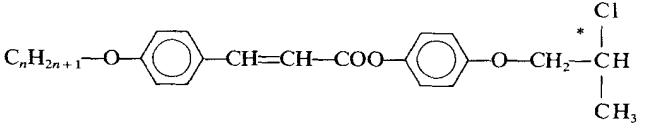

50

32 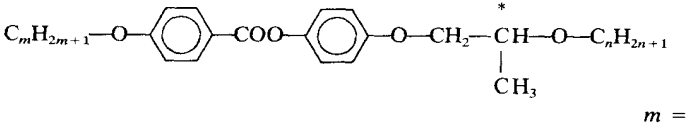

51

$m = 10$	2		15	52
$m = 10$	2	(9–28)	15	53
$m = 10$	3	(25–37.5)	15	53

Downloaded by [Tomsk State University of Control Systems and Radio] at 12:54 19 February 2013

TABLE I (*continued*)

No.	Structural formula	n	Range of C* phase, grad.†	P_s, 10^{-9} $C \cdot cm^{-2}$	Ref.
33	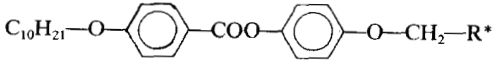		(15–56.5)	4	53
34	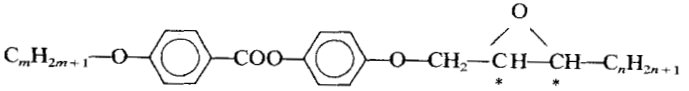 $m = 10$	3	75–80	45	54
35	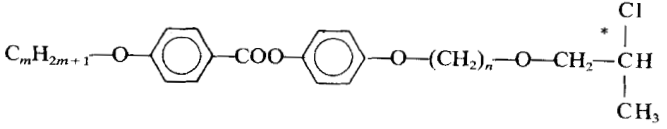	3 5			91
36	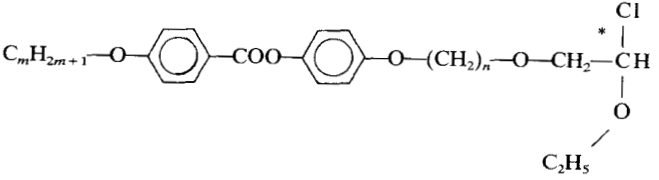				91
37	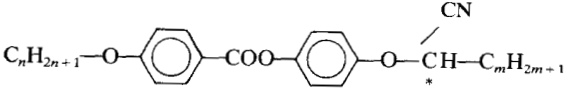				225

†Temperature in the parentheses refers to the cooling cycle.

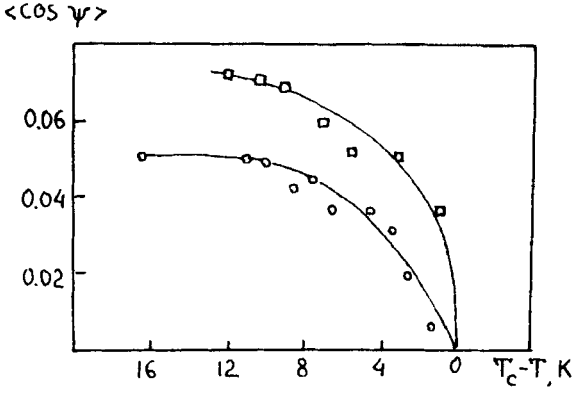

FIGURE 23 The polar order parameter ⟨cos ψ⟩ for the —C=O group as a function of temperature for DOBAMBC (○) and HOBACPC (□).

gible. For compound No 2, the dipole moment formed by an oxygen atom —O— is situated closer to the asymmetric carbon atom and the P_s value is easily detected. In compound No 3 the same dipolar —O— group is directly coupled with the asymmetric atom and the P_s value is one or two orders of magnitude higher.

A similar increase in P_s with decreasing distance between a dipolar group and a chiral moiety was also observed for other chemical classes of ferroelectric liquid crystals, see for example.[115]

The effect of the variation of other molecular fragments on the value of the spontaneous polarization is rather weaker. For instance, compounds No 10, 12, 19–23 and 24 from Table I have nearly the same $P_s \approx 10^{-9}C \cdot cm^{-2}$ though the central cores of their molecules are quite different. An increase in the number n of carbon atoms in an alkyl chain results, as a rule, in some decrease in the P_s value (look at, e.g., compound 10, 12, 24 in Table I). The latter effect can be accounted for by the zig-zag overall form of the molecules,[82] see Fig. 24, which, with increasing n, results in a decrease in the effective tilt angle θ_t for the chiral tails defining the polarization value (3).

3.4. Ferroelectricity in mixtures.

The conditions which are sufficient for the origin of the spontaneous polarization may be satisfied not only in single-compounds but in binary or multi-component mixtures as well. The most important case corresponds to mixtures of nonchiral smectic C compounds with chiral dipolar additives.[70,116,117] Such mixtures have the same point symmetry (C_2) which is typical of single component ferroelectric liquid

Downloaded by [Tomsk State University of Control Systems and Radio] at 12:54 19 February 2013

Downloaded by [Tomsk State University of Control Systems and Radio] at 12:54 19 February 2013

TABLE 2

The correlation between spontaneous polarization and the relative positions of the transverse dipole moment and the chiral moiety.

N	Structure formula	T_c	P_c, C·cm^{-2}	Reference
1	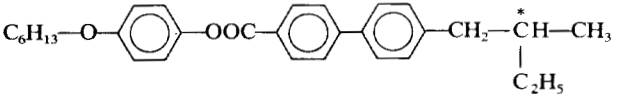	76°C	0	G. Chilaya private communication, 112
2	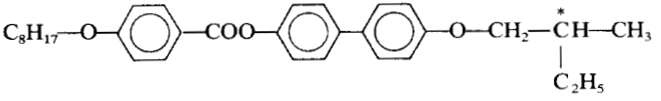	131°C	1.10^{-9}	110
	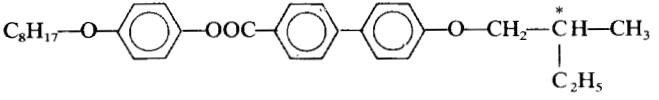	136°C	2.10^{-9}	author's measurements
3	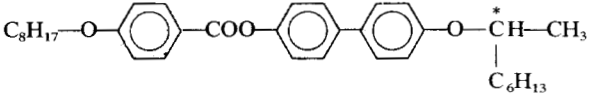	101°C	55.10^{-9}	110

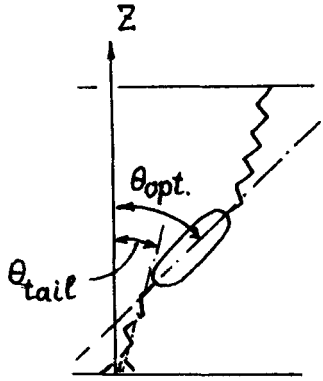

FIGURE 24 A zig-zag model for molecular packing in the C* phase.

crystals. Thus, the mixture composed from non-ferroelectric components are ferroelectric and the value of the spontaneous polarization can be of the same order of magnitude or even higher than that for single component liquid crystals.[118] The mechanisms for dipolar ordering in the two cases are similar, Fig. 21.

From a practical point of view, it is much easier to synthesize separately achiral smectic C matrices and chiral dipolar additives. The matrix should satisfy only some requirements with respect to the temperature range, stability and optical properties and there are a lot of compounds[119] of this kind. The chiral dipolar additive determines the P_s value and, on the one hand, must have rather complicated molecular structure but, on the other hand, may be non-mesogenic.

The exact value of the spontaneous polarization in mixtures is determined by a variety of factors. We can list the dipole moment and its vicinity to the chiral moiety of additives, the molecular tilt angle for the matrix and the mutual accordance in molecular lengths of the matrix and the additive. For small concentrations of additives (C) the induced polarization is proportional to C,[118] Fig. 25. The chiral impurity, naturally, twists the director of an achiral smectic C matrix and the corresponding wave vector is also proportional to concentration (for small C). In this respect the situation is similar to the case of the induced chirality in nematic mixtures.[120]

The microscopic theory[121,122] also predicts the possibility of inducing the spontaneous polarization in mixtures of the same symmetry (C_2) but containing other components. For instance, one may compose a ferroelectric mixture from an achiral tilted smectic C matrix with dipolar molecules and chiral but non-polar additives. Another

Downloaded by [Tomsk State University of Control Systems and Radio] at 12:54 19 February 2013

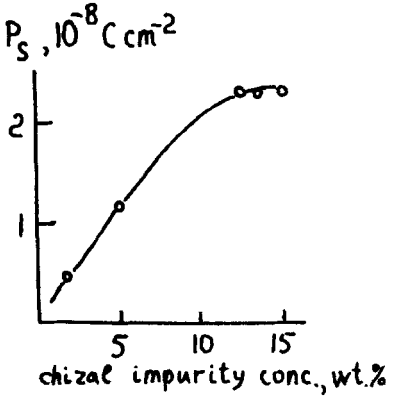

FIGURE 25 The value of the spontaneous polarization P_s induced by a chiral additive in an achiral smectic C matrix as a function of the concentration (C) of the additive.

way is to combine a chiral non-polar smectic C* with achiral but strongly polar impurities. However, the last two combinations do not result in high values of P_s—because of weak coupling between the dipolar and chiral moieties.

There are attempts to control the P_s value of single component ferroelectrics by introducing dipolar or chiral additives. A monotonic decrease in P_s was observed for DOBAMBC doped with small (<10 wt%) amounts of an achiral dipolar impurity.[58] The further increase in impurity concentration usually results in disappearance of both the smectic C* phase and the polarization.[100,123]. The small chiral molecules of L- or D-carvone

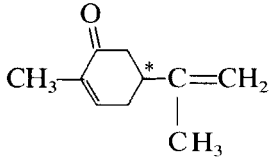

dissolved in DOBAMBC change its polarization in a rather complicated way,[124] Fig. 26. The behaviour depends on the sign of the chirality and is due to specific packing effects of the small impurity molecules between the tails of the relatively large DOBAMBC molecules.[125] The asymmetry of the influence of the left and right isomers on the concentration dependence of P_s can probably be connected with a different change in the angle formed by the tails of the DOBAMBC molecules with the smectic planes. Similar behaviour was observed in bilayers of optically active phospholipids doped with left and right amino-acids.[126]

Downloaded by [Tomsk State University of Control Systems and Radio] at 12:54 19 February 2013

Downloaded by [Tomsk State University of Control Systems and Radio] at 12:54 19 February 2013

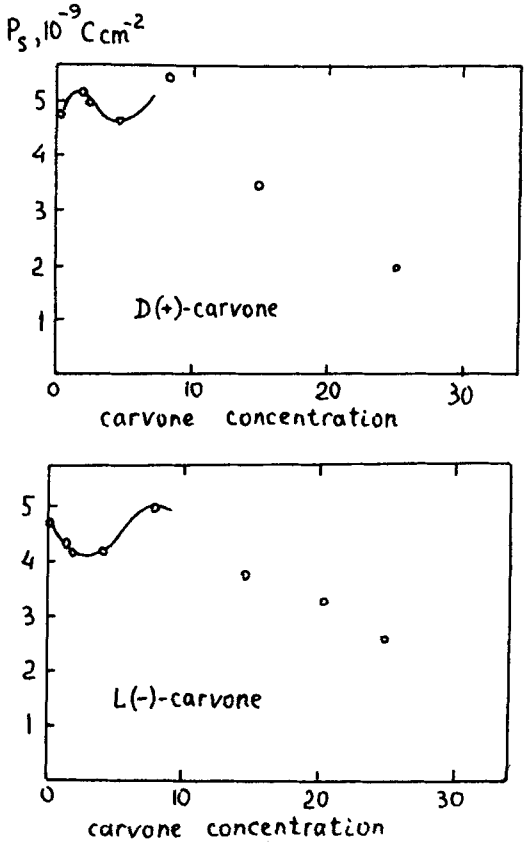

FIGURE 26 The spontaneous polarization of L-DOBAMBC as a function of the concentration of D-carvone (upper) and L-carvone (lower).

Let us return to the ferroelectric mixtures. From high temperature compounds of various classes one can compose room-temperature mixtures suitable for technical applications. For example,[110] a six-component mixture:

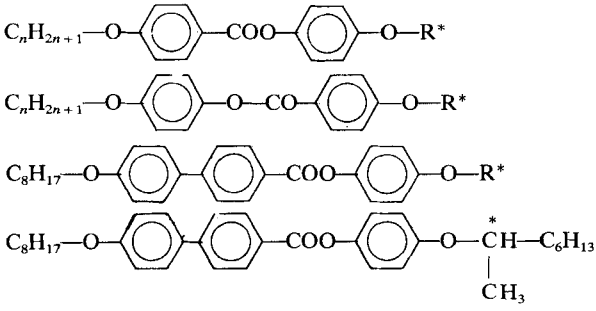

n = 9, 25 wt %,
n = 10, 20 wt %,
n = 9, 10 wt %,
n = 10, 10 wt %,
15 wt %,

20 wt %,

with the following phase transition temperatures:

Smectic III $\xrightarrow{25°C}$ smectic C* $\xrightarrow{58°C}$ smectic A $\xrightarrow{73°C}$ nematic $\xrightarrow{82°C}$ isotropic—has (at T = 28°C) the polarization $P_s = 9.4 \cdot 10^{-9}$ $C \cdot cm^{-2}$, tilt angle $\theta = 22°$ and helical pitch $h = 4\mu$.

3.5. Non-helical liquid crystalline ferroelectrics

The chirality of the compounds which form the smectic C* phase results in two consequences. First, it removes the inplane mirror symmetry and gives rise to a polar microscopic structure. Second, the chirality induces a macroscopic helical structure with a pitch exceeding the thickness of the smectic layers by two or three orders of magnitude. The microscopic mechanisms of these two effects are different and one may imagine a specific case when the helical structure vanishes but the polar direction remains.

In electro-optical devices, the helical structure, as a rule, is undesirable because of numerous defects and inhomogeneities of the orientation of the director even at zero field.[127,128] Thus, it is of practical importance to have an untwisted but ferroelectric liquid crystal.

There are several ways to prepare untwisted structures with a finite value of the spontaneous polarization. In thin cells where the thickness of a liquid crystal layer is less than the helical pitch, $d < h$, the helix is unwound for the interaction of a liquid crystal with solid surfaces. Another way is to compose a mixture of two (right and left) components with different molecular structures (otherwise we would obtain a racemic non-ferroelectric mixture). Two different components compensate for their twisting abilities.

For the first time a non-helical ferroelectric has been prepared from two classical single-component liquid crystals, DOBAMBC and HOBACPC with different signs of chirality.[129] For a certain concentration of HOBACPC (c = 55 wt %) the spiral is completely unwound, Fig. 27, but the value of the spontaneous polarization remains finite ($P_s = 4 \cdot 10^{-9}$ $C \cdot cm^{-2}$ at $T_{CA} - T = 20°$, wave vector $q_0 = 0$). Another example is a mixture of an achiral smectic C matrix with right and left additives which are not mirror isomers of the same compound.[32] Further, for some specific set of parameters the twist may be compensated for even in a single component ferroelectric liquid crystals.[130] And, lastly, the twist can disappear for the specific elastic properties of other ferroelectric phases (besides the SmC*) which occur at lowered temperatures.[131]

Downloaded by [Tomsk State University of Control Systems and Radio] at 12:54 19 February 2013

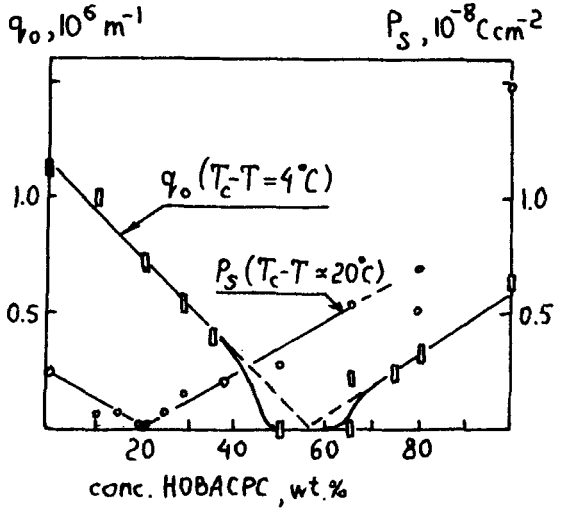

FIGURE 27 Compensation for the helical structure and the vanishing of the polarization in a mixture of DOBAMBC and HOBACPC.

3.6. The effect of the steric and dipolar interactions on the value of the spontaneous polarization

From the conventional point of view the dipolar ordering in chiral tilted smectics is a secondary effect which results from a more fundamental, primary reason, namely, from the hinderance of molecular rotation around their long axes caused by some steric interactions (the model with molecular tripods discussed above is an example of these interactions). The spontaneous polarization, as a secondary parameter, is proportional to the true order parameter (the tilt angle θ) of the smectic C* phase, Eqn. (3). The role of steric factors could be seen if one compares the P_s-values for substances N 6 and 7 ($n = 10$) in Table I. The chiral moiety of substance N 7 is a little more forked than that of substance N 6 because of an extra $-CH_2$ group and this factor enhances the P_s value more than two times.

Besides the main part of P_s, which is a linear function of the tilt angle θ, there exists an additional contribution to P_s which is cubic in θ.[23] The relaxation time for this novel part of the polarization is less than 10^{-8} S, which is markedly shorter than the tilt angle relaxation times (soft mode). To explain this contribution to P_s one should consider the additional degree of freedom for molecular motion. For example, the fast part of the polarization may result from fast motion of the chiral dipolar tail of a molecule. In that case, the tilt of the

Downloaded by [Tomsk State University of Control Systems and Radio] at 12:54 19 February 2013

molecule as a whole, which is necessary to have P_s for symmetry considerations, represents a slow background against which the fast process of the relaxation of a dipolar tail occurs. The experiment confirms the predicted (cubic) dependence

$$P_t \sim \mu_t \theta^3 \tag{55}$$

for the fast contribution. The two terms (slow and fast) can be separated using the pulse pyroelectric technique.[58] For DOBAMBC the fast polarization is small, $P_t \approx 0.03\ P_s$ but is easily detected thanks to the time selection. The temperature behaviour of the slow, $P_\theta(T)$, and fast, $P_t(T)$, polarization modes is shown in Fig. 28 for DOBAMBC.[23] The fast term of P_s can be more pronounced in multicomponent mixtures.

Apart from steric interactions the ordering of the short molecular axes may also be caused by long-range forces. According to the microscopic theory[121,122] (see below, part IV), an increase in the transverse component of the dipole moment $d_{\perp 2}$ in a chiral moiety of a molecule results in increasing interactions of the type "dipole-induced dipole." These interactions also increase with increasing transverse polarization of neighbouring molecules $\chi_\perp$.

To discuss the role of the dipole–dipole interactions let us look at the well known compounds DOBAMBC and HOBACPC. Their main difference is due to the compact but strongly polar C—Cl group

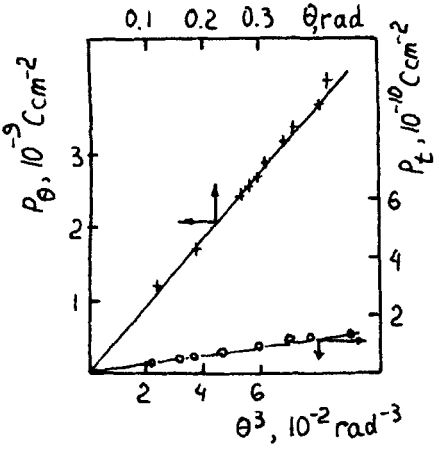

FIGURE 28 Slow (P_θ) and fast (P_t) contributions to the spontaneous polarization of DOBAMBC as functions of the tilt angle.

Downloaded by [Tomsk State University of Control Systems and Radio] at 12:54 19 February 2013

instead of non-polar but "forked" C—C_2H_5 group in the chiral moiety. As a result of this compactness one can anticipate the smaller order parameter ⟨cos ψ⟩ for the short molecular axis (labelled, for example, by $\diagdown$ C=O group) of HOBACPC versus that of DOBAMBC (may-be, two-times or more in analogy with substances No 6 and 7 from Table I). However, experiments[114] show that ⟨cos ψ⟩ for the C=O bond of HOBACPC is higher than that for DOBAMBC, Fig. 23. In our opinion, this increase in ⟨cos ψ⟩ of the $\diagdown$ C=O bond is a result of the dipole–dipole interactions between the C—Cl bonds of neighbouring molecules[121,122] which are stronger than the interactions between the ethyl groups in DOBAMBC.

The measurements of the spontaneous polarization in specially composed mixtures allowed us to separate the contributions from steric and dipolar interactions to the total dipolar ordering.[132] The slow and fast components of the polarization were measured for a mixture of an achiral smectic C NOBAPC.

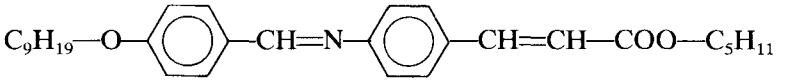

and its chiral isomer L-NOBAMBC

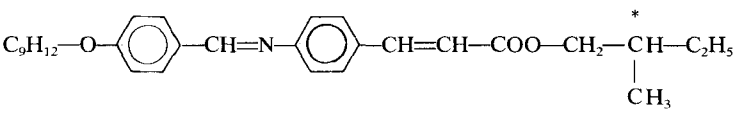

which differs from NOBAPC only by the location of the CH_3-group in the molecular tail. With this mixture it is possible to change smoothly the steric and dipolar intermolecular interactions. Let, for example, the concentration of the "forked" component (NOBAMBC) in a mixture be increased. Then the hinderance of the rotation of the molecules around their long axes caused by steric factors also increases. At the same time, the interaction between the dipolar $\diagdown$ C=O groups in neighbouring molecules becomes weaker for an increase in the distance l between them, Fig. 29 (the dipole–dipole interaction energy strongly depends on l, $W_{dd} \sim d^2/l^3$).

Downloaded by [Tomsk State University of Control Systems and Radio] at 12:54 19 February 2013

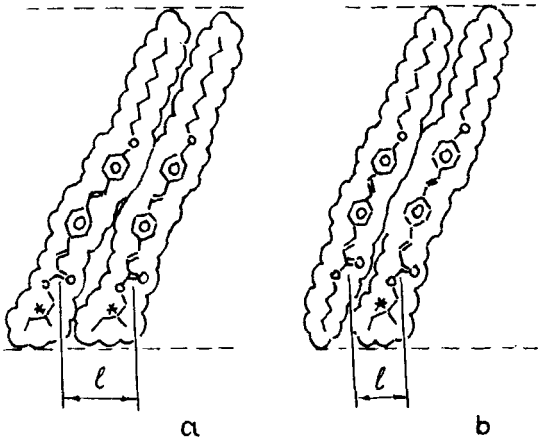

FIGURE 29 A model for mutual packing in the chiral C* phase of two chiral molecules of NOBAMBC (a), and of a chiral (NOBAMBC) and achiral (NOBAPC) molecule (b).

The concentration dependences of P_θ and P_t reduced to the same tilt angle θ of the director (data taken from[133]) are demonstrated in Fig. 30. The corresponding values for the piezocoefficients μ_θ and μ_t calculated with Eqns. (3) and (55) are also shown. It is easily seen that an increase in the concentration of the chiral component results in an increase in the "steric" piezo-coefficient μ_θ and a decrease in the "dipolar" piezo-coefficient μ_t. Thus, though the energy for the

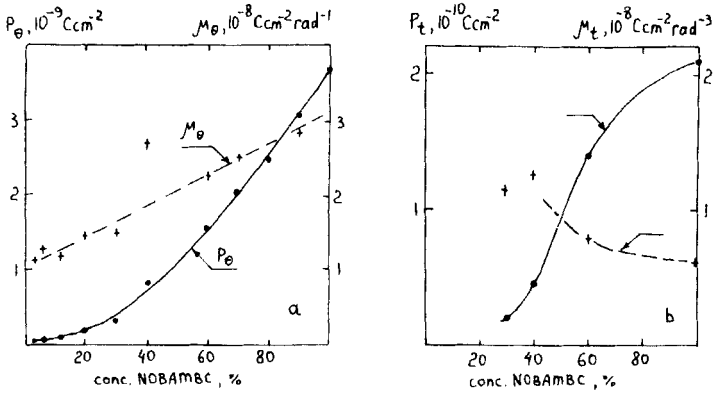

FIGURE 30 Maximum values of slow (P_θ) and fast (P_t) polarizations and the corresponding piezo-moduli μ_θ and μ_t in the smectic C* phase of a NOBAPC-NOBAMBC mixture as functions of the NOBAPC concentration.

Downloaded by [Tomsk State University of Control Systems and Radio] at 12:54 19 February 2013

dipole–dipole interactions $W_{dd} \approx 0.2$ kT (T = 350 K, $d_{\perp} \approx 2D$, $l \approx$ 5 – 7 Å, $W_{dd} \approx 10^{-21}$ J) can not control the transition to a ferroelectric phase it does give an additional contribution to the dipolar ordering and spontaneous polarization as soon as the ferroelectric phase occurs for some other (e.g. steric) reasons. This contribution is small for DOBAMBC and for the discussed mixture ($P_t \sim$ 3–5% of P_θ) but it becomes essential for mixtures of achiral smectics C and chiral additives with a large dipole moment in the chiral moiety. For instance, in a mixture of HOPE OOBA and HOBACNPC (5 wt %)

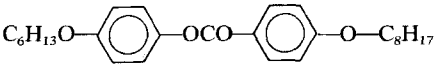

(HOPE OOBA)

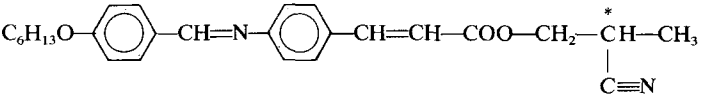

(HOBACNPC)

the fast dipolar contribution $P_t = 0.43\ P_\theta$[23]. The temperature dependences of the fast components of the spontaneous polarization P_t and pyro-electric coefficient γ_t as well as of the total polarization $P_s = P_\theta + P_t$ are shown in Fig. 31 for the above discussed mixture.

The increase in the transverse dipole moment $d_{\perp 2}$ in a chiral molecular fragment of an additive increases sharply the polarization P_s. This may be seen from Fig. 32a. Various chiral additives with a general

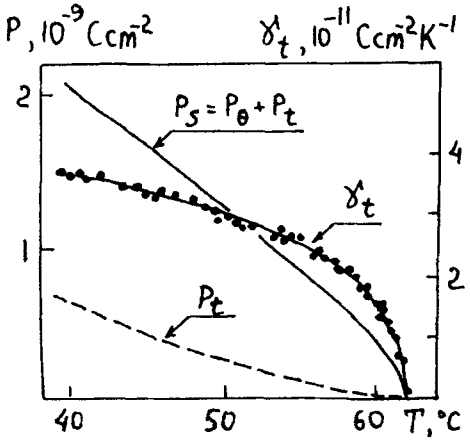

FIGURE 31 Temperature dependences of the fast contributions in the pyro-coefficient γ_t and polarization P_t and of the total polarization $P_S = P_\theta + P_t$ for a mixture of the achiral smectic HOPE OOBA and the chiral additive HOBACNPC (5 wt%).

Downloaded by [Tomsk State University of Control Systems and Radio] at 12:54 19 February 2013

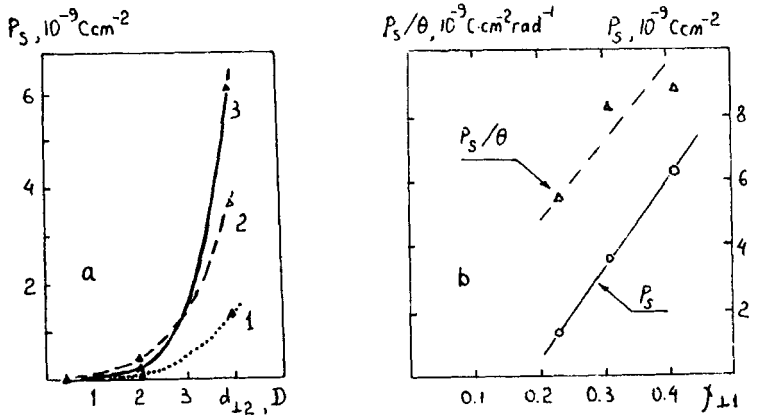

FIGURE 32 Spontaneous polarization P_s induced in achiral smectic C matrices OOOPP (1), HOPE OOBA (2), HOHSA (3) by chiral additives as functions of the dipole moment $d_{\perp 2}$ of the additive (a) and of the transverse component $\chi_{\perp 1}$ of the matrix (b). Concentration of the additive is 5 wt% everywhere.

formula

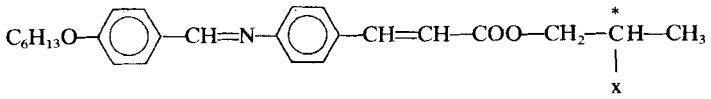

where $X_1 = -C_2H_5$ (HOBAMBC, $d \sim 0.3 - 1\ D$), $X_2 = -Cl$ (HOBACPC, $d \sim 2\ D$), $X_3 = -C{\equiv}N$ (HOBACNPC, $d \sim 4\ D$) were introduced in three different smectic C matrices. The increase in P_s value agrees with the theoretically predicted dependence $P_s \sim d_\perp^3$. The spontaneous polarization also increases markedly with increasing value of the transverse molecular polarizability $\chi_\perp$ of an achiral matrix. Fig. 32b shows the data for P_s for three mixtures based on different smectic C matrices (OOPOP, HOPE OOBA and HOHSA)

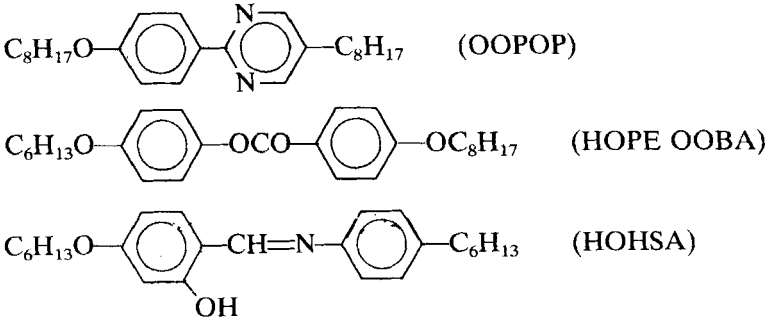

Downloaded by [Tomsk State University of Control Systems and Radio] at 12:54 19 February 2013

with the same additive (HOBACNPC). The additive concentration was held to be constant (C = 5 wt %) and the P_s-values were reduced to the same tilt angle of the smectic C matrices. The linear dependence of P_s on $\chi_\perp$ predicted by the theory[121,122] for small impurity concentrations agrees well with the experimental data.

Our experiments[23,132,134] have shown that high values of P_s can be provided only for high values of the parameter μ_t and its value, in turn, correlates with the dipolar properties of both the matrix and the additive. This result should be taken into account when preparing mixtures with high spontaneous polarization for applications.

3.7. Polymorphism of ferroelectric phases

From symmetry considerations, the appearance of spontaneous polarization is allowed for all chiral smectic phases with the director tilted with respect to the layers. The most studied case is the smectic C* phase, especially for DOBAMBC and HOBACPC. There are also data on the temperature behaviour of the spontaneous polarization for other, low-temperature ferroelectric phases of the same compounds.[102,135] For instance, at the transition from the C*-phase of HOBACPC into phase III[136] one may observe a sharp peak of the pyroelectric coefficient $\gamma(T)$,[102] Fig. 33, and a corresponding rise in the spontaneous polarization.[135] The critical exponent of the relaxation time for the soft mode appeared to be equal to 1.0 ± 0.1 on both sides of the transition[102] which is indicative of its second order character. At the same time, the DSC measurements show that this transition is of the first order. The reason for the discrepancy lies, in our opinion, in the fact that the spontaneous polarization is mainly determined by the tail part of the molecules, where the chiral and dipolar groups are located, and the phase transition occurs in a different way for flexible tails and for rigid molecular skeletons.

Rich polymorphism is typical of ferroelectric mixtures. An example is shown in Fig. 34. The temperature dependence of the pyro-coefficient for a mixture of achiral NOBAPC with chiral HOBACPC reveals a rather complicated behaviour.

There are only smectic A, smectic C and smectic B phases[119] in pure NOBAPC while the mixtures have four pyroelectric phases or even more. For one of them the molecular packing is presumably anti-ferroelectric, Fig. 34.

The low temperature phases are, as a rule, more viscous and the switching times for the director are markedly longer.[67,98] However, they appear to be suitable for some memory devices. Some low tem-

Downloaded by [Tomsk State University of Control Systems and Radio] at 12:54 19 February 2013

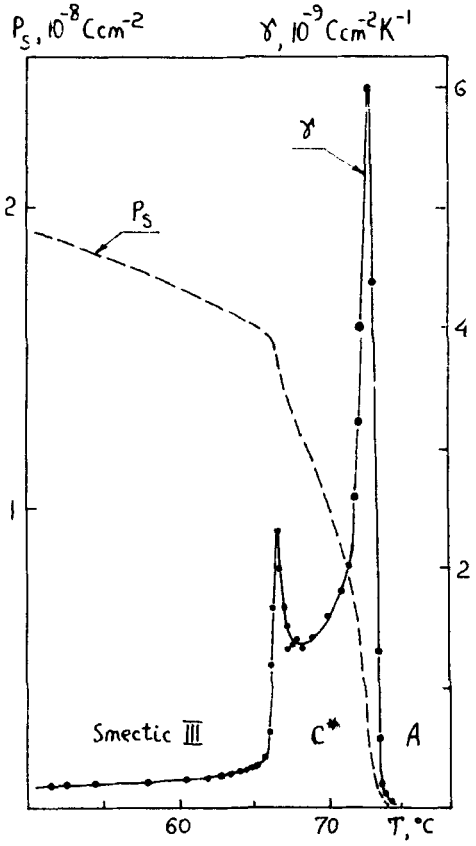

FIGURE 33 Temperature behaviour of the pyroelectric coefficient γ and the spontaneous polarization P_s of HOBACPC.

perature ferroelectric phases of single component substances are untwisted even in the zero-field condition[137] and may be referred to as both liquid crystalline and solid ferroelectrics.

3.8. Polymeric liquid crystalline ferroelectrics

In some cases, polymeric liquid crystals may be considered as consisting of two independent sub-systems, namely, mesogenic fragments and flexible chains. For example, a flexible chain, in the first approximation, does not influence such static parameters as refractive indices, magnetic susceptibility, etc. The same may be said of the point symmetry of a polymeric liquid crystal. When mesogenic moieties form a structure satisfying the symmetry requirements, which are

Downloaded by [Tomsk State University of Control Systems and Radio] at 12:54 19 February 2013

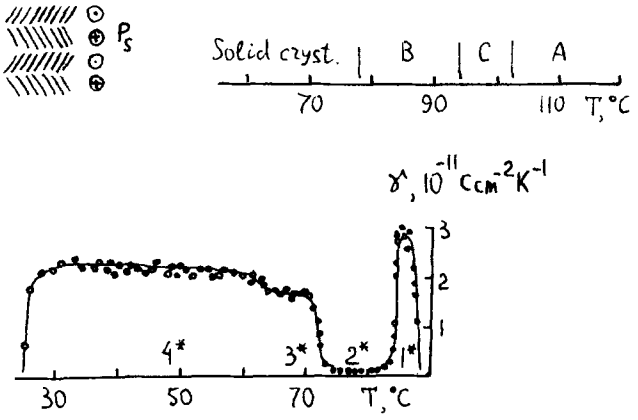

FIGURE 34 Temperature dependence of the pyro-coefficient for a mixture of NOBAPC and HOBACPC (20 wt%). 1*–4* are different smectic phases. Upper right: the sequence of phase transitions for pure NOBAPC. Upper left: a herring-bone antiferroelectric structure.

necessary and sufficient for ferroelectricity, spontaneous polarization appears in the polymeric liquid crystal. The comb-like polymers of the general formula

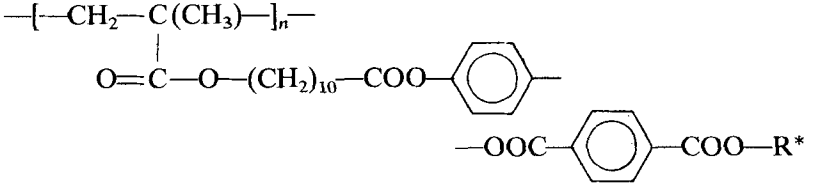

where $R_1^* = -CH_2-\overset{*}{C}H(CH_3)-C_2H_5$ (polymer P5*M)

and $R_2^* = -CH_2-\overset{*}{C}H(Cl)-CH_2-CH(CH_3)_2$ (polymer P6 CM)

were synthesized[138,139] with the aim of producing a ferroelectric structure.

Downloaded by [Tomsk State University of Control Systems and Radio] at 12:54 19 February 2013

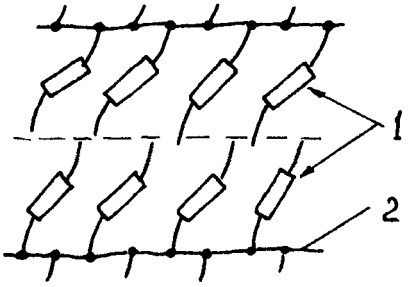

FIGURE 35 The packing of mesogenic groups (1) and polymeric chains (2) in the smectic C* phase of the comb-like ferroelectric polymers P5*M and P6CM.

X-ray analysis showed the layered smectic structure with the tilted orientation of the side mesogenic groups, Fig. 35, in the temperature ranges 43–73°C (P5*M) and 52–71°C (P6 CM).

As was anticipated, the spontaneous polarization was detected in both polymers. Its value, $P_s \approx 10^{-9}$C · cm^{-2} is typical of liquid crystalline (low molecular) ferroelectrics. The temperature dependences of the pyro-coefficient and the spontaneous polarization measured by the pulse pyroelectric technique are shown in Fig. 36.

Polymeric liquid crystalline ferroelectrics have some specific features. First, polarization and the pyro-effect remain even in the glassy state at temperatures below the vitrification point (T_v = 43°C for P5*M and T_v = 52°C for P6 CM). Second, when we use a polarizing

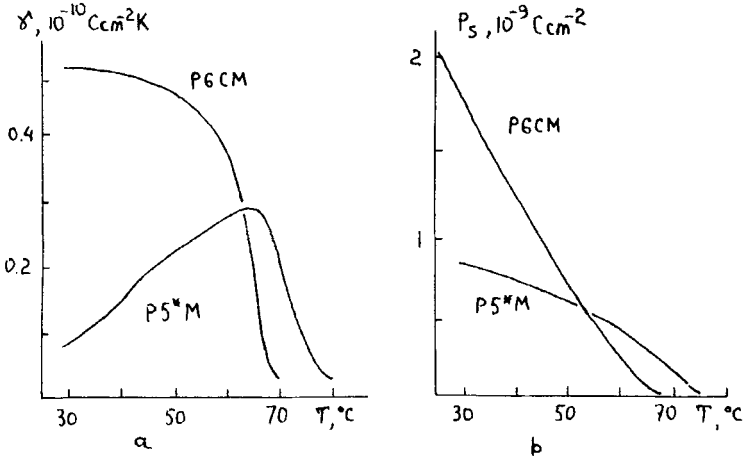

FIGURE 36 Temperature behaviour of the pyro-coefficient γ(T) (a) and the spontaneous polarization (b) of polymers P5*M and P6CM.

Downloaded by [Tomsk State University of Control Systems and Radio] at 12:54 19 February 2013

electric field to obtain a monodomain state in the smectic C* phase this state relaxes very slowly (hours) because of the high viscosity of the polymer. Third, near the transition into the smectic A phase the critical behaviour of the soft mode relaxation times is strongly extended and the corresponding times are two order of magnitude longer (1 mS) than those for low-molecular analogs of the polymeric ferroelectrics. In fact, polymeric chains influence the fluctuations in the tilt of the mesogenic groups.

A ferroelectric liquid crystalline polymer P6 CM has been made[138] by polymerization of a low-molecular liquid crystal. To this aim a double-bond group —CH=CH— was introduced in the molecular structure of the latter. The monomer itself (M6 CM)

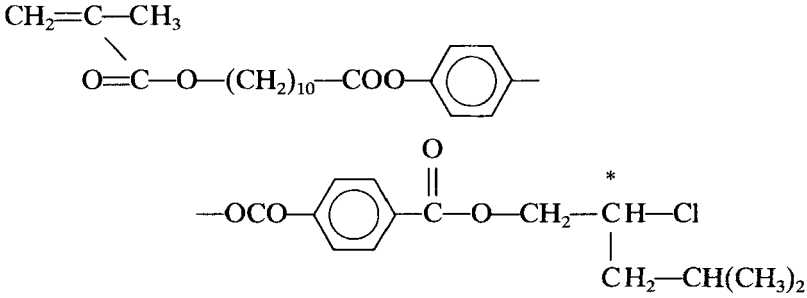

has a monotropic ferroelectric C*-phase in the range 15–25°C and its ferroelectric properties are standard. For example, polarization $P_s \approx 2 \cdot 10^{-8} C \cdot cm^{-2}$ almost coincides with the P_s value of HOBACPC which has the same —C*—Cl bond in the chiral center. However, it is worth noting that the double unsaturated bond sharply decreases the temperature range of the mesophase. This may be useful for the development of low temperature materials for applications.

Thus, the main features of the ferroelectricity in low- and high-molecular weight compounds are similar. However, the presence of spontaneous polarization in the glassy state opens up the possibilities for investigations and technical applications of the pyro- and piezoelectric properties of the corresponding solid films. In addition, the polarization measurements allow the mutual influence of the flexible chain and the mesogenic groups to be studied.

3.9. The possibility of ferroelectric ordering in living tissues

There are some reasons for a search of ferroelectricity in biological systems. Some biological structures are lamellar (e.g. membranes),

Downloaded by [Tomsk State University of Control Systems and Radio] at 12:54 19 February 2013

others are chiral[140,141] and, lastly, there are examples of polar biological structures (e.g. pyroelectric tissues[142,135]).

In paper Ref. 143 an idea was given for a search for ferroelectricity in lamellar membrane structures with chiral additives. This possibility is due to the analogy in the structure of the membranes and ferroelectric liquid crystals. The chirality of biologically active molecules included in membranes (e.g. cholesterol) provides automatically one of the necessary conditions for the presence of spontaneous polarization. The second condition, namely, the molecular tilt in the lamellar structure is also satisfied in bilayers with the tilt of the lipid molecules with respect to the normal of the bilayer,[144,125] Fig. 37. Such a tilt may occur, for example, locally under the action of some external factors (chemical, mechanical, etc.). The vector of spontaneous polarization must lie in the bilayer plane perpendicular to the tilt plane.

To evaluate the polarization value which can be induced by biologically-active, chiral molecules in bilayers, the polarization induced by cholesterol in achiral smectic C liquid crystals was measured. The in-plane polarization appeared to be surprisingly high, $P_s \approx 10^{-10} - 10^{-9} C \cdot cm^{-2}$, even for rather small concentrations of the additive, Fig. 38. The extrapolation of the P_s value to the concentrations of cholesterol typical of natural membranes gives the magnitude $P_s \approx 10^{-8} C \cdot cm^{-2}$. Similar results were obtained in experiments with antibiotics.

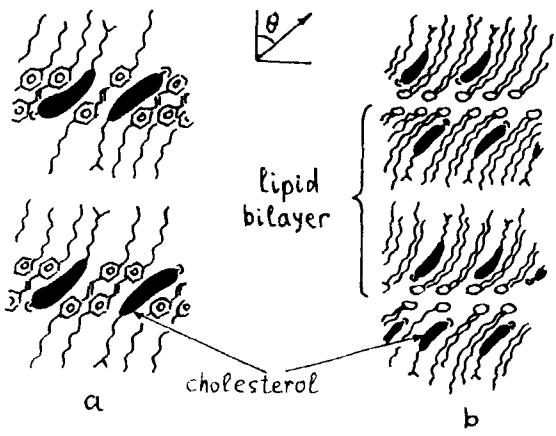

FIGURE 37 Structure of the smectic C* phase (a) and lipid bilayers (b) with spontaneous polarization induced by cholesterol.

Downloaded by [Tomsk State University of Control Systems and Radio] at 12:54 19 February 2013

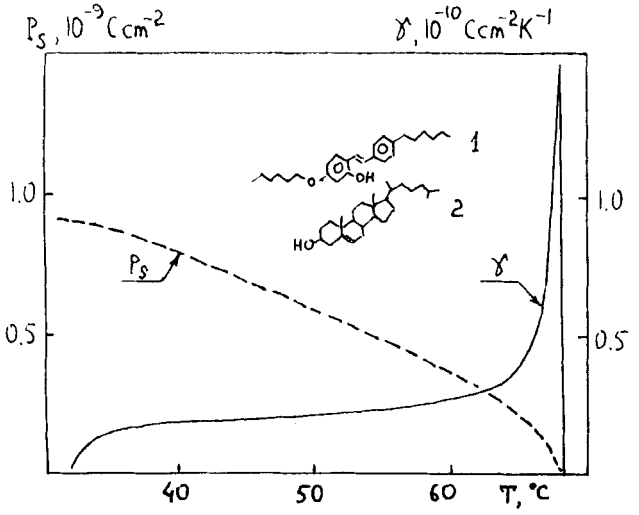

FIGURE 38 Temperature behaviour of the pyro-coefficient γ and spontaneous polarization P_s in a mixture of smectic C HOHSA(1) and cholesterol (2). The concentration of cholesterol is 6 wt%.

The direct detection of spontaneous polarization in biomembranes would, in our opinion, help in understanding the physical nature of such biological processes as excitation transfer, ion transport, ensyme action, etc.

IV. MOLECULAR-STATISTICAL THEORY OF FERROELECTRIC LIQUID CRYSTALS

4.1. Microscopic origin of spontaneous polarization in liquid crystals

The spontaneous polarization in ferroelectric liquid crystals appears as a result of the partial ordering of transverse molecular dipoles (Fig. 39). In the chiral smectic C* phase the average dipole moment is parallel to the smectic layer and orthogonal to the director **n**. The microscopic origin of spontaneous polarization can be clarified if one considers first the orientation of a given molecule in the smectic C* phase, represented in Fig. 39. The orientation of molecule "i" can be specified by two unit vectors $\mathbf{a}_i$ and $\mathbf{b}_i$ which determine the orientation of the long and short axes of the molecule, respectively, $(\mathbf{a}_i\mathbf{b}_i) = 0$. In liquid crystals the average orientation of the long molecular axis $\mathbf{a}_i$ is determined by the director **n**, which is tilted with

Downloaded by [Tomsk State University of Control Systems and Radio] at 12:54 19 February 2013

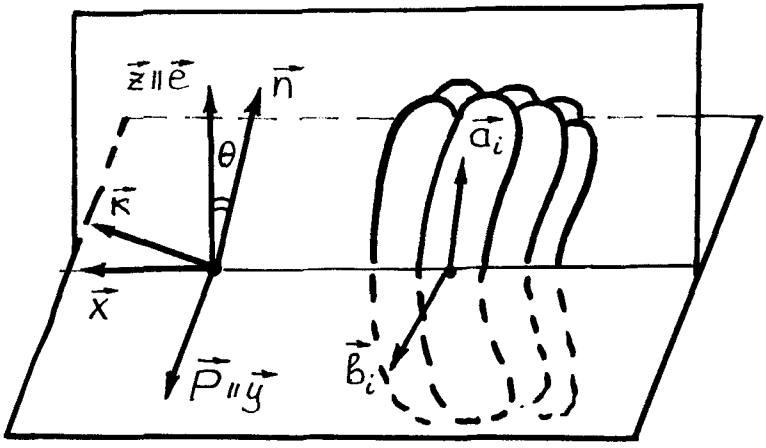

FIGURE 39 Relative orientation of the director **n**, the spontaneous polarization **P** and the smectic plane normal **e** in the ferroelectric smectic C* phase.

respect to the smectic plane normal **e**. In the smectic C phase the orientational order is rather high[145] and the long molecular axis $\mathbf{a}_i$ does not deviate strongly from the average direction. At the same time the experiments of Zagar, Blinc *et al.*[146] show that in the achiral smectic C phase the molecules rotate freely about their long axes. On the contrary, in the chiral ferroelectric C* phase a small hindrance of rotation is observed[146] and hence the dipole order parameter $\langle(\mathbf{x}\mathbf{b}_i)\rangle \neq 0$, where vector **x** is fixed in the laboratory frame. For typical ferroelectric liquid crystals the dipole order parameter is very small. For example, $\langle(\mathbf{b}_i\mathbf{x})\rangle \sim 10^{-2}$ for the liquid crystal DOBAMBC.[146] Thus, in the smectic C* phase the molecules rotate almost freely about the long axes, but the opposite directions of the short axis $\mathbf{b}_i$ become nonequivalent. This results in the nonzero spontaneous polarization of the smectic layer in the direction determined by the symmetry of the C* phase.

If the short axis $\mathbf{b}_i$ is parallel to the transverse molecular dipole $\mathbf{d}_{\perp i}$ the spontaneous polarization can be written as

$$\mathbf{P} = \rho d_\perp \langle \mathbf{b}_i \rangle \tag{56}$$

where ρ is the number density. The Eq. (56) can be rewritten in the familiar form (see Eq. (7) of Section 2.1) which corresponds to the phenomenological theory

$$\mathbf{P} = \rho d_\perp \mathcal{H} [\mathbf{ne}] \tag{57}$$

Downloaded by [Tomsk State University of Control Systems and Radio] at 12:54 19 February 2013

where $\langle \mathbf{b}_i \rangle = \mathcal{H}[\mathbf{ne}]$ and the parameter $\mathcal{H} << 1$ is the dipole order parameter of the short axes. The direction of the average dipole is determined by the vector [**ne**], as shown in Fig. 39. The parameter $\mathcal{H}$ can be estimated also from the ratio of the experimentally measured polarization **P** and the maximum polarization $\mathbf{P}_{max} = \rho d_\perp$ which would appear under the condition of perfect dipolar ordering. In DOBAMBC $\rho \simeq 1.5 \cdot 10^{-9}$Cu/cm^3 $d_\perp \simeq$ 1D and $\rho \sim 10^{21}$cm^{-3} which also yields $\mathcal{H} \sim 10^{-2}$. Therefore, the dipolar ordering in the smectic C* phase is rather weak in comparison with the strong orientational order of long molecular axes which determine the structure of the C* phase.

The weak ordering of transverse molecular dipoles in the smectic C* phase confirms the conclusion of the phenomenological theory that chiral smectics C* are the pseudoproper ferroelectrics with the spontaneous polarization being the consequence of the symmetry of the chiral C* phase.

So far we have considered only the dipolar ordering within a smectic layer. In the adjacent layers the direction of spontaneous polarization is slightly changed due to the helicoidal twisting of the director about the smectic plane normal. It should be noted that helicoidal twisting in the smectic C* phase is analogous to the twisting in cholesterics and is determined only by the molecular chiralty. The spontaneous macroscopic twist results in an additional contribution to the spontaneous polarization of the smectic layer due to the flexoelectric effect. This effect has been described in Section 2.2. The molecular theory of the flexoelectric effect in the smectic C* phase is presented in Refs. 21 and 147.

4.2. Model potentials of interaction between chiral molecules in smectics C*

Perhaps the most important problem in the molecular theory of ferroelectric liquid crystals is the origin of the intermolecular forces which can cause the spontaneous polarization. In the majority of classical ferroelectrics the interaction between permanent dipoles is usually responsible for the ferroelectric ordering. In contrast, the electrostatic dipole–dipole interaction cannot account for the ordering of dipoles in the smectic C* phase. Indeed, the spontaneous polarization is observed only in chiral smectics, while the interaction between permanent dipoles is the same in chiral and nonchiral liquid crystals, since this interaction does not reflect the molecular chirality. Thus, the ferroelectric ordering in the smectic C* phase can be ex-

Downloaded by [Tomsk State University of Control Systems and Radio] at 12:54 19 February 2013

plained only on the basis of some other intermolecular forces which are sensitive to molecular chirality. The corresponding intermolecular interactions will be discussed in the following section. In this Section we shall follow another way and construct appropriate model interaction potentials which can be used to describe ferroelectric ordering in the C* phase. As mentioned above, this potential should reflect the chirality of interacting molecules. In the theory of liquid crystals the expression for the chiral interaction energy was first proposed by Goosens.[148] The simplest chiral interaction between molecules i and j can be written as

$$V^*(i,j) = -J^*(r_{ij})(\mathbf{a}_i\mathbf{a}_j)([\mathbf{a}_i\mathbf{a}_j]\mathbf{u}_{ij}) \tag{58}$$

where r_{ij} is the intermolecular distance and $\mathbf{u}_{ij} = \mathbf{r}_{ij}|\mathbf{r}_{ij}|^{-1}$. In Eq. (58) the pseudoscalar $([\mathbf{a}_i\mathbf{a}_j]\mathbf{u}_{ij})$ changes sign under the inversion operation. The coupling constant $J^*(r_{ij})$ also changes sign if one changes the handedness of the molecules. Thus $J^*(r_{ij}) = 0$ for achiral molecules. Note that the interaction energy $V^*(i,j)$, being a scalar, is invariant under the inversion. The interaction (58) is equal to zero if both molecules i and j are achiral.

The interaction potential (58) is widely used in the description of helical twisting in cholesterics and smectics C*.[148–151] However, it is evident that ferroelectric ordering cannot be caused by this interaction since the potential (58) corresponds to cylindrically symmetric molecules. In the theory of ferroelectric liquid crystals one can use only those model potentials which depend on the direction of the short molecular axis $\mathbf{b}_i$ (i.e. the direction of the transverse dipole). The appropriate potential should be even in $\mathbf{u}_{ij}$, also, since this interaction contributes to the free energy of the undistorted (unwound) smectics C*. Then the simplest potential of interaction between chiral and polar molecules can be written in the form

$$\begin{aligned} U^*(ij) &= U_{ij} + U_{ji}; \\ U_{ij} &= -U^*_{ij}(r_{ij})(\mathbf{a}_i\mathbf{a}_j)(\mathbf{a}_i\mathbf{u}_{ij})([\mathbf{b}_i\mathbf{a}_j]\mathbf{u}_{ij}) \end{aligned} \tag{59}$$

The interaction (59) is even in $\mathbf{a}_{ij}\mathbf{a}_j$, $\mathbf{u}_{ij}$ and odd in $\mathbf{b}_i$ and hence it is sensitive to the direction of the molecular transverse dipole. At the same time the interaction (59) is chiral, similar to the potential (58), since the quantities $([\mathbf{b}_i\mathbf{a}_j]\mathbf{u}_{ij})$ and $V^*(r_{ij})$ are pseudoscalars which change sign under the inversion. Similar to the potential (58), the coupling constant $V^*_{ij}(r_{ij}) = 0$ if both molecules i and j are achiral.

Downloaded by [Tomsk State University of Control Systems and Radio] at 12:54 19 February 2013

Downloaded by [Tomsk State University of Control Systems and Radio] at 12:54 19 February 2013

The simple potential (59) was used in the first statistical theory of ferroelectric liquid crystals.[122] The general statistical theory of ferroelectric ordering in smectics C* will be presented in section 4.3. However, one does not need the general theory in order to be convinced of the fact that interaction (59) can be responsible for the dipolar ordering.

Indeed, let us consider for simplicity the smectic C* phase with a perfect orientational and translational order. In this case the contribution from the interaction (59) to the internal energy of the smectic C* is given by

$$\Delta U = \frac{1}{2} \sum_{i,j} \langle U^*(i,j) \rangle \tag{60}$$

where the $\langle \ldots \rangle$ stands for the averge over the intermolecular distance $\mathbf{r}_{ij}$ and the short axis $\mathbf{b}_i$. Let us assume now that the interaction $U^*(i,j)$ is a short-ranged one, and consider only interactions between nearest neighbours. In the case of ideal smectic order the centres of mass are located in equidistant smectic planes and move freely in the planes. Then the average over $\mathbf{r}_{ij}$ is different for the two molecules, located in the same plane in the adjacent planes. In the former case the vector $\mathbf{r}_{ij}$ lies in the smectic plane ($\mathbf{u}_{ij} \perp \mathbf{e}$) while in the latter one $\mathbf{r}_{ij}$ is perpendicular to the plane ($(\mathbf{u}_{ij}\mathbf{e})^2 = 1$). Finally, the average interaction (60) can be written as

$$\begin{aligned} \Delta U &= -U_0^* \rho^2 \{(1 - \sigma)(\mathbf{ne})([\mathbf{ne}]\langle \mathbf{b}_i \rangle) \\ &\quad + \sigma \int (\mathbf{nu}_{ij})([\mathbf{nu}_{ij}]\langle \mathbf{b}_i \rangle)\delta(\mathbf{u}_{ij}\mathbf{e}) d^2\mathbf{u}_{ij}\} \\ &= U_0^* \rho^2 \left(\frac{3}{2}\sigma - 1\right)(\mathbf{ne})([\mathbf{ne}]\langle \mathbf{b}_i \rangle) \end{aligned} \tag{61}$$

where σ is a fraction of the nearest neighbours located in the same plane as the central molecule, and

$$U_0^* = \int [U_{ij}^*(r_{ij}) + U_{ji}^*(r_{ij})] r_{ij}^2 dr_{ij}$$

With the help of Eq. (56) we have

$$\begin{aligned} \Delta U &= -\mu(\mathbf{ne})([\mathbf{ne}]\mathbf{P}) \\ \mu &= U_0^* \rho d_\perp^{-1}; \end{aligned} \tag{62}$$

The expression (62) has the same form as the so-called "piezoelectric" term in the phenomenological free energy of the ferroelectric smectic C* phase (see Eq. (21)). As shown in Section 2.2, this "piezoelectric" term is responsible for the appearance of spontaneous polarization in the C* phase, i.e.

$$\mathbf{P} = -\mu\chi[\mathbf{ne}],$$

where χ is the dielectric susceptibility.

The oversimplified derivation, presented above, has been included here to demonstrate the main ideas only. The general theory, presented in Section 4.3, enables one to obtain the same result in a more consistent manner.

4.3. Induction interaction between polar and chiral molecules

Let us now proceed to the discussion of concrete intermolecular interactions which can be responsible for the ferroelectric ordering in the smectic C* phase. As mentioned above, these interactions should be sensitive to the chiral and polar molecular properties. Then it is useful to analyze the molecular structure of typical ferroelectric liquid crystals.

Ferroelectric liquid crystals can be obtained from the achiral smectogens through the replacement of a hydrogen atom in the alkyl chain by an appropriate group (CH_3, Cl, CN, etc.).[1,10,132] The same method is used in the synthesis of chiral nematics.[120] The schematic model of such chiral molecule is presented in Fig. 40. The chirality of the molecule i, in Fig. 40 is determined by the orientation of the substitution group with the long axis $\mathbf{o}_i$ with respect to the long axis of the whole molecule $\mathbf{a}_i$. The molecule is chiral if the vectors $\mathbf{a}_{ij}$, $\mathbf{m}_i$ $\mathbf{o}_i$ are not coplanar, i.e. $([\mathbf{a}_i\mathbf{m}_i]\mathbf{o}_i) \neq 0$. A possible effective bend angle $\epsilon << 1$ of the molecule is also shown in Fig. 40. Using the terminology proposed by Derzhanski and Petrov[152] one can say that the molecule i possesses the so-called steric dipole $|\mathbf{s}_i| = \epsilon D$, where D is the molecular diameter. It should be noted that an analogous molecular model was used by Van der Meer and Vertogen in the theory of cholesteric ordering.[153]

The chiral interaction between molecules, presented in Fig. 40, is determined by the interaction of the substitution group (i.e. the chiral centre) with the polarizable core of the neighbouring molecule. It should be stressed that maximum spontaneous polarization has been observed in smectics C* with a large dipole in the chiral part of the

Downloaded by [Tomsk State University of Control Systems and Radio] at 12:54 19 February 2013

Downloaded by [Tomsk State University of Control Systems and Radio] at 12:54 19 February 2013

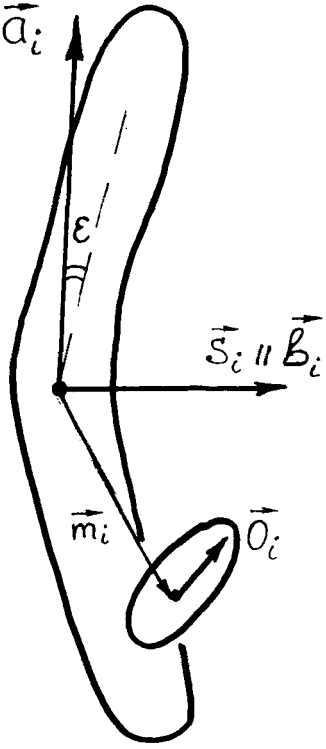

FIGURE 40 Model for a chiral molecule with transverse steric dipole s_i and substitution group of long axis o_i.

molecule.[118] The best known example of such ferroelectric liquid crystals is 4-hexybenzylidene-4′-amino(2-chloropropyl) cinnamate HOBACPC which possesses the dipole moment $d \simeq 2D$ due to the polar bond C—Cl in the chiral moiety. Thus, at least in the case of molecules with large transverse dipoles in the chiral part, the chiral interaction is mainly determined by the induction interaction between this dipole and the polarizable core of the neighbouring molecule.[121,122] The energy of the induction interaction, averaged over the rotation of molecule i about its long axis, is given by

$$V^*_{\text{ind}}(\mathbf{o}_i, \mathbf{a}_i, \mathbf{u}_{ij}) = J_1(i,j)[(\mathbf{o}_i\mathbf{a}_j) - 3(\mathbf{o}_i\mathbf{u}_{ij})]([\mathbf{o}_i\mathbf{a}_j]\mathbf{u}_{ij}), \tag{63}$$

with

$$J_1(i,j) = 3r_{ij}^{-7}\,\Delta\alpha_j d^2_{\perp i}(\mathbf{o}_i\mathbf{a}_i)([\mathbf{o}_i\mathbf{a}_i]\mathbf{m}_i) \tag{64}$$

where $\mathbf{d}_i = d_i\mathbf{o}_i$ is the dipole moment located in the chiral moiety of molecule i and $\Delta\alpha_j$ is the anisotropy of the polarizability of molecule j. Note that the chiral potential (63) cannot be used directly in the theory of ferroelectricity since it does not depend on the direction of the short molecular axis, and hence it cannot cause the ordering of transverse dipoles. Therefore, it is necessary to take into account the polar asymmetry of the molecule. A simple model of an asymmetric molecule is presented in Fig. 41. The anisotropic polarizability of molecule j in Fig. 41 is located at two effective centres 0_{i1} and 0_{j2} with point polarizabilities $\hat{\alpha}_{j1}$ and $\hat{\alpha}_{j2}$. The tensor $\hat{\alpha}_{j2}$ can be transformed into $\hat{\alpha}_{j1}$ by a small rotation. As a result the two induced dipoles make a small angle $\epsilon << 1$ as shown in Fig. 41. The present model represents the asymmetric molecular polarizability which can be related to the asymmetric molecular hard core.

Now the symmetry of chiral induction interaction between mole-

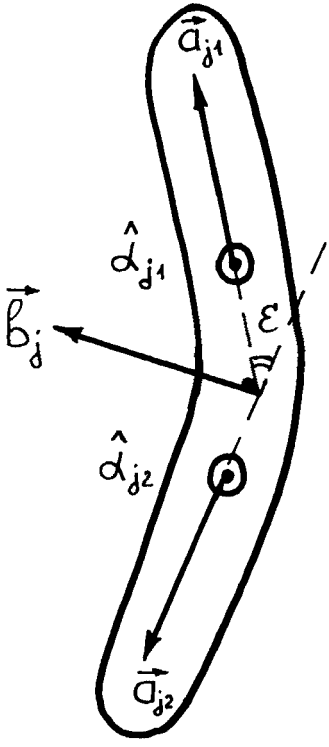

FIGURE 41 Model for an asymmetric molecule with polarizable centers.

Downloaded by [Tomsk State University of Control Systems and Radio] at 12:54 19 February 2013

cules i and j can be written as

$$V^*(i,j) = V^*_{ij} + V^*_{ji};$$

$$V^*_{ij} = V^*_{\text{ind}}(\mathbf{o}_i, \mathbf{a}_{j1}, \mathbf{r}_{ij1}) + V^*_{\text{ind}}(\mathbf{o}_i, \mathbf{a}_{i1}, \mathbf{r}_{ij1}) \tag{65}$$

where

$$\mathbf{r}_{ij\alpha} = |\mathbf{r}_{ij\alpha}|\mathbf{u}_{ij\alpha} = \mathbf{r}_{ij} + l\mathbf{a}_{j\alpha}; \quad \alpha = 1,2;$$

$$a_{j1,2} = \pm a_j + \epsilon b_j;$$

and l is the distance between two polarizable centres. The induction interaction V^*_{ind} between the chiral group and one of the polarizability centres is given by Eqs. (63), (64).

Expanding the interaction (65) in powers of ϵ one readily obtains

$$V^*(i,j) = V^*_{ij} + V^*_{ji};$$

$$V^*_{ij} = -U^*(r_{ij})(\mathbf{a}_i\mathbf{a}_j)(\mathbf{a}_j\mathbf{u}_{ij})([\mathbf{a}_i\mathbf{u}_{ij}]\mathbf{b}_j) + \mathbf{o}(\epsilon^2), \tag{66}$$

with

$$U^*(r_{ij}) = 72r_{ij}^{-8}l\epsilon d_i^2\Delta\alpha_j(\mathbf{o}_i\mathbf{a}_i)([\mathbf{o}_i\mathbf{a}_i]\mathbf{m}_i). \tag{67}$$

Thus, the consideration of the induction interaction between the dipole of the chiral group and the asymmetric polarizability of the neighbouring molecule results in the effective interaction potential which has the same mathematical form as the model one (see Eq. 59), constructed in the preceding section with the help of symmetry arguments. However, the analysis of the particular model yields an explicit expression (67) for the coupling constant $U^*(r_{ij})$. Note that $U^*(r_{ij})$ is proportional to the pseudoscalar $\Delta_i = (\mathbf{o}_i\mathbf{a}_i)([\mathbf{o}_i\mathbf{a}_i]\mathbf{m}_i)$ which reflects the molecular chirality and changes sign if the handedness of the molecule is reversed. The coupling constant $U^*(r_{ij})$ is proportional also to the square of the molecular transverse dipole, located in the chiral part, and to the parameter ϵ which characterizes the polar asymmetry of the molecule.

The model of a chiral molecule, presented in Fig. 40, enabled us to find some intermolecular forces which can be responsible for ferroelectric ordering in the smectic C* phase. These forces represent

Downloaded by [Tomsk State University of Control Systems and Radio] at 12:54 19 February 2013

Downloaded by [Tomsk State University of Control Systems and Radio] at 12:54 19 February 2013

the induction interaction between the constant dipole in the chiral center of the molecule and the polarizability of the nearest neighbours. Clearly, it is only an example of such forces. For example, the molecular polarity can influence the chiral intermolecular interaction through the polar asymmetry of molecular shape and not through the asymmetry of the quadrupole molecular polarizability. The general case will be considered in Section 4.3 with the help of the general molecular statistical theory.

Nevertheless, the qualitative arguments, presented here, enable one to conclude that the spontaneous polarization is influenced by every chiral intermolecular interaction potential which changes sign under rotation over 180° about one of the principal axes of the interacting molecules.

It is interesting to note that the chiral intermolecular interaction (59), (66) is essential only in tilted smectic phases. Indeed, in the cholesteric phase the molecular centres are randomly distributed (locally) and the potential (59) can be averaged over the intermolecular unit vector $\mathbf{u}_{ij}$. Then it can be readily shown that the averaged potential vanishes. On the other hand, for the smectic A phase the smectic plane normal $\mathbf{e}$ is parallel (or antiparallel) to the director $\mathbf{n}$ and the averaged potential (59) also vanishes since $[\mathbf{ne}] = 0$. Thus the chiral intermolecular interaction, considered above, is specific for ferroelectric liquid crystals.

4.3. The general theory of ferroelectric ordering

*4.3.1. Free energy of the smectic C**. It has been mentioned already that the dipole ordering is very weak in the smectic C* phase and the energy, associated with this ordering, is small compared with typical orientational intermolecular potentials. Therefore, ferroelectric ordering can be described with the help of a perturbation theory. Then the orientational distribution function $f_1(i)$ can be approximately expressed in the form: $f_1(i) = f_0(i)[1 + g_1(i)]$, where $f_0(i)$ is the distribution function of the nonchiral smectic C and the function $g_1(i)$ is small. The function $g_1(i)$ depends upon the direction of the short molecular axis $\mathbf{b}_i$ and hence determines the ferroelectric ordering in the smectic C* phase. Then the spontaneous polarization of the ferroelectric smectic C* can be written in the form

$$\mathbf{P} = \rho d_\perp \langle \mathbf{b}_i \rangle = \rho d_\perp \int \mathbf{b}_i f_0(i) g_1(i) d(i) \tag{68}$$

where $d(i) = \delta(\mathbf{a}_i \mathbf{b}_i) d^2\mathbf{a}_i d\mathbf{b}_i$. In Eq. (68) the short axis $\mathbf{b}_i$ is taken in the direction of the transverse molecular dipole $\mathbf{d}_\perp$, $\mathbf{d}_{\perp_i} = d_\perp \mathbf{b}_i$.

The functions $f_0(i)$ and $g_1(i)$ can be determined by minimization of the free energy density of the smectic C* phase. Let us consider the different contributions to this free energy.

In the molecular theory of liquid crystals the total intermolecular interaction potential is written as a sum of two parts which represent the hard core repulsion and the intermolecular attraction.[154,155] Then the attractive interaction is taken into account in the molecular field approximation while the repulsion is treated more exactly. As a result the free energy of a liquid crystal can be written in the form

$$F(\mathbf{r}_i) = \frac{1}{2}\rho^2 \int \Omega(\xi_{ij} - r_{ij})V(i,j)f_1(i)f_1(j)d^3\mathbf{r}_{ij}d(i)\mathrm{d}(j)$$

$$+ \frac{1}{2}\rho^2\lambda k_B\mathrm{T} \int \Omega(\xi_{ij} - r_{ij})f_1(i)f_1(j)d^3\mathbf{r}_{ij}d(i)\mathrm{d}(j)$$

$$- k_B\mathrm{T}\rho \int f_1(i)\ \ln f_1(i)d(i) \tag{69}$$

where $V(i,j)$ is the attractive interaction energy between molecules i and j and ξ_{ij} is the closest distance of approach for these molecules. $\Omega(\xi_{ij} - r_{ij})$ is a stepfunction, $\Omega(\xi_{ij} - r_{ij}) = 0$ if the molecules penetrate, i.e. $r_{ij} < \xi_{ij}$, and $\Omega(\xi_{ij} - r_{ij}) = 1$ if $r_{ij} > \xi_{ij}$. The function ξ_{ij} is completely determined by the molecular shape and depends on the relative orientation of the molecules i and j. The constant λ is a function orelative orientation of the molecules i and j. The constant λ is a function of the number density ρ and molecular dimensions. In the first approximation $\lambda = 1$.[156]

The first term in Eq. (69) is the internal energy of a liquid crystal. The stepfunction $\Omega(\xi_{ij} - r_{ij})$ determines the excluded volume for the centers of the two molecules and hence the attraction is modulated by the asymmetric molecular shape. The second term in Eq. (69) is the so-called packing entropy and the third one is the mixing entropy of a liquid crystal.

The distribution function $f_1(i)$ can be determined by minimization of the free energy density (69) taking into account the normalization conditions for the functions $f_1(i)$ and $f_o(i)$. Note that the distribution function $f_o(i)$ correspond to a minimum of the free energy (69) in the case of an achiral liquid crystal. When the molecular chirality is included, the attration interaction energy $V(i,j)$ is changed slightly and the free energy minimum is determined by the distribution function $f_1(i)$. Then the function $g_1(i)$ is determined by the chiral part of the intermolecular attraction and repulsion. The resulting expression for $g_1(i)$ can be substituted into Eq. (68). Finally one obtaines the fol-

Downloaded by [Tomsk State University of Control Systems and Radio] at 12:54 19 February 2013

lowing general equation for the spontaneous polarization of smectic C*

$$\mathbf{P} = -\rho^2\beta d_\perp \int \mathbf{b}_i \Omega(\xi_{ij} - r_{ij})[V(i,j) + k_B T] f_o(i) f_o(j) d^3\mathbf{r}_{ij} d(i) d(j). \quad (70)$$

It can be shown that the spontaneous polarization (70) vanishes in the nematic (cholesteric) phase for an arbitrary intermolecular interaction. This general result can be obtained based on symmetry grounds as discussed in Section 4.2. It is obvious also that the spontaneous polarization vanishes if the functions $V(i,j)$ and $\Omega(\xi_{ij} - r_{ij})$ are odd in $\mathbf{b}_i$, i.e. if the molecules are nonpolar in the transverse direction. However, the polar asymmetry of a molecule is not a sufficient property for ferroelectric ordering since the spontaneous polarization (70) vanishes also in the case of a nonchiral liquid crystal. Thus, ferroelectric ordering in the smectic C* phase is determined by chiral and polar terms in the intermolecular interaction potential.

In the general case the dipolar ordering can be caused by chiral and polar asymmetry of the molecular shape. Then it is sufficient to consider the isotropic attraction $V(i,j) = V(r_{ij})$. On the other hand, the experimental facts indicate[132] that the polarization in the smectic C* phase is affected more by the molecular dipole than by the molecular shape. Therefore, it is reasonable to neglect the chirality of the molecular shape and take into account only the chiral part of the dispersion interaction $V^*(i,j)$. In this case Eq. (70) can be rewritten in the form

$$\mathbf{P} = -\rho^2\beta d_\perp \int \mathbf{b}_i \Omega(\xi_{ij} - r_{ij}) V^*(i,j) d^3\mathbf{r}_{ij} d(i) d(j) \quad (71)$$

Eq. (71) indicates that the spontaneous polarization is determined by chiral attraction interaction $V^*(i,j)$ modulated by anisotropic repulsion.

According to Eq. (71) the polarization $\mathbf{P}$ does not vanish only if the product $\Omega(\xi_{ij} - r_{ij})V^*(i,j)$ is odd in $\mathbf{b}_i$. This property can be related to the asymmetry of the chiral attraction potential $V^*(i,j)$ or (and) to the polar asymmetry of the molecular shape. In the latter case the closest distance of approach for molecules i and j can be approximately written as

$$\xi_{ij} = \xi_{ij}^0 + (D/4L)[(\mathbf{S}_i\mathbf{u}_{ij}) + (\mathbf{S}_j\mathbf{u}_{ij})] \quad (72)$$

where $\mathbf{S}_i = D\epsilon\mathbf{s}_i$ is the transverse steric dipole of molecule i, $|\mathbf{s}_i| = 1$, and $\epsilon << 1$ is the effective bend angle. The function ξ_{ij}^0 is the closest distance of approach for the two molecules without steric dipoles, i.e. $\xi_{ij} \to \xi_{ij}^0$ when $\epsilon \to 0$.

Downloaded by [Tomsk State University of Control Systems and Radio] at 12:54 19 February 2013

Downloaded by [Tomsk State University of Control Systems and Radio] at 12:54 19 February 2013

The general Eq. (71) can be symplified in the case of ideal orientational and translational order. Indeed, in the smectic phase the orientational order is rather high, $S \simeq 0.8$–0.9.[145] The translational order is also high in ferroelectric smectics C* since the majority of ferroelectric liquid crystals exhibit the smectic A phase at higher temperatures. Therefore, it is possible to neglect the influence of the orientational and translational order variation on the spontaneous polarization of the smectic C* phase. In this case one obtaines

$$\mathbf{P} = -\rho^2\beta d_\perp[(1-\sigma)\int \mathbf{W}(\mathbf{n},\mathbf{u}_{ij})\delta(\mathbf{u}_{ij}\mathbf{e})d^2\mathbf{u}_{ij} + \sigma\mathbf{W}(\mathbf{n},\mathbf{e}), \quad (73)$$

with

$$\mathbf{W}(\mathbf{n},\mathbf{u}_{ij}) = \int \mathbf{b}_i\left\{\int \Omega(\xi_{ij}^0 - r_{ij})V^*(i,j)r_{ij}^2 dr_{ij} + (D/4L)V^*(i,j)\Big|_{r_{ij}=\xi_{ij}^0}^{(\xi_{ij}^0)^2}[(\mathbf{S}_i\mathbf{u}_{ij}) + (\mathbf{S}_j\mathbf{u}_{ij})]\right\}d\mathbf{b}_i d\mathbf{b}_j \quad (74)$$

where σ is the fraction of the nearest neighbors of a given molecule located in the same plane. The first term in Eq. (73) determines the contribution from the interaction of the molecules located in the same smectic plane, while the second term corresponds to molecules located in the adjacent smectic layers. The spontaneous polarization is determined by the effective potential $\mathbf{W}(\mathbf{n},\mathbf{u}_{ij})$ which in turn is a sum of two terms given by Eq. (74). The first term in Eq. (74) is a contribution from the asymmetric polar part of the chiral attraction $V^*(i,j)$ modulated by the averaged (uniaxial) molecular shape. In contrast, the second term in Eq. (74) is a contribution from the symmetric part of the chiral interaction potential $V^*(i,j)$ modulated by the asymmetric molecular shape. Thus, ferroelectric ordering can be explained with the help of two different molecular models which will be considered below.

4.3.2. Ferroelectric ordering in smectic C composed of molecules with steric dipoles.* The steric dipole $\mathbf{S}_i$ characterizes the polar asymmetry of the molecular shape. For a banana-like molecule presented on Fig. 40 the steric dipole is expressed as $|\mathbf{S}_i| = D\epsilon$, where ϵ is the bend angle. It is clear that the asymmetric shape of many real molecules cannot be approximated by the banana-like model. Then the parameter ϵ has no direct interpretation and can be considered as an effective measure of the asymmetry.

Downloaded by [Tomsk State University of Control Systems and Radio] at 12:54 19 February 2013

Let us consider again the model of a chiral molecule presented on Fig. 40. As mentioned in section 4.2, the chiral interaction between such molecules is determined by the interaction between the chiral center of one molecule and the polarizable core of another one. In the general case the chiral attractive interaction is a part of the dispersion interaction between chiral molecules. The dispersion interaction can be divided into the induction interaction between permanent multipoles and the polarizability of the neighboring molecules, and the purely dispersion interaction between molecular polarizabilities.[157] In this section we consider the model of a chiral molecule with a large dipole in the chiral part. In this case the predominant part of the chiral attraction is the induction interaction between the dipole $\mathbf{d}_i$ and the polarizability of the neighboring molecule. Note that the corresponding purely dispersion interaction is much weaker since the polarizability of the chiral group is small.

The simplest chiral induction interaction which contributes to the spontaneous polarization of the smectic C*[121] is the dipole–dipole, dipole–quadrupole induction interaction,

$$V_{ddq}(i,j) = V_{ij} + V_{ji} \tag{75}$$

with

$$V_{ij} = r_{ij}^{-7} \sum_{nj} (E_{oj} - E_{nj})^{-1} \langle o_j|U_{dq}(i,j)|n_j\rangle\langle n_j|U_{dd}(i,j)|o_j\rangle + c.c. \tag{76}$$

where $\langle o_j|$ and $\langle n_j|$ represent the ground state and the excited state of molecule j, respectively, and $E_{oj} - E_{nj}$ is the excitation energy of the molecule. The potentials $U_{dd}(i,j)$ and $U_{dq}(i,j)$ correspond to dipole–dipole and dipole–quadrupole interaction energies, respectively, which can be written as

$$U_{dd}(i,j) = \int e(\boldsymbol{\rho}_j)[3(\boldsymbol{\rho}_j\mathbf{u}_{ij})(\mathbf{d}_i\mathbf{u}_{ij}) - (\boldsymbol{\rho}_j\mathbf{d}_i)]d^3\boldsymbol{\rho}_j; \tag{77}$$

$$\begin{aligned} U_{dq}(i,j) = \int e(\boldsymbol{\rho}_j)\Bigg[&\frac{3}{2}\, d_i^2(\boldsymbol{\rho}_j\mathbf{u}_{ij}) + 3(\mathbf{d}_i\boldsymbol{\rho}_j)(\mathbf{d}_i\mathbf{u}_{ij}) \\ &- \frac{15}{2}\,(\mathbf{d}_i\mathbf{u}_{ij})^2(\boldsymbol{\rho}_j\mathbf{u}_{ij}) - \frac{3}{2}\,(\boldsymbol{\rho}_j)^2(\mathbf{d}_i\mathbf{u}_{ij}) \\ &- 3(\mathbf{d}_i\boldsymbol{\rho}_j)(\boldsymbol{\rho}_j\mathbf{u}_{ij}) + \frac{15}{2}\,(\boldsymbol{\rho}_j\mathbf{u}_{ij})^2(\mathbf{d}_i\mathbf{u}_{ij})\Bigg]d^3\boldsymbol{\rho}_j; \end{aligned} \tag{78}$$

where $\mathbf{d}_i$ is the permanent dipole of molecule i, $e(\boldsymbol{\rho}_j)$ is the charge density of molecule j and $\boldsymbol{\rho}_j$ is the vector pointing from the center of mass of molecule j to the given point.

Substituting Eqs. (75)–(78) into the general Eq. (73) one obtains, after some mathematical manipulations, the final expression for the spontaneous polarization of smectic C*

$$\mathbf{P} = \mu(\mathbf{n}\ \mathbf{e})[\mathbf{n}\ \mathbf{e}] \tag{79}$$

with

$$\mu = -\frac{1}{4}(\rho^2/k_B\mathrm{T})(\mathbf{S}\ \mathbf{d})\Delta(D^6/L)\sigma(2\chi_\perp + 15\ \Delta\chi + \Delta\chi_\perp), \tag{80}$$

and

$$\Delta = (\mathbf{d}_i\mathbf{a}_i)([\mathbf{d}_i\mathbf{m}_i]\mathbf{a}_i) \tag{81}$$

Here $\Delta\chi = \chi_{zz} - (\chi_{xx} + \chi_{yy})/2$ is the anisotropy of molecular polarizability, $\chi_\perp = \chi_{xx} + \chi_{yy}$ is the transverse molecular polarizability and $\Delta\chi_\perp = \chi_{xx} - \chi_{yy}$ is the anisotropy of the transverse polarizability.

Note that the spontaneous polarization (79, 80) is proportional to the fraction of nearest neighbors located in the smectic plane. It can be shown[121] that the contribution from molecules located in adjacent planes is proportional to the small parameter $(D/L)^5$ and hence it can be neglected. It is interesting to note also that the polarization $\mathbf{P}$ depends on the angle between the steric dipole $\mathbf{S}$ and the electric dipole $\mathbf{d}$ of the same molecule. In the limiting case, when $\mathbf{S}\perp\mathbf{d}$, the steric dipoles can be still ordered due to the steric intermolecular interaction while the electric dipoles are disordered and the spontaneous polarization is absent.

In conclusion, ferroelectric ordering in the smectic C* phase consisting of molecules with large steric dipoles is determined mainly by the induction interaction between the chiral group and the polarizable core of neighboring molecules. The latter interaction is modulated by short range steric forces.

4.3.3. Ferroelectric ordering in the system of symmetric molecules. When the molecules do not possess steric dipoles the ferroelectric ordering can be determined by the polar part of the chiral dispersion intermolecular interaction. In this case one is interested in the chiral attraction potential which changes sign under the 180°

Downloaded by [Tomsk State University of Control Systems and Radio] at 12:54 19 February 2013

rotation of the molecular coordinate frame about the long axis $\mathbf{a}_i$. It can be shown that the dipole–dipole, dipole–quadrupole induction (or dispersion) interaction, considered in the previous section, does not possess all the necessary properties. The simplest chiral and polar dispersion interaction potential is related to the r_{ij}^{-8} term in the general expansion of the dispersion interaction

$$V_{dq}(i,j) = V_{dqj} + V_{dqi}, \tag{82}$$

with

$$V_{dqi} = r_{ij}^{-8} \sum_{ki} (E_{oi} - E_{ki})^{-1} \langle o_i | U_{dq}(i,j) | k_i \rangle \langle k_i | U_{dq}(i,j) | o_i \rangle \tag{83}$$

where $U_{dq}(i,j)$ is the dipole–quadrupole interaction potential given by Eq. (78). Substituting Eqs. (83) and (78) into the general Eq. (73) one arrives at the familiar expression for the spontaneous polarization

$$\mathbf{P} = \mu(\mathbf{n}\ \mathbf{e})[\mathbf{n}\ \mathbf{e}] \tag{84}$$

with

$$\mu = -0.45(\rho^2/k_B T)\ \Delta D^{-5}\ \sigma(Q_{xx} + Q_{yy})\chi_\perp, \tag{85}$$

where the pseudoscalar parameter Δ and the transverse molecular polarizability $\chi_\perp$ are given by Eqs. (81) and (80), respectively, and Q_{xx}, Q_{yy} are the components of the molecular quadrupole.

The parameter μ in Eq. (85) is determined by the interaction between the permanent quadrupole $Q_{\alpha\alpha}$ of the given molecule and the induced dipoles of nearest neighbors. Therefore, it depends on the dipolar polarizability $\chi_\perp$. Note that in the derivation of Eq. (85) we have neglected the contribution from the interaction between the permanent dipole and the quadrupolar polarizability since it is expected to be small.[121]

4.3.4. Discussion. In sections 4.3.2 and 4.3.3 we have considered two different intermolecular interactions which can be responsible for ferroelectric ordering in the smectic C* phase. The first contribution is related to the induction interaction between the dipole of the chiral group and the polarizability of the neighboring molecule modulated by the asymmetric molecular shape. In this case the molecule possesses a steric dipole (which is proportional to the average

Downloaded by [Tomsk State University of Control Systems and Radio] at 12:54 19 February 2013

bend angle ϵ in the case of banana-like molecules) and the ferroelectric ordering is a consequence of the ordering of steric dipoles. Note that the corresponding contribution to the spontaneous polarization is proportional to $\cos\psi = (\mathbf{Sd})$, where ψ is the angle between the electric and steric dipoles.

Thus, in smectic C* composed of molecules with large steric dipoles, the phenomenological constant μ is related to the following molecular model parameters: the electric dipole **d**, the steric dipole **S**, the components of the molecular polarizability $\chi_{\alpha\alpha}$, $\alpha = x,y,z$, the molecular length L and the diameter D.

The second contribution to the spontaneous polarization is determined by the chiral induction interaction between the permanent quadrupole and the polarizability of neighboring molecules. Therefore, if the steric dipole is small enough, the constant μ is related to the dipole $\mathbf{d}_\perp$, quadrupole $Q_{\alpha\alpha}$, ($\alpha = x,y,z$) and the transverse polarizability $\chi_\perp$.

In the general case the spontaneous polarization is determined by both contributions and it is difficult to conclude which contribution is predominant in real ferroelectric liquid crystals. The answer to this question depends on the detailed experimental information. However, at present there is an argument in favor of the interaction associated with steric dipoles. Indeed, it will be shown in section 5.3 that the steric interaction between asymmetric banana-like molecules results in the strong temperature variation of the helical pitch in the smectic C* phase. Thus the model of a molecule with steric dipole enables one to explain different properties of ferroelectric liquid crystals.

The general statistical theory supports the main qualitative results which have been obtained in sections 4.2, 4.1 with the help of a simple model. In both cases the spontaneous polarization is proportional to the pseudoscalar parameter $\Delta = (\mathbf{da})([\mathbf{da}]\mathbf{m})$ which characterizes the chirality of the molecule with a substitution group, presented on Figs. 40, 42. The parameter Δ determines the variation of the spontaneous polarization with the change in position and orientation of the chiral group with respect to the molecular hard core. The polarization depends also on the molecular dipole **d**. Note that $P \sim d^3$ within the model of molecules with steric dipoles. This result enables one to explain the large value of the spontaneous polarization in ferroelectric liquid crystal HOBACPC which possesses the strongly polar C—Cl bond in the chiral part of the molecule. The correlations between the experimentally observed spontaneous polarization and the dipole **d**

Downloaded by [Tomsk State University of Control Systems and Radio] at 12:54 19 February 2013

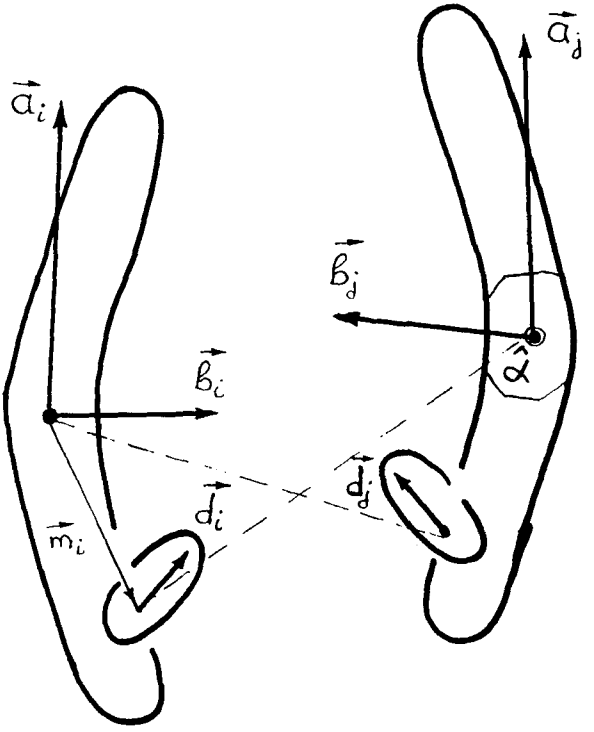

FIGURE 42 Interaction of molecules "*i*" and "*j*" with large dipoles.

and the polarizability χ of the molecule will be discussed in more detail in the following section.

It should be stressed that in the present model the molecule is considered to be rigid and possible rotations of the dipole with respect to the chiral group are not taken into account. It is clear that such rotations can reduce the spontaneous polarization substantially. In the first approximation the reduction of the spontaneous polarization is determined by the parameter $\langle \cos \psi \rangle$, which characterizes the rotational freedom of the dipole. Then the polarization $P \approx P_o \langle \cos \psi \rangle$, where P_o is calculated in the model of rigid molecules. The analysis of experimental data shows that the reduction of the spontaneous polarization is large when the dipole is located far from the chiral center. For example, in the ferroelectric smectic DOBAMBC the predominant contribution to the dipole moment of a molecule is related to the polar bond C=O which is separated from the chiral

Downloaded by [Tomsk State University of Control Systems and Radio] at 12:54 19 February 2013

Downloaded by [Tomsk State University of Control Systems and Radio] at 12:54 19 February 2013

center by the CH_2 group. As a result, the spontaneous polarization in DOBAMBC is rather low, $P \sim 10^{-9}$ C/cm^2. On the other hand, the molecular structure of the ferroelectric liquid crystal DOBA—I—MPC is the same as that of DOBAMBC with the only exception that the C=O group is directly attached to the chiral center. This minor change in the molecular structure results in a substantial growth of the spontaneous polarization which acquires the value of $1.8\ 10^{-8}$ C/cm^2.[105] The large spontaneous polarization in DOBA—I—MPC is related also to the location of the dipole, which is attached directly to the chiral group. Therefore, the dipole takes part in the chiral induction interaction with the neighboring molecules according to the theory presented above. In contrast, when the dipole is located far from the chiral center the chiral intermolecular interaction potential is determined by the relatively weak dispersion interaction between the polarizability of the chiral group and the polarizability of the neighboring molecule. In this case the spontaneous polarization is proportional to d (and not to d^3, as in section 4.3.2) and to the parameter $\Delta' = (\mathbf{a}_i\mathbf{o}_i)([\mathbf{o}_i\mathbf{a}_i]\mathbf{m}_i)$, where $\mathbf{o}_i$ is a unit vector in the direction of the long axis of the chiral substitution group.

4.4. Ferroelectricity in mixtures

The statistical theory of ferroelectric ordering in the smectic C* phase can be generalized to the case of many-component liquid crystals.[121] In the general situation the spontaneous polarization of the mixture is a sum of the contributions from all the components $l = 1,2$.

$$\mathbf{P} = \sum_l \rho x_l d_{\perp l} \langle \mathbf{b}_{il} \rangle, \tag{86}$$

where ρx_l is the number density of component l, $\Sigma x_l = 1$. Taking into account only pair intermolecular interactions we arrive at the following expression for the internal energy of the mixture

$$U = \frac{1}{2} \rho^2 \sum_{k,l} x_l x_k \langle V_{kl}(i,j) \rangle, \tag{87}$$

where $V_{kl}(i,j)$ is the interaction potential for molecule i of component k and molecule j of component l. Then the spontaneous polarization of the mixture is also a quadratic function of the concentrations x_l

$$\mathbf{P} = \mu(\mathbf{n}\ \mathbf{e})[\mathbf{n}\ \mathbf{e}]$$

with

$$\mu = \sum_{k,l} x_k x_l \mu_{kl} \tag{88}$$

Here the constant μ_{kl} $(k,l = 1,2, \ldots)$ is determined by the interaction between a molecule of component k and a molecule of component l. The constant μ_{kk} is determined by the interaction of identical molecules and is given by Eq. (80) in the case of molecules with large steric dipoles. The constants μ_{kl} $(k \neq l)$ are related to the interaction between different molecules and depend on the molecular parameters of both components k and l. In the model of molecules with large steric dipoles the constants μ_{kl} are given by the following expressions

$$\mu_{kl} = (\mathbf{S}_k \mathbf{d}_k)(\Delta_k w_{kl1} + \Delta_l w_{kl2}), \tag{89}$$

with

$$w_{kl1} = -\frac{1}{4}(\rho^2/k_B T)\sigma\, D_k^{-4} L_k^{-1} (2\,\chi_{\perp l} + 15\,\Delta\chi_l), \tag{90}$$

$$w_{kl2} = -\frac{1}{4}(\rho^2/k_B T)\sigma\, D_k^{-4} L_k^{-1}\, \Delta\chi_{\perp l}, \tag{91}$$

and

$$\Delta_k = (\mathbf{d}_k \mathbf{a}_k)([\mathbf{d}_k \mathbf{m}_k]\mathbf{a}_k). \tag{92}$$

Here the parameter Δ_k reflects the chirality of the component k. Note that $\mu_{kl} \neq \mu_{lk}$.

At present many-component ferroelectric liquid crystals are considered to be the promising materials for technical applications. It is reasonable, therefore, to discuss different kinds of such mixtures in more detail.

4.4.1. Binary mixtures of ferroelectric liquid crystals. In this case both components exhibit the ferroelectric smectic C* phase and the spontaneous polarization of the mixture is a quadratic function of the concentrations x_A and x_B, $x_A + x_B = 1$. In fact the concentration dependence of the polarization is even more complicated since the transition temperature T_{AC}, and hence the tilt angle θ, is also a function of a x_A, x_B. The nonlinear concentration dependence of the

Downloaded by [Tomsk State University of Control Systems and Radio] at 12:54 19 February 2013

Downloaded by [Tomsk State University of Control Systems and Radio] at 12:54 19 February 2013

spontaneous polarization has been observed by different authors.[129,158] It should be noted, however, that the strongly nonlinear concentration dependence is expected only for mixtures of liquid crystals which correspond to different chemical classes. In mixtures of smectics C* composed of similar molecules one can neglect the concentration dependence of the tilt angle θ and put $\mu_{AB} + \mu_{BA} = \mu_{AA} + \mu_{BB}$. Then the general Eq. (88) results in a linear concentration dependence of the phenomenological constant

$$\mu = \mu_{AA}x_A + \mu_{BB}x_B \tag{93}$$

The nearly linear concentration dependence of the spontaneous polarization has been observed in mixtures of different members of a homologous series,[97] of smectics C* with similar molecular structure[158] and even in mixtures of DOBAMBC and HOBACPC.[129] Note that in mixtures of a right-handed and left-handed smectics C* the constants μ_{AA} and μ_{BB} have opposite signs and hence the spontaneous polarization can vanish at an appropriate concentration ratio x_A/x_B. This effect has been observed in Ref. 129.

4.4.2. Achiral smectics C doped with chiral molecules. The spontaneous polarization in an achiral smectic C doped with various chiral molecules has been observed by many authors.[70,100,116,118,132,159] The ferroelectric properties of such mixtures can be naturally explained by the present theory. Indeed, let us denote the concentration of the chiral molecules by x_B. Then the general Eq. (88) for the spontaneous polarization can be rewritten as

$$\mathbf{P} = \mu\,(\mathbf{n}\,\mathbf{e})\,[\mathbf{n}\,\mathbf{e}]$$

with

$$\mu = \tilde{\mu}_{AB}\,x_A x_B + \mu_{BB}x_B^2, \qquad \mu_{AB} = \mu_{AB} + \mu_{BA} \tag{94}$$

The parameter $\mu_{AA} = 0$ because component A is achiral.

When the concentration of chiral molecules is small ($x_B << 1$) the second term in Eq. (94) can be neglected and we arrive at

$$\mu = \tilde{\mu}_{AB}x_B, \qquad x_B << 1. \tag{95}$$

i.e. the polarization is proportional to the concentration of chiral molecules. This concentration dependence has been observed in all experiments at small x_B.

Thus, the spontaneous polarization in an achiral smectic C doped with chiral molecules is caused by the interaction between the nonchiral molecules of the matrix and the chiral molecules of the admixture. This interaction results in nonzero μ_{AB}. The explicit expression for μ_{AB} can be obtained with the help of Eqs. (89)–(91). In the model of molecules with steric dipoles one obtains

$$\mu_{AB} = -\frac{1}{4}(\rho^2/k_B\mathrm{T})\sigma\Delta_B\,[(\mathbf{S}_A\mathbf{d}_A)\,D_A^{-4}\,L_A^{-1}\,\Delta\chi_{\perp B} + (\mathbf{S}_B\mathbf{d}_B)\,D_B^{-4}L_B^{-1}\,(2\,\chi_{\perp A} + 15\,\Delta\chi_A)], \quad (96)$$

where the parameter Δ_B, given by Eq. (92) with $k = B$, characterizes the chirality of the admixture.

It follows from Eq. (96) that the maximum spontaneous polarization can be obtained in mixtures of strongly chiral molecules with large transverse dipoles and an appropriate smectic C composed of molecules with transverse dipoles. When $d_{\perp B} >> d_{\perp A}$, the contribution from the second term in Eq. (96) is predominant and the spontaneous polarization strongly depends on the dipole moment of the chiral molecule, $\mathrm{P} \sim d_B^3$. This correlation between the spontaneous polarization and the dipole moment is supported by experiment.[132] The correlations between the polarization and the polarizability of the matrix χ_A are discussed in Ref. 132.

4.4.3. Ferroelectric liquid crystals doped with nonchiral molecules. In this case the constant μ is given by

$$\mu = \mu_{AA}x_A^2 + \mu_{AB}x_Ax_B$$

where x_B is the concentration of achiral molecules. The spontaneous polarization $\mathrm{P} = \mathrm{P}_o - \gamma x_B$ is a decreasing function of the concentration of achiral molecules. This result is also in agreement with experiment.[58,160]

In conclusion, it should be noted that the general theory, discussed in this section, can be used also in the description of ferroelectric liquid crystals composed of molecules with different structure which can not be represented by the model of Fig. 40. For example, one can use cholesterol derivatives, etc. In this case the explicit expressions for the spontaneous polarization, obtained in this review, are not valid. However, one can obtain new results with the help of the general expressions presented in section 4.3 provided the appropriate

Downloaded by [Tomsk State University of Control Systems and Radio] at 12:54 19 February 2013

expressions for the chiral intermolecular interaction potential are available. In the most general case we can conclude that the chiral part of the dispersion interaction, modulated by the asymmetric molecular shape, can be responsible for the ferroelectric ordering.

Downloaded by [Tomsk State University of Control Systems and Radio] at 12:54 19 February 2013

5. MOLECULAR THEORY OF FLEXOELECTRICITY AND HELICOIDAL TWISTING IN FERROELECTRIC LIQUID CRYSTALS

5.1. Introduction

The flexoelectric effect in liquid crystals manifests itself in the appearance of an induced polarization under the condition of applied strain. The origin of flexoelectricity is not related to the molecular chirality and hence the flexoelectric properties of the ferroelectric smectic C* phase are analogous to those of achiral smectics C. On the other hand, the flexoeffect influences the ferroelectric properties of the C* phase. Indeed, in the chiral smectic C* phase the spontaneous twist of the director around the smectic plane normal results in the additional flexoelectric contribution to the polarization of the smectic layer. Thus the flexoelectric effect contributes to the spontaneous polarization, static dielectric constant and other parameters of ferroelectric liquid crystals. Then it becomes obvious that a consistent microscopic description of the ferroelectric state is impossible without a molecular theory for the flexoelectricity in the smectic C phase.

In smectics, the flexoelectricity can be related both to the inhomogeneous director field and to the distortion of the smectic layers.[17] In the present paper, however, we shall not take into account the latter effect since smectic layers can be distorted only by strong external fields or stresses. The corresponding effect is important in smectics A because the director is always normal to the smectic plane in the A phase. On the other hand, in the smectic C phase the inhomogeneous orientation of the director is the most important effect and the flexoelectric properties of smectics C are partially analogous to those of nematics.

In the nematic phase there are two independent contributions to the induced polarization

$$\mathbf{P} = e_1\, \mathbf{n}(\nabla\mathbf{n}) + e_3\, (\mathbf{n}\nabla)\mathbf{n}. \tag{97}$$

The smectic C phase is biaxial and is characterized by two independent unit vectors: the director **n** and the smectic plane normal **e** (see Fig. 39), (**ne**) = cos θ. Note that the unit vector **e** is fixed in the laboratory frame while the director orientation is changed in the deformed smectic C. As a result one can distinguish between three orthogonal contributions to the polarization induced by the flexoelectric effect: $\mathbf{P}_o$, $\mathbf{P}_\perp$, $\mathbf{P}_\parallel$. The vectors $\mathbf{P}_o$, $\mathbf{P}_\perp$, $\mathbf{P}_\parallel$ are shown on Fig. 39. Note that the vector $\mathbf{P}_o$ is in the direction of the spontaneous polarization in the chiral smectic C* phase, i.e. $\mathbf{P}_o \| [\mathbf{ne}]$. Three contributions to the induced polarization correspond to three independent flexocoefficient μ_f, μ_f' and μ_f'', as discussed in section 2.2. The corresponding contributions to the free energy of the smectic C phase are given by Eq. (21). For the comparison with the results of the molecular theory discussed in the following section it is convenient to rewrite this expression in the form

$$\Delta F_{fe} = -\mu_f n_z\left(\mathbf{P}_o \frac{\partial \mathbf{n}}{\partial z}\right) - \mu_f^\perp n_z\left(\mathbf{P}_\perp \frac{\partial \mathbf{n}}{\partial z}\right) - \mu_f^\parallel (\mathbf{P}_\parallel \mathbf{n})(\nabla_\perp \mathbf{n}), \quad (98)$$

where the **z** axis is parallel to the smectic plane normal **e** and $\nabla_\perp = \nabla - \mathbf{e}\nabla_z$. It should be noted that in the smectic A phase the vectors $\mathbf{P}_o$ and $\mathbf{P}_\perp$ are equivalent and hence $\mu_f - \mu_f^\perp \sim \theta^2$ when $\theta << 1$. At small tilt angle θ

$$\mathbf{P}_o \sim \mu_f \theta \frac{\partial \varphi}{\partial z}, \qquad P_\perp \sim \mu_f^\perp \frac{\partial \theta}{\partial z}, \quad (99)$$

where φ is the azimuthal angle which determines the orientation of the director in the projection to the smectic plane

$$n_x = \sin\theta \cos\varphi, \qquad n_y = \sin\theta \sin\varphi, \qquad n_z = \cos\theta.$$

Thus, the induced polarizations $\mathbf{P}_o$ and $\mathbf{P}_\perp$ correspond to different distortions of the director field **n**(**r**) in the C phase. The polarization $\mathbf{P}_o$ is nonzero when the orientation of the director **n**(**r**) is different in the adjacent smectic layers, while the polarization $\mathbf{P}_\perp$ is related to the gradient of the tilt angle $\theta(z)$. The polarization $\mathbf{P}_\parallel$ is induced by a bending strain within the smectic layer.

From the microscopic point of view there exist two different interpretations of the flexoelectric effect in liquid crystals. The first interpretation (dipolar flexoeffect) was proposed by R. Meyer[161] who

Downloaded by [Tomsk State University of Control Systems and Radio] at 12:54 19 February 2013

assumed that the macroscopic polarization is related to the orientation of asymmetric polar molecules in the distorted liquid crystal. One can assume that the molecule possess a geometrical asymmetry which can be related to different end chains (effective wedge-like shape) or to a small molecular bend (effective banana-like shape). In the general case the polar geometrical asymmetry can be represented by the steric dipole. In the distorted liquid crystal the opposite directions of the steric dipole are nonequivalent and hence the dipoles are partially ordered. In this situation the macroscopic polarization is observed if the molecules also possess electric dipoles.

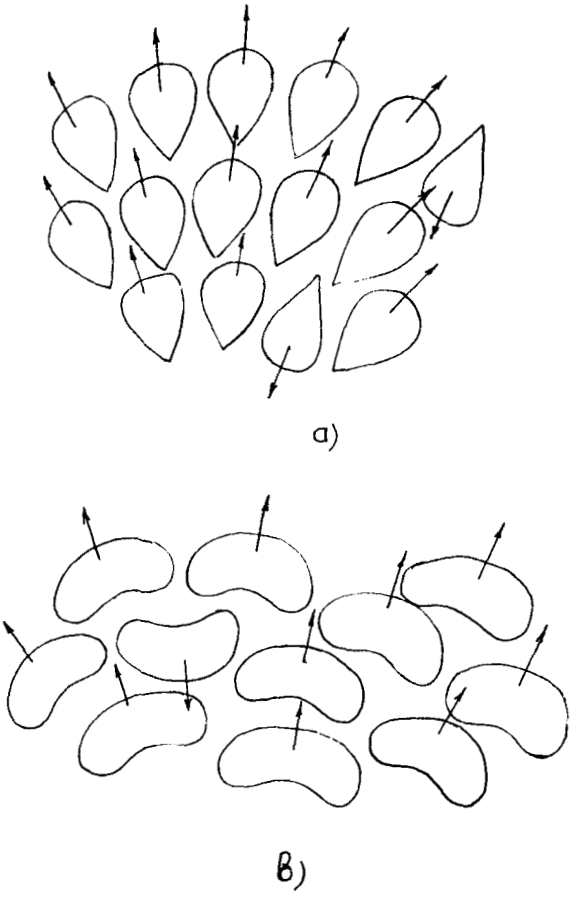

FIGURE 43 Ordering of electric and steric dipoles in distorted liquid crystals composed of cone-like (a) or banana-like (b) molecules.

Downloaded by [Tomsk State University of Control Systems and Radio] at 12:54 19 February 2013

The quadrupolar interpretation of the flexoelectricity is related to the fact that the very symmetry of liquid crystals leads to nonzero quadrupole density. Then the macroscopic polarization can be caused by the gradient of the quadrupole density in a distorted liquid crystal. The quadrupolar flexoeffect is more general since it does not require steric or electric molecular dipoles.

In the smectic C phase both contributions to the flexoelectric effect are important. It will be shown, however, that these contributions correspond to essentially different θ dependences of the flexocoefficients. The quadrupolar contribution to the flexocoefficient μ_f appears to be a constant while the dipolar one strongly depends on the tilt angle θ. This result enables one to explain the strong temperature variation of the helical pitch in the chiral smectic C* phase as shown in section 5.3.

5.2. Dipolar and quadrupolar flexoelectricity

In the most general case the macroscopic polarization in a liquid crystal can be written as

$$\mathbf{P} = \rho\langle\mathbf{d}_i\rangle + \rho\boldsymbol{\nabla}\cdot\langle\hat{Q}_i\rangle \tag{100}$$

where $\mathbf{d}_i$ is the dipole and $\hat{Q}_i$ is the quadrupole of the molecule "i". Let us consider first the quadrupolar flexoeffect which is determined by the second term in Eq. (100).

Let us assume for simplicity that the molecular quadrupole tensor $\hat{Q}$ is diagonal in the molecular reference system which is determined by the long axis $\mathbf{a}_i$ and short axes $\mathbf{b}_i$ and $\mathbf{c}_i$, $\mathbf{b}_i \perp \mathbf{c}_i \perp \mathbf{a}_i$. Then the averaged quadrupolar density in the smectic C phase is given by

$$\langle Q_{\alpha\beta}\rangle = Q_0 S(n_\alpha(\mathbf{r})n_\beta(\mathbf{r}) - (1/3)\delta_{\alpha\beta}), \tag{101}$$

where $Q_o = Q_{zz} - (Q_{xx} + Q_{yy})/2$. The polarization induced by the gradient of the quadrupole density can be written in the familiar form

$$P_q = \rho Q_o S[\mathbf{n}(\boldsymbol{\nabla}\mathbf{n}) + (\mathbf{n}\boldsymbol{\nabla})\mathbf{n}] \tag{102}$$

It follows from Eq. (102) that the quadrupolar contribution to all flexocoefficients μ_f, $\mu_f^\perp$ and $\mu_f^\parallel$ is the same, i.e. $\mu_{fq} = \rho Q_o S$. This contribution is approximately constant in the smectic C phase and does not depend on the tilt angle θ. Note that in the ferroelectric smectic C* phase the dielectric constant is a function of the difference

Downloaded by [Tomsk State University of Control Systems and Radio] at 12:54 19 February 2013

of flexocoefficients $\mu_f - \mu_f^{\perp}$ and hence it does not depend on the quadrupolar contribution.

The dipolar flexoelectricity is described by the first term in Eq. (100). The averaging of the dipolar moment $\mathbf{d}_i = \mathbf{a}_i d_{\parallel} + \mathbf{b}_i d_{\perp}$ in Eq. (100) is performed with the one-particle distribution function of the nonuniform liquid crystal $f_1(\mathbf{n}(\mathbf{r}))$. This function can be determined by the minimization of the free energy of the nonuniform smectic C. In section 4.3.1 we have discussed the free energy of the smectic C phase in the molecular field approximation. In the case of nonuniform smectic C the free energy (69) can be rewritten as

$$\begin{aligned} \mathrm{F} = & -\frac{1}{2}\rho^2 \int f_1(\Omega_i,\mathbf{r}_i)\tilde{U}(i,j)f_1(\Omega_j,\mathbf{r}_j)d\Omega_i d\Omega_j d\mathbf{r}_i d\mathbf{r}_j \\ & + k_B \mathrm{T}\rho \int f_1(\Omega_i,\mathbf{r}_i)\ln f_1(\Omega_i,\mathbf{r}_i)d\Omega_i d\mathbf{r}_i \end{aligned} \tag{103}$$

with
$$\tilde{U}(i,j) = U(i,j) - k_B \mathrm{T}\Omega(\zeta_{ij} - r_{ij}) \tag{104}$$

where $U(i,j)$ is the intermolecular attraction potential and the step-function $\Omega(\zeta_{ij} - r_{ij})$ describes the steric intermolecular repulsion.

The flexoelectric effect describes the coupling between the induced polarization and the orientational deformation of the medium. In the case of small distortions the free energy of the nonuniform liquid crystal can be calculated with the help of the expansion of the first term in Eq. (103) in powers of $\nabla_\alpha f_1(\Omega_j,\mathbf{r}_j)$. The flexoeffect is described by the first term of this expansion. In the smectic C phase the positional dependence of the distribution function is related both to the periodic density modulation and to the nonuniform orientation of the director $\mathbf{n}(\mathbf{r})$. As mentioned above, we consider only the flexoelectric effect related to the director orientation and hence only this kind of positional dependence will be taken into account.

The distribution function of the nonuniform smectic C can be written as

$$f_1(j) = f_1(\Omega_j,\mathbf{n}(\mathbf{r}_j)) \approx f_1(\Omega_j,\mathbf{n}(\mathbf{r}_i)) + (\mathbf{r}_{ij}\nabla)f_1(\Omega_j,\mathbf{n}(\mathbf{r}_i)) \tag{105}$$

where $\mathbf{r}_{ij} = \mathbf{r}_i - \mathbf{r}_j$. Substituting Eq. (105) into Eq. (103) we arrive at the following free energy correction

$$F(\mathbf{r}) = F_o - \frac{1}{2}\rho^2 \int f_1(\Omega_i)\tilde{U}(i,j)(\mathbf{r}_{ij}\nabla)f_1(\Omega_j,\mathbf{n}(\mathbf{r}_i))d^2\mathbf{r}_{ij}d\Omega_i d\Omega_j, \tag{106}$$

Downloaded by [Tomsk State University of Control Systems and Radio] at 12:54 19 February 2013

where F_o is the free energy density of the uniform smectic C. In Eq. (106) we have written down only the terms linear in the gradient of the distribution function. The second order terms determine the elastic constants of smectic C.

In the case of weak nonuniformity the distribution function can be written in the form $f_1(i) = f_o(i)[1 + \psi(i)]$, where $f_o(i)$ is the distribution function of the uniform liquid crystal and the small correction $\psi(i)$ is proportional to the gradients of the director $\nabla_\alpha n_\beta(\mathbf{r})$. Then the induced polarization in the nonuniform liquid crystal takes the form

$$\mathbf{P}_d = \rho \int \mathbf{d}_i f_o(i)\psi(i) d\Omega_i \tag{107}$$

The function $\psi(i)$ can be determined by the minimization of the free energy of the nonuniform liquid crystal (103) taking into account the normalization conditions for the functions $f_o(i)$ and $f_1(i)$. The resulting expression can be substituted into Eq. (107). The result is substantially simplified in the case of ideal orientational and translational order. As discussed already in section 4.3, real ferroelectric smectics C are rather close to this ideal model. Then the induced polarization in the smectic C phase is given by

$$\begin{aligned}\mathbf{P} = \rho\beta \int (d_\parallel \mathbf{n} + d_\perp \mathbf{b}_i)\{\sigma \int (\mathbf{u}_{ij}\nabla_{\perp j})V(i,j)d\mathbf{u}_{ij} \\ + (1 - \sigma)(\mathbf{e}\nabla_j)V(\mathbf{n}_i,\mathbf{n}_j,\mathbf{b}_i,\mathbf{e})\}d\mathbf{b}_i,\end{aligned} \tag{108}$$

with

$$V(i,j) = V(\mathbf{n}_i,\mathbf{n}_j,\mathbf{b}_i,\mathbf{u}_{ij}) = \int \bar{U}(\mathbf{n}_i,\mathbf{n}_j,\mathbf{b}_i,\mathbf{b}_j,\mathbf{r}_{ij})d\mathbf{b}_j r_{ij}^2 dr_{ij}$$

Here σ is the fraction of nearest neighbors located in the same smectic plane. The contribution from σ molecules, located in the same smectic plane, is given by the first term in Eq. (108). Note that these molecules are characterized by the intermolecular unit vector $\mathbf{u}_{ij} \perp \mathbf{e}$. The contribution from the remaining $1 - \sigma$ nearest neighbors, located in adjacent smectic planes, is given by the second term in Eq. (108).

Eq. (108) is the general expression for the polarization of the smectic C phase induced by the dipolar flexoeffect. Eq. (108) can be used to obtain detailed information about the flexocoefficients μ_f, $\mu_f^\perp$, $\mu_f^\parallel$, taking into account different kinds of intermolecular in-

Downloaded by [Tomsk State University of Control Systems and Radio] at 12:54 19 February 2013

teractions. In the following section we consider the contributions from the multipolar and steric intermolecular interactions.

5.3. Flexoelectric coefficients in the smectic C phase

Dipolar flexoelectricity is determined by the intermolecular interactions which can cause the ordering of the molecular dipoles. Therefore, the corresponding interaction potential should change sign under the inversion of the molecular dipole. It can be shown that the dipole–quadrupole interaction is the simplest interaction of this kind.

The dipole–quadrupole interaction potential is given by Eq. (78). Substitution of Eq. (78) into the general Eq. (108) yields the following contribution to the induced polarization of smectic C

$$\mathbf{P}_{dq} = \mathbf{P}_{\perp} + \mathbf{P}_{\parallel},$$

$$\mathbf{P}_{\perp} = -\frac{1}{2}\rho^2\beta(1-\sigma)Q_o\left[d_{\perp}^2 3n_z\frac{\partial n_z}{\partial z} - \frac{15}{2}d_{\perp}^2\mathbf{k}\sin 2\theta n_z\frac{\partial n_z}{\partial z} + d_{\parallel}^2\cdot\mathbf{n}(2-5n_z^2)\frac{\partial n_z}{\partial z}\right], \quad (109)$$

where the unit vector $\mathbf{k}$ is shown on Fig. 39, $\mathbf{k} = [\mathbf{n}[\mathbf{ne}]]/\sin\theta$.

At small tilt angles $\theta << 1$ the polarization $\mathbf{P}_{\parallel}$ reads

$$\mathbf{P}_{\parallel} = \frac{3}{8}\sigma d_{\parallel}^2(5n_z^2-1)\mathbf{n}(\nabla_{\perp}\mathbf{n}) \quad (110)$$

Eqs. (109) and (110) can be compared with the phenomenological expression (21) for the flexoelectric contribution to the free energy of the nonuniform smectic C. The comparison yields the following expression for the flexocoefficients

$$\mu_f = \frac{1}{2}\rho^2(k_B\mathrm{T})^{-1}(1-\sigma)Q_o d_{\perp}^2; \quad (111)$$

$$\mu_f - \mu_f^{\perp} = -\frac{15}{2}\rho^2(k_B\mathrm{T})^{-1}(1-\sigma)Qd_{\perp}^2\theta^2; \quad (112)$$

$$\mu_f^{\parallel} = \frac{3}{2}\rho^2(k_B\mathrm{T})^{-1}\sigma Q_o d_{\parallel}^2. \quad (113)$$

Downloaded by [Tomsk State University of Control Systems and Radio] at 12:54 19 February 2013

The dipole–quadrupole contribution to the flexocoefficients (111)–(113) can be compared with the quadrupolar one $\mu_{fq} = \rho Q_o/3$. Indeed, the ratio of the two contributions is determined by the molecular dipole, i.e. $\mu_{fq}/\mu_{fdq} \sim \rho d^2/k_B T$. In the case of molecules with small dipoles $d < 1D$, $\rho d^2/k_B T << 1$ and the dipole–quadrupole contribution is small compared with the quadrupolar one. However, in the case of strongly polar molecules, which are used in the synthesis of ferroelectric smectics with large spontaneous polarization ($d = 3 \div 4D$), both contributions are of the same order of magnitude. On the other hand, it is important that the dipole–quadrupole interaction contributes to the difference of flexocoefficients $\Delta\mu_f = \mu_f - \mu_f^{\perp}$ which is equal to zero in the case of the purely quadrupolar effect. Note that $\mu_f - \mu_f^{\perp} = \delta\mu_f' \theta^2$ in accordance with the phenomenological theory.

It is interesting to note also that the dipole–quadrupole interaction does not contribute to flexoelectricity in nematics[147] and hence this contribution is specific for the smectic C phase.

The steric interaction between asymmetric molecules, which determines the dipolar flexoeffect in the nematic phase, also contributes to the flexocoefficients of the smectic C phase. The steric contribution can be calculated substituting the following effective interaction potential $\bar{U}(i,j)$ into the Eq. (108)

$$\bar{U}(i,j) = -k_B T \{\exp[-\beta U_s(i,j)] - 1\} = -k_B T \Omega(\zeta_{ij} - r_{ij}) \quad (114)$$

where ζ_{ij} is the closest distance of approach for the molecules i and j. and $\Omega(\zeta_{ij} - r_{ij})$ is a stepfunction. $\Omega(\zeta_{ij} - r_{ij}) = 0$ if the molecules do not overlap and $\Omega(\zeta_{ij} - r_{ij}) = -1$ otherwise. Note that for molecules with steric dipoles the function ζ_{ij} is sensitive to the direction of the dipole.

The steric contribution to flexocoefficient μ_f has been considered in reference 21 using the simple model for a banana-like molecule (see Fig. 40). The banana-like molecule possess the transverse steric dipole $s_\perp = \epsilon D$, where ϵ is the effective molecular bend angle. Note that this model has been used in the theory of ferroelectric ordering discussed in section 4.3. The steric contribution to the flexocoefficient μ_f is given by

$$\mu_f^s = \frac{1}{4\sqrt{2}} \rho^2 (1 - \sigma) L^4 (L/D)^2 d_\perp \epsilon \frac{[1 + (\theta/\epsilon)^2]^{1/2}}{[1 + (\theta L/D)^2]^{7/2}} \quad (115)$$

It follows from Eq. (115) that the steric interaction between asymmetric molecules results in the strong θ dependence of the flexo-

Downloaded by [Tomsk State University of Control Systems and Radio] at 12:54 19 February 2013

Downloaded by [Tomsk State University of Control Systems and Radio] at 12:54 19 February 2013

coefficient μ_f in the smectic C phase. From the experimental point of view, Eq. (115) predicts a strong temperature variation of the constant μ_f since $\theta \sim (T - T_c)^\beta$ near the phase transition point. This strong variation is associated with two small parameters of the asymmetric molecule: the average bend angle $\epsilon << 1$ and the breadth to length ratio D/L, $\epsilon << D/L$. The θ dependence of the flexocoefficient μ_f is scaled by these small parameters, i.e. $\mu_f^s(\theta) = \mu_f^s(\theta/\epsilon, \theta L/D)$. Therefore, when the tilt angle θ is small ($\theta \sim \epsilon$ or $\theta \sim D/L$) one still cannot neglect the temperature dependence of μ_f^s since $\theta/\epsilon \sim 1$ or $\theta L/D \sim 1$. In this case the expansion of the flexocoefficients in powers of θ^2 is incorrect even in the vicinity of the A-C phase transition point when $|T - T_{AC}| \simeq 1 \div 2°$ and $\theta \sim 10^{-1} \div 10^{-2}$. Indeed, the expression $[1 + (\theta/\epsilon)^2]^{1/2}$, for example, cannot be approximated by a few terms of the Taylor expansion in powers of θ^2 when $\theta \gtrsim \epsilon$.

For typical ferroelectric smectics C* the parameter D/L is not very small, $D/L \simeq 1/5$. Then one can consider the range of tilt angles $\epsilon << \theta << D/L$, since $\epsilon \sim 10^{-1} \div 10^{-2}$. In this range Eq. (115) is simplified to

$$\mu_f^s = \frac{1}{4\sqrt{2}} \rho^2(1 - \sigma)d_\perp L^4(L/2R_o)\epsilon[1 + (\theta/\epsilon)^2]^{1/2}, \qquad (116)$$

where R_o is the radius of curvature at the top of the molecule.

It should be noted that Eq. (115), which is valid for an arbitrary tilt angle θ, has been obtained only for a model of slightly bent ellipsoidal particles. This model, however, overestimates the value of the flexocoefficient μ_f^s at small tilt angles θ. Indeed, when the tilt angle is small, $\theta << 1$, the molecules, located in the adjacent smectic planes, touch each other at their ends. In this case the flexocoefficient μ_f^s is determined by the radius of curvature at the end of the molecule. Now it is clear that the model of the ellipsoidal particle is quantitatively incorrect since the ellipsoid possess a very small radius of curvature at the top, $R_o = (D/2)(D/L)$, while it is natural to expect that $R_o = D/2$. Thus, the coefficient $L^4(L/D)^2$ in Eq. (115) should not be taken too seriously and only the θ dependence of the steric contribution to the flexocoefficient should be taken into account.

5.4. Macroscopic helicoidal structure of the ideal smectic C*

In the chiral smectic C* phase the long molecular axes are tilted with respect to the smectic plane normal **e** and the partial ordering of the transverse molecular axes results in the nonzero polarization of the

smectic layer. At the same time the molecular chirality causes the helicoidal twisting of the director **n**(**r**) and the polarization **P**(**r**) around the smectic plane normal **e** (See Fig. 2). From the microscopic point of view this spontaneous twist is analogous to that in the cholesteric phase and hence it is not determined by the ferroelectric ordering. Then one can imagine smectic C* with helical structure and without spontaneous polarization of the layer. For example, the spontaneous polarization vanishes when the total transverse molecular dipole is equal to zero. Perhaps, this property can be attributed to the smectic C* liquid crystal synthesised by Gray and McDonnel.[162] However, the spontaneous polarization has not been measured in this material.

From the phenomenological point of view the helical twisting is related to the so called Lifshitz invariant in the free energy expansion for the smectic C* phase. (See Eq. (6)). In ferroelectric smectics C* the helical twisting influences the spontaneous polarization of the layer since the spontaneous twist along the z-axis results in an additional contribution to the polarization due to the flexoelectric effect. As a result, in the first approximation the helical pitch p is given by

$$p = 2\pi/q = 2\pi|\tilde{K}/\tilde{\lambda}| \tag{117}$$

with

$$\begin{aligned} \tilde{K} &= K - \chi\mu_f^2, \\ \tilde{\lambda} &= \lambda + \chi\mu_p\mu_f \end{aligned} \tag{118}$$

where the phenomenological constants λ, μ_f, μ_p and K are discussed in section 2. Thus, according to Eqs. (117), (118) the helical pitch of smectic C* is a function of the flexocoefficient μ_f and the piezocoefficient μ_p. For comparison, in the cholesteric phase the helical pitch is written as $p = |K'/\lambda'|2\pi$, where the constants K' and λ' have the same physical interpretation as the parameters K and λ in Eq. (118). In Eq. (118) both λ and μ_p are related to the molecular chirality. On the other hand, the parameters λ and μ_p are determined by different intermolecular interactions. Indeed, as shown in section 4.3, the piezoelectric coefficient μ_p is determined by polar interactions between chiral molecules, while parameter λ is related to any nonpolar anisotropic chiral intermolecular potential. Therefore, the parameters μ_p and λ are different functions of the molecular parameters and hence the ratio of these contributions to the helical pitch can depend strongly on the molecular structure. The most interesting situation can be found in mixtures of liquid crystals since in this case the

Downloaded by [Tomsk State University of Control Systems and Radio] at 12:54 19 February 2013

Downloaded by [Tomsk State University of Control Systems and Radio] at 12:54 19 February 2013

parameters μ_p and λ are functions of the concentrations of the components. In the two-component smectic C* parameter μ_p is written as (See Eq. (88))

$$\mu_p = \mu_{AA}x_A^2 + \mu_{AB}x_Ax_B + \mu_{BB}x_{BB}^2 \tag{119}$$

where x_A,x_B are the normalized number densities of the components "A" and "B", $x_A + x_B = 1$, and the constants $\mu_{\alpha\beta}(\alpha,\beta = A,B)$ are determined by the interaction between the molecules of components A and B. A similar expression can be obtained also for parameter λ

$$\lambda = \lambda_{AA}x_A^2 + \lambda_{AB}x_Ax_B + \lambda_{BB}x_B^2 \tag{120}$$

Now let us consider the mixture of two smectics C* composed of molecules with opposite chirality. In this case the constants μ_{AA} and μ_{BB} (and also λ_{AA} and λ_{BB}) will have opposite signs. Then the constant $\tilde{\lambda}$ in Eq. (117) can vanish at a certain concentration x_A^*, x_B^* and one will have smectic C* without a helical structure. At the same time the constant μ_p in Eq. (119) is not equal to zero at $x_A = x_A^*$, $x_B = x_B^*$ and hence the spontaneous polarization does not vanish. This nonhelicoidal ferroelectric liquid crystal has been observed by Beresnev and Blinov.[129]

It should be noted that in this section we considered only the helical twisting in the ideal smectic C* phase and neglect the influence of the boundary conditions. In real ferroelectric smectics C* the situation is more complex as discussed by Glogarova *et al.*[26]

5.5. Temperature variation of the helical pitch in the smectic C* phase

In contrast to the cholesteric phase, the helical pitch in the ferroelectric smectic C* phase depends strongly on the temperature in the vicinity of the phase transition point. The typical temperature variation of the pitch is presented in Fig. 4. The most interesting feature of this temperature variation is the location of the maximum pitch which does not correspond to the transition temperature. Indeed, in all ferroelectric liquid crystals, investigated so far, the helical pitches attain their maximum within 0.5–2°C below the A–C transition point.[10,11,163] Thus, the strong temperature variation of the pitch is not related to the critical behaviour at the phase transition point.

The temperature variation of the pitch in the smectic C* phase has been measured in different classes of ferroelectric liquid crys-

tals.[11,163,164] At the same time one may be puzzled by the large differences in the helical pitches determined by some investigators for the same compound. These differences are shown in Fig. 44 which presents the temperature variation of the pitch in DOBAMBC, determined by three experimental groups.[11,39,163] It can be easily seen that the results obtained by the different investigators are qualitatively similar while the absolute values of the pitch differ by a factor of two or three. The results presented in Fig. 44 have been obtained using different methods and this fact could be considered as a reason for the observed disagreement. However, the results of Ref. 165 make

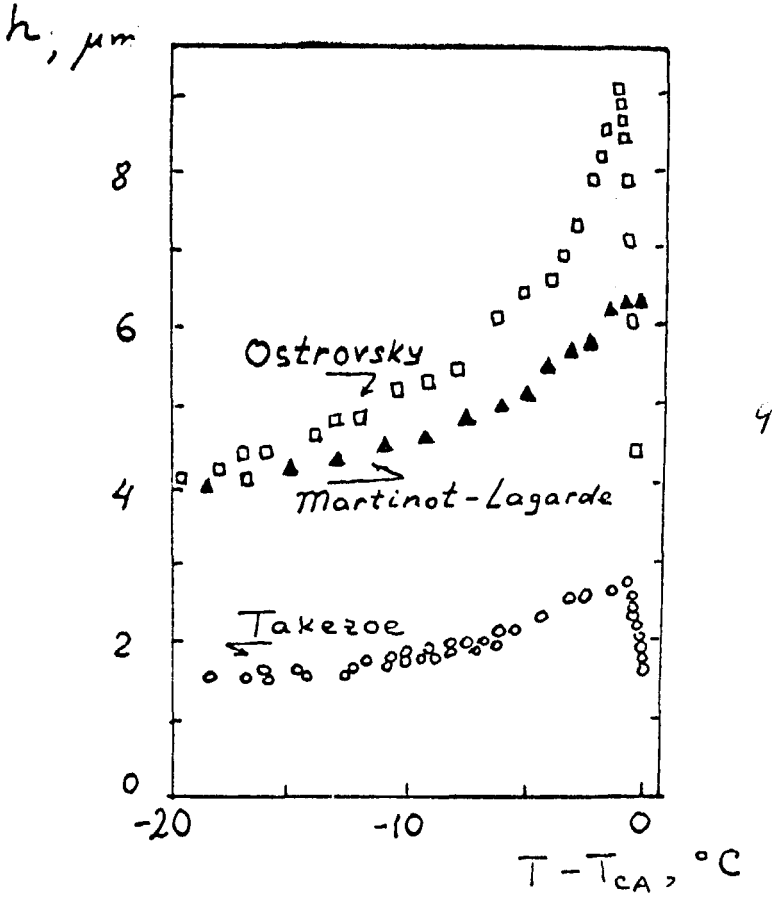

FIGURE 44 Temperature variation of the helical pitch in DOBAMBC determined by Ostrovskii et. al.,[11] Martinot-Hagarde et. al.[39] and Takezoe et. al.[163]

Downloaded by [Tomsk State University of Control Systems and Radio] at 12:54 19 February 2013

this conclusion doubtful. Indeed, Rozanski measured the pitch in DOBAMBC by four different methods used by other investigators and was able to show that the results agree very well. Then the disagreement, presented on Fig. 44, can be attributed only to different treatments of the cell surface or to the difference in the concentration of defects and disclinations which can play a substantial role in the formation of the helical structure.[26] It should also be noted that the typical temperature variation of the pitch observed only in relatively thick samples. In thin cells the boundary conditions influence the pitch as shown on Fig. 45.

In general one can point out the following peculiar features of the helical pitch behaviour in the smectic C* phase.:

1. Finite value of the pitch at the A–C phase transition point (extrapolation),
2. The pronounced maximum at $|T-T_c| \sim 1 \div 2°C$,
3. The slower diminishing of the pitch with decreasing temperature.

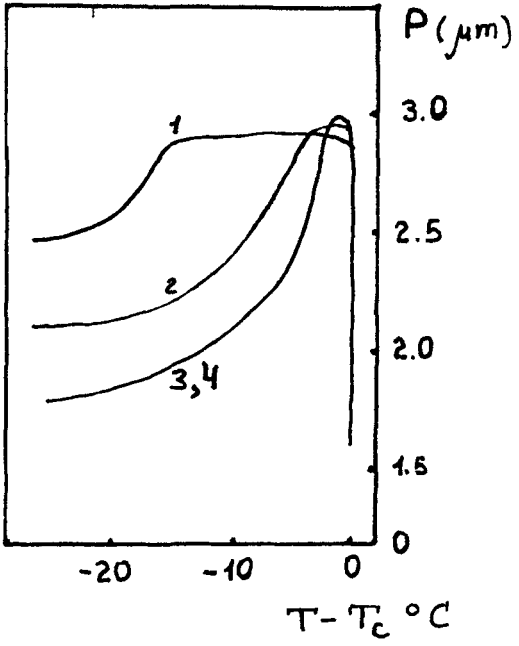

FIGURE 45 The cell thickness dependence of the helical pitch in DOBAMBC.[164] Cell thickness: 100 μm (1), 150 μm (2), 250 μm (3), 350 μm (4).

Downloaded by [Tomsk State University of Control Systems and Radio] at 12:54 19 February 2013

Downloaded by [Tomsk State University of Control Systems and Radio] at 12:54 19 February 2013

Within the frame work of the phenomenological theory the helical pitch is determined by Eq. (117) where the constants λ and K are independent on the temperature in the first approximation. It is obvious that the temperature variation of the pitch in the smectic C* phase can be described with the help of the phenomenological theory taking into account the higher order invariants in the free energy expansion. However, it remains unclear if one can describe the observed strong variation with the help of the first few terms in the expansion. In this connection we shall show that the temperature variation of the pitch plotted in Fig. 4 can not be described by the expansion in powers of θ^2. Indeed, let us expand the pitch p as follows:

$$p = p_o[1 + a\theta^2 + b\theta^4 + \ldots] \tag{121}$$

Note that the maximum value of the pitch corresponds to the very small tilt angle $\theta = \theta_o \sim 10^{-1}$. At the same time the pitch is changed by a factor of two with increasing tilt angle, from $\theta = 0$ to $\theta = \theta_o$. Then it follows from Eq. (121) that $a\theta^2 \sim 1$ and hence the coefficient a is anomalously large, $a \sim 10^2$. Moreover, the maximum of the pitch at $\theta = \theta_o$ can be described by Eq. (121) only if $b \sim 10^4, a \sim 10^2$. Thus the coefficients in the expansion (121) grow rapidly with increasing power of θ^2 and all the terms in the expansion are of the same order of magnitude even at small tile angle $\theta << 1$. As a result expansion (121) is useless.

Attempts to describe the unusual temperature variation of the pitch in the ferroelectric smectic C* phase have been made by different authors.[26,166,167] However, Musevic *et al.* have shown that the critical fluctuations considered by Yamashita and Kimura[167] can not cause the observed temperature variation of the pitch. The interpretations suggested by Blinc *et al.*[166] and Glogarova *et al.*[26] are more consistent. It should be noted, however, that the model presented by Glogarova *et al.* is only qualitative and is not supported by a theory. The possible theoretical description of the temperature variation of the pitch, taking into account the energy of disclinations, is a matter of great interest.

Now let us consider in more detail the theory developed by Blinc *et al.*[166]. As mentioned already, the helical pitch is independent of temperature in the first approximation of the phenomenological theory. Then it is clear that the temperature variation of the pitch can be explained taking into account additional terms in the free energy expansion. Blinc and Zeks considered the following correction of the

free energy of the smectic C* phase

$$\Delta F = -\frac{1}{2}\Omega(P_x\xi_2 - P_y\xi_1)^2 + \frac{1}{4}\eta(P_x^2 + P_y^2) - d(\xi_1^2 + \xi_2^2)\left(\xi_1\frac{\partial\xi_2}{\partial z} - \xi_2\frac{\partial\xi_1}{\partial z}\right) \quad (122)$$

Note that the first two terms in Eq. (122) are not chiral while the third term is the first correction to the Lifshitz invariant in Eq. (21). The numerical calculations presented by Blinc *et al.*[166] show that the free energy expansion including the terms in Eq. (122) can be used to describe qualitatively the temperature variation of the pitch in the smectic C* phase. At the same time this interpretation is open to criticism for the same reason as the simple expansion of the inverse pitch in powers of θ^2. Indeed, the rapid growth of the pitch within $T - T_c < 1K$ can be explained only if $d/\lambda \sim \theta_o^{-2} >> 1$, where the tilt angle θ_o corresponds to the maximum pitch $p_{max} = p(\theta_o)$. Therefore, the correction to the Lifshitz invariant is of the same order of magnitude as the invariant itself even at small tilt angles. However, the most serious shortcoming of this theory is the prediction of nonzero spontaneous polarization in the achiral smectic C phase. Indeed, the minimum of the free energy corresponds to the nonzero value of $P^2 = (\Omega/\eta)(\theta^2 - \theta_o^2)$ at $\theta > \theta_0$ in achiral smectic C. Therefore, nonchiral smectic C should possess the corresponding spontaneous polarization **P**. The latter conclusion is in contradiction to the existing experimental data. Thus the theory developed by Blinc *et al.* requires some modification.

In this section we consider another interpretation of the temperature variation of the pitch in the chiral smectic C* phase, taking into account the temperature dependence of the flexoelectric coefficient μ_f discussed in section 5.3. The most important consequence of Eqs. (115) and (116) is the strong dependence of the steric contribution to the flexocoefficient μ_f on the tilt angle θ in the smectic C phase. As mentioned above, this unusual behaviour is associated with two small parameters of the molecule: the average bend angle ϵ and the breadth to length ratio D/L, $\epsilon << D/L$. Then one can not neglect the temperature variation of the constant μ_f even at small $\theta \sim \epsilon$ or $\theta \sim D/L$, since μ_f is a function of the combinations $\theta/\epsilon \sim 1$ or $\theta L/D \sim 1$.

It seems reasonable to explain the experimentally observed strong temperature variation of the pitch in the smectic C* phase by the

Downloaded by [Tomsk State University of Control Systems and Radio] at 12:54 19 February 2013

strong temperature variation of the flexocoefficient μ_f. At small tilt angle $\theta \lesssim \epsilon$, $\mu_f \sim [1 + \theta^2/2\epsilon^2]$. Substitution of this expression into Eq. (117) yields the following expression for the pitch

$$p \approx p_o[1 + \delta_o(T - T_c)\epsilon^{-2}], \ \theta \lesssim \epsilon \tag{123}$$

where the constants p_o and δ_o are composed of the parameters of Eqs. (117), (116). Thus, when the tilt angle is small, the pitch is growing linearly with temperature in the smectic C* phase in accordance with experiment.

Note that the large growth rate of the pitch within 1° of the transition temperature is determined by the parameter $\epsilon^{-2} >> 1$. When the temperature is decreased, the growth rate of the constant μ_f (and hence the growth rate of the pitch) is reduced since $\mu_f \sim \epsilon[1 + (\theta/\epsilon)^2]^{1/2} \sim \theta \sim (T_c - T)^\beta$ when $\epsilon < \theta < D/L$. At lower temperatures $\theta \sim D/L$ and in this region one has to use Eq. (115) which is valid for arbitrary tilt angle $\theta < 1$. The dependence of μ_f on $(\theta L/D)$ reduces the flexocoefficient μ_f and it can be shown that the maximum pitch corresponds to $\theta_0 \simeq D/L$. For the typical ferroelectric liquid crystal DOBAMBC $\theta_0 \simeq 1/5$ and hence $L \simeq 5D$. The slow decrease of the pitch far from the transition temperature T_{AC} can be explained by the weak temperature variation of the constants λ and K in Eq. (117) according to the theory of Van der Meer and Vertogen.[151]

The present molecular model enables one to explain also the odd-even effect observed in the dependence of the maximum pitch in ferroelectric liquid crystals nOBAMBC, $n = 6 - 10$.[164] It is interesting to note that the odd-even effect is not observed in the dependence of the Sm A* – Sm C* transition temperature on the alkoxy chain length. Thus the odd-even effect can not be explained in the same way in the nematic phase since the well known odd-even effect in nematics manifests itself in the phase transition temperature. At the same time the odd-even effect in the dependence of the maximum pitch in the smectic C* phase can be readily explained by the odd-even variations of the average bend angle ϵ. The transition temperature T_{AC} does not depend on the parameter ϵ in the first approximation and hence it is not sensitive to the odd-even variations.

In conclusion we want to emphasize that the real origin of the strong temperature variation of the helical pitch in the smectic C* phase is still unclear and the solution of this problem requires new experiments.

Downloaded by [Tomsk State University of Control Systems and Radio] at 12:54 19 February 2013

Downloaded by [Tomsk State University of Control Systems and Radio] at 12:54 19 February 2013

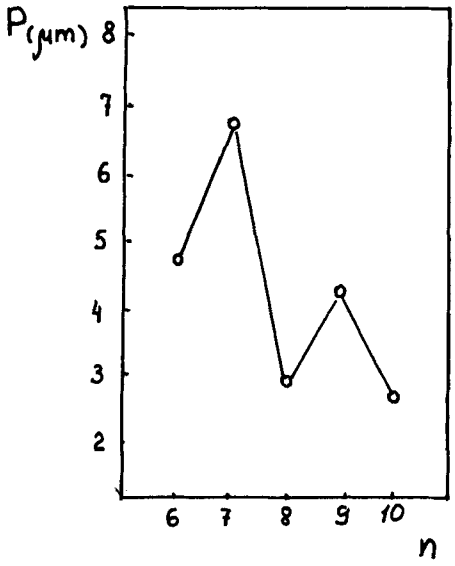

FIGURE 46 Odd-even variation of the maximum pitch in DOBAMBC.[164]

VI. OPTICAL PROPERTIES OF THE CHIRAL SMECTIC C* PHASE

6.1. A mirror-symmetrical smectic C

Before the consideration of the optical properties of the helical smectic C* phase let us discuss the simplest case of an achiral smectic C, Fig. 47. As the director **n** is tilted by the angle θ with respect to the normal z to the smectic layers a smectic C is described by the point symmetry group C_2 and is optically biaxial.[168] For such symmetry only one principal axis of the dielectric tensor is strictly defined.[169] It is a second order axis C_2 which coincides with the y-axis (or axis 1) in Fig. 47. Directions of the other two principal axes (axes 2 and 3 in Fig. 47) depend on the exact properties of a substance and, in general, do not coincide, say, with the director or the z-normal.

In the general case, the tensor of the dielectric permittivity of the smectic C phase has four linearly independent terms[55]:

$$\epsilon_{ij} = a\,\delta_{ij} + b\,z_i z_j + c\,n_i n_j + d(n_i \tilde{z}_j + \tilde{z}_i n_j)(\mathbf{n}\,\mathbf{z}) \qquad (124)$$

where $\mathbf{n} = (\sin\theta, 0, \cos\theta)$ is a director, **z** is the unit vector of the smectic normal. This tensor can be reduced to a diagonal form and,

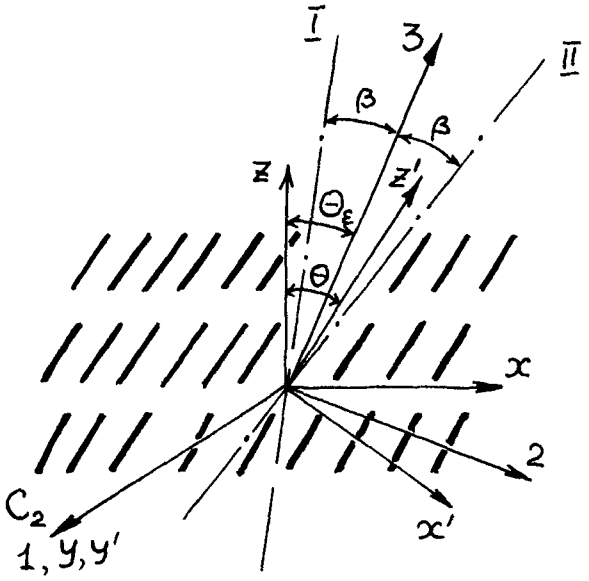

FIGURE 47 The choice of the coordinate frames for an achiral smectic C. x, y, z is the Cartesian system coupled with the smectic normal z; x', y', z' is the system coupled with the director $z' = n$; 1, 2, 3 are principal axes of the dielectric tensor; I, II are the optical axes.

in this way, one can find the directions of its principal axes with respect to the director. The corresponding expression is rather bulky and, to discuss the idea, we shall limit ourselves to the case of small θ-angles. For $\theta << 1$ the angle θ_ϵ between the z-axis and one of the principal axes of the dielectric ellipsoid (in this case we speak of the longest axis) is a linear function of θ[55]:

$$\theta_\epsilon = -\frac{c + d}{b + c + 2d}\theta \tag{125}$$

and may, in principle, be expressed as a function of the principal values of the dielectric tensor

$$\theta_\epsilon = f(\epsilon_1, \epsilon_2, \epsilon_3)\theta \tag{126}$$

and θ_ϵ may be either more or less than θ. In experiments, the values of θ_ϵ obtained from optical measurements seem often to be more than the corresponding angles θ obtained from X-ray data (see paragraph 6.4).

Downloaded by [Tomsk State University of Control Systems and Radio] at 12:54 19 February 2013

In the frame of the axes 1, 2, 3 shown in Fig. 47 the dielectric tensor is diagonal and its components may be related to the corresponding refractive indices

$$n_1 = \sqrt{\epsilon_1}; \quad n_2 = \sqrt{\epsilon_2}; \quad n_3 = \sqrt{\epsilon_3}$$

For other directions, for example for the direction of the director, these simple relationships are not fulfilled.

Sometimes it is important to find the dielectric permittivities in a frame system x, y, z connected with the smectic layers (we meet such a case when discussing spiral structures with the helical axis parallel to z). Then one should use a dielectric tensor introduced by Berreman

$$\epsilon_{ij} = \begin{pmatrix} \epsilon_1 & 0 & (\epsilon_3 - \epsilon_2)\sin\theta_\epsilon \cos\theta_\epsilon \\ 0 & \epsilon_2\cos^2\theta_\epsilon + \epsilon_3\sin^2\theta_\epsilon & 0 \\ (\epsilon_3 - \epsilon_2)\sin\theta_\epsilon \cos\theta_\epsilon & 0 & \epsilon_2\sin^2\theta_\epsilon + \epsilon_3\cos^2\theta_\epsilon \end{pmatrix} \tag{127}$$

where, in contrast to[170,171] we use θ_ϵ instead of θ.

The refractive indices in the x, y, z system are defined by formulas

$$n_z = \frac{n_3 n_2}{\sqrt{n_3^2 \sin^2\theta + n_2^2 \cos^2\theta}}$$

$$n_x = \frac{n_3 n_2}{n_3^2 \cos^2\theta + n_2^2 \sin^2\theta} \tag{128}$$

$$n_y = n_1$$

obtained in a standard way.[172]

Using the tensor (127) and the angle $\theta_\epsilon - \theta$ between the principal axis 3 and the direction z' of the director one can calculate the dielectric permittivities ϵ'_{ij} in the frame system of the director and, after that, according to (128) one can find the corresponding refractive indices n'_z, and $n'_x(n'_y = n_1)$. Thus, the relationships between the values of ϵ_i and n_i in the two coordinate systems are derived.

Unfortunately, up to now such a treatment of experimental data was not realized. Usually one considers a smectic C either to be uniaxial with an optical axis parallel to the director or to be biaxial

Downloaded by [Tomsk State University of Control Systems and Radio] at 12:54 19 February 2013

with one of the principal axis of the dielectric tensor coinciding with the director. The latter approximation was made, for instance, in paper[173] where refractive indices were studied in the frame system x', y', z' fixed to the director. In this case the maximum refractive index corresponds to the direction of the director z'-direction in Fig. 47), and the two other indices are nearly equal, $n_{y'} = n_1 \gtrsim n_{x'}$, Fig. 48. The observed temperature behaviour is accounted for when taking pair correlations between molecules into account and neglecting all interaction forces apart from the steric ones.[174]

Knowledge of the principal values for the refractive indices allows the calculation of the angle 2β between the two optical axes of a smectic C[175]

$$tg\beta = \pm\sqrt{\frac{n_2^{-2} - n_1^{-2}}{n_1^{-2} - n_3^{-2}}}$$

Here, the angle $\pm\beta$ is reckoned from the principal axis 3 of the dielectric tensor. The optical axes I and II are also shown in Fig. 47. The temperature behaviour of the angle β for thioester compounds was shown[173] to differ markedly from that of the director tilt angle $\theta \approx \theta_\epsilon$.

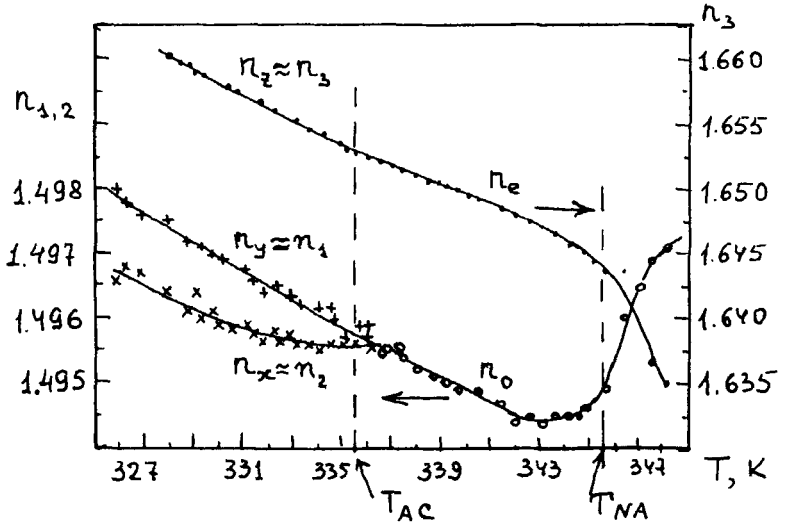

FIGURE 48 The refractive indices of 4-pentylphenylthio-4′-n-nonyloxybenzoate (from Ref. 173).

Downloaded by [Tomsk State University of Control Systems and Radio] at 12:54 19 February 2013

Since the difference between ϵ_1 and ϵ_2 is small the angle β in smectics C is also small, namely, of the order of several degrees. Hence, in many cases, a smectic C is considered to be uniaxial with $n_3 = n_{\parallel}$, $n_1 = n_2 = n\perp$. In this approximation the principal axis 3 coincides with the direction z' of the director. Such an approximation allows the tilt angle θ of the director to be calculated from optical measurements (see 6.4).

6.2. The ideal helical structure of a smectic C*

In the chiral smectic C* phase the director is rotated by angle $\varphi = q\,z$ when proceeding along the normal to smectic planes. The tensor of dielectric permittivity is rotated together with the director[170,171]:

$$\hat{\epsilon} = \begin{pmatrix} \epsilon_{11}^0 + \epsilon_a\cos 2\varphi & \epsilon_a\sin 2\varphi & \epsilon_a^1\cos\varphi \\ \epsilon_a\sin 2\varphi & \epsilon_{22}^0 - \epsilon_a\cos\varphi & \epsilon_a^1\sin\varphi \\ \epsilon_a^1\cos\varphi & \epsilon_a^1\sin\varphi & \epsilon_{33}^0 \end{pmatrix}$$

Here

$$\epsilon_{11}^0 = \epsilon_{22}^0 = \frac{1}{2}(\epsilon_1 + \epsilon_2\cos^2\theta_\epsilon + \epsilon_3\sin^2\theta_\epsilon)$$

$$\epsilon_{33}^0 = \epsilon_2\sin^2\theta_\epsilon + \epsilon_3\cos^2\theta_\epsilon$$

$$\epsilon_a = \frac{1}{2}(\epsilon_1 - \epsilon_2\cos^2\theta_\epsilon - \epsilon_3\sin^2\theta_\epsilon)$$

$$\epsilon_a' = (\epsilon_3 - \epsilon_2)\sin\theta_\epsilon\cos\theta_\epsilon$$

and the principal values ϵ_1, ϵ_2, ϵ_3 are defined as earlier, Fig. 47.

An infinite sample being locally biaxial became macroscopically uniaxial with the optical axis z parallel to the helical axis. This has been shown by a conoscopic technique in the same pioneering studies where ferroelectric phases have been discovered.[1,4]

Optical properties of the chiral smectic C* phase are similar to those of the cholesteric phase. A smectic C* strongly rotates the light polarization plane and reveals selective light scattering and circular dichroism. However, there is a serious difference between the optical properties of the two phases. The period of a change in all the physical properties of a smectic C* is equal to the pitch of the helix while it

Downloaded by [Tomsk State University of Control Systems and Radio] at 12:54 19 February 2013

coincides with half of the pitch in the cholesteric phase. This difference, however, is not seen in the light incident along the helical axis. In this case ($\xi = \pi/2$) only the second order ($m = 2$) reflection is observed at wavelength $\lambda_2 = h\,\bar{n}$ according to the Bragg formula

$$2\,\bar{n}\,\sin\,\xi = m\,\lambda$$

Here $\bar{n}$ is the refractive index averaged over a smectic plane. If a locally biaxial smectic C* is considered to be uniaxial ($\theta_\epsilon \approx \theta$) the index $\bar{n}$ for light incident along the normal to layers is equal to $1/2\,\sqrt{n_x^2 + n_y^2}$ where $n_y = n_1$ and $n_x = n_\parallel n_\perp/\sqrt{n_\parallel^2 \cos^2\theta + n_\perp^2 \sin^2\theta}$ In the limiting case $\theta \rightarrow \pi/2$ we have $n_x = n_\parallel$, $n_z = n_y = n_\perp$, that is the situation characteristic of a cholesteric liquid crystal. The case of $\theta \rightarrow 0$ corresponds to a smectic A, $n_z = n_\parallel$, $n_x = n_y = n_\perp$.

The measurements of refractive indices in the smectic C* phase are difficult because of the very existence of the helical structure. As a rule, the values $n_\parallel$ and $n_\perp$ are calculated by an extrapolation of the corresponding temperature dependences for the smectic A phase, see, e.g. Refs. 82, 163 and 176. An exception is the paper[176] where independent measurements were carried out of the refractive indices for two linearly polarized and two circularly polarized beams incident on a chiral smectic C* along the helical axis. In addition, the wavelength for the maximum selective scattering λ_2 was measured. From these data with the help of the tensor (127) all the three principal values ϵ_1, ϵ_2 and ϵ_3 as well as the angle θ_ϵ were calculated.[176] The experimental data for a sample of the 4-n-hexyl-oxyphenyl ester of 4-(2″-methyl-butyl)biphenyl-4-carboxylic acid (HOPE MBBCA) are shown in Fig. 49. A weak temperature dependence of the angle θ_ϵ reflects a weak temperature dependence of the tilt angle $\theta(T)$ which is due to the absence of the smectic A phase and the first order nature of the cholesteric-smectic C* phase transition. This substance has a small pitch of the helix which allows the second order reflection to be observed using ordinary light sources. In other cases, e.g. for DOBAMBC, the second order reflection takes place in the IR spectral range and one must use a more complicated technique, for example, a tunable laser on F-centers.[177]

The measurements of the optical rotatory power for light incidence along the helical axis of a smectic C* are carried out in paper Refs. 177 and 178 and agree qualitatively with theoretical results[16] obtained for the cholesteric phase.

For an oblique incidence of light on the helical smectic C* structure a local tilt of the director results in the periodicity of the optical

Downloaded by [Tomsk State University of Control Systems and Radio] at 12:54 19 February 2013

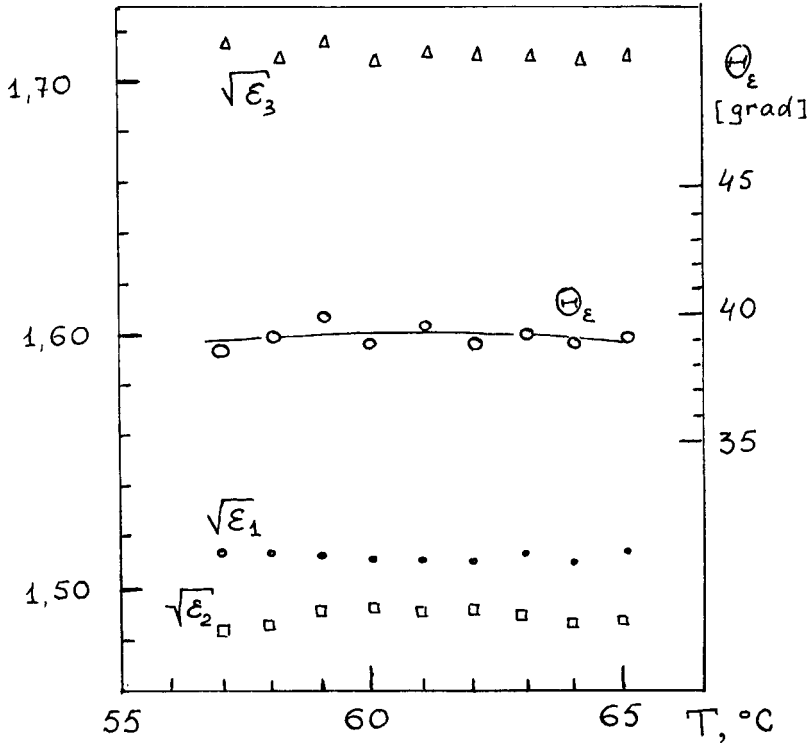

FIGURE 49 The principal values of the dielectric tensor ($n_i = \sqrt{\varepsilon_i}$) and the inclination angle for the principal axis of the tensor ε_{ij} as functions of temperature for HOPE MBBCA (from Ref. 179).

properties corresponding to the full pitch of the helix.[170] A new maximum for the Bragg reflection appears at the wavelength $\lambda_1 = 2\,\bar{n}h$. For the first time, the first order reflection was observed by Chilaya *et al.*[179] in the same substance HOPE MBBCA, see also Ref. 180. For the classical ferroelectric DOBAMBC the first order reflection is observed in the IR spectral range.[165]

The polarization properties of light reflected into the first diffraction order are markedly differ from those for the second order. For instance, the right-polarized wave transforms into a left-polarized one and vice versa [170] (by the way, in cholesterics one circular polarization does not reflect at all and the other keeps the polarization after reflection). For oblique incidence of light with a wavelength considerably less than the helical pitch a strong forward diffraction is observed with a change of linear polarization by the angle $\pi/2$. This

Downloaded by [Tomsk State University of Control Systems and Radio] at 12:54 19 February 2013

effect is magnified under certain phase matched conditions for the wave vectors.[181]

In an absorbing medium, e.g., when some dyes are dissolved in a smectic C* matrix one can observe[179] a diffractional decrease in light absorption near the selective reflection band (Bormann's effect).

6.3. Preparation of optically homogeneous samples

In fact, the ideal helical structure of a smectic C* is never realized in experiments since the solid boundaries play an important role even in the case of thick samples. Usually one tries to prepare as perfect a sample as possible, however it is very difficult to avoid various structural defects such as walls, disclinations, focal-conic domains, spherulites, etc. The most important, from the practical point of view, are the two orientation geometries of the smectic layers with respect to the limiting solid surfaces, shown in Fig. 50.

The first one, called homeotropic, corresponds to smectic planes parallel to the limiting boundaries. As the molecular tilt angles θ are usually small (< 45%) the boundaries are treated by surface-active substances which force the molecules of a liquid crystal to stay per-

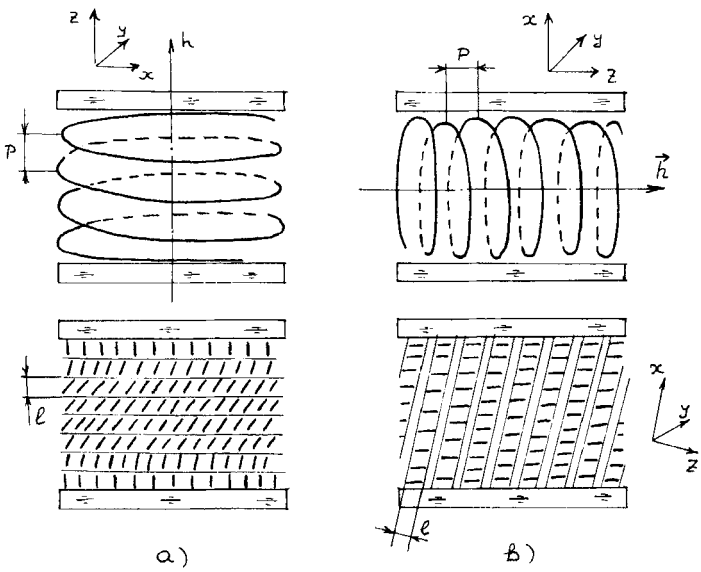

FIGURE 50 Upper: Two typical geometries for the investigation of the helical structure of smectic C*. The helical axis is perpendicular (a) and parallel (b) to the limiting surfaces. Lower: The same structures under conditions of helix unwinding in thin cells.

Downloaded by [Tomsk State University of Control Systems and Radio] at 12:54 19 February 2013

Downloaded by [Tomsk State University of Control Systems and Radio] at 12:54 19 February 2013

pendicular to the support. Conventional orienting substances for DOBAMBC are cetyl-trimethylammonium bromide,[1,165] hexadecyl-trimethylammonium bromide,[123] and others. Usually a liquid crystal is oriented in the smectic A phase (if it exists) and an additional strong shear of one plate with respect to the other favours the orientation of the smectic layers parallel to the plates. The reason is the easy sliding of the smectic A layers relative to each other.

After preparing the uniform homeotropic orientation in the smectic A phase the substance is cooled down into the smectic C* phase. In the volume of the sample the molecular tilt and the helical structure appear and the surface parts of the sample become distorted (bend-deformation). In the case of small thickness (microns) the helix is untwisted and the sample becomes homeotropically oriented, Fig. 50 (left lower part).

The second type of orientation corresponds to the case (Fig. 50, right part) when the smectic layers are perpendicular and the helical axis is parallel to the limiting surfaces. It is very difficult to obtain a high quality orientation of such a type since the helical structure in the volume of a sample does not *joint* with the uniform molecular orientation at the surface. In this case, the system of linear defects, disclinations appear. The disclinations are perpendicular to the director at the surface and the distance between them is equal to the pitch, Fig. 51. A similar system of defects occurs in the cholesteric phase, however, in that case, its period is equal to half of the pitch. The difference is accounted for by the fact that in addition to the second order diffraction the first order one is allowed in the smectic C* phase.

To obtain the homogeneous planar molecular orientation at the boundaries one usually uses some combination of a surface treatment and the influence of external fields. First of all one should provide for the anisotropy of the surface forces. For this purpose one often uses either the vacuum deposition of SiO with oblique incidence of the molecular beam[182,183] or the depositon of a polymeric layer with its subsequent unidirectional rubbing. Good results may be obtained using an adhesion promoter.[184] Such a technique allows planarly oriented layers of DOBAMBC, HOBACPC and some ferroelectric mixtures to be obtained even without external fields.

As external factors one often uses a magnetic field[185] or a weak mechanical shear of the supports either manually with microscopic screws[186] or electrically with an acoustic diffuser[187]. When the initial planar orientation is made at the cell walls and the magnitude of the

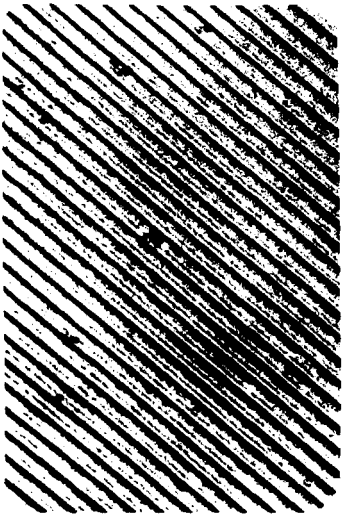

FIGURE 51 Linear domains characteristic of chiral smectic C* with the helical axis lying in the plane of the sample (from Ref. 127).

shear does not exceed 100μ the smectic layers would stay perpendicular to the walls with their planes oriented along the shear direction. This method is especially effective in the case of thin cells when the spiral structure is absent and a so-called "bookshelf" geometry is achieved, Fig. 50 (right lower part).

An electric field[188,189] and a temperature gradient[190] are sometimes applied as additional orienting agents. For example, homogeneous samples of the smectic A phase of DOBAMBC were grown in a temperature gradient using the edge of a polymeric spacer as the seed.

6.4. Optical methods for measuring the pitch of the helical structure and the molecular tilt angle

Following[165] let us briefly describe various experimental techniques for measuring the helical pitch of the smectic C* phase. The most popular is the method of measurement of the distance between parallel strips (domains) in the planar texture when the helical axis is parallel to the cell boundaries. This method allows the full pitch to be directly measured.[10,11,22] However, as was shown recently[12,163] the value of the pitch and its qualitative temperature behaviour as well

Downloaded by [Tomsk State University of Control Systems and Radio] at 12:54 19 February 2013

as other parameters strongly depend upon the sample thickness.[191] This method may be recommended only for sufficiently thick samples (hundreds microns).

The same difficulties are characteristic of the diffraction method[32,163] of measuring the pitch by the deviation angle for a light beam incident perpendicular to the helical axis on the planarly oriented sample.

In the case of homeotropically oriented samples with the helical axis perpendicular to the limiting plates one measures either the distance between Grandjean disclinations in a wedge-form cell,[165] or the spectral position of the Bragg reflection maxium.[163] In the latter case, to calculate the pitch one should have data of the refractive indices. In general, for thick cells the different methods give close agreement for the pitch.

There are several optical means for measuring the tilt angle θ for both achiral (C) and chiral (C*) smectics. As a rule, smectic C is considered to be uniaxial. For example, for achiral smectics there have been developed interferometric[192] and conoscopic[82,193] techniques. The angle θ may be also determined from dichroism measurements in an electric field (guest-host effect). In the latter case,[194] a dye is dissolved in a liquid crystalline matrix. In all the cases mentioned, the angle measured is considered to be equal to the angle of deviation of the director from the normal to the smectic layers. However, there are significant discrepancies between θ values obtained from optical and X-ray data. This may be explained, first, by neglecting the biaxiality and, second, by the different contributons of various molecular moieties (flexible tails and rigid skeletons) to the scattering of X-ray and optical beams.[82]

For chiral smectics C* the angle θ may be determined optically either for sufficiently thin samples where the helix is unwound or in a strong field unwinding the helix. If the director has no preferrable orientation in the plane of a cell the defect structures may be observed in polarized light different parts of which are darkened at different angles of orientation of an analyser with respect to a polarizer. From these observations the angle θ may be determined.[186,191] More convenient, however, is an electro-optical technique[10,11] which uses field-induced switching of the director by an angle 2θ which is easily measured when rotating an LC-cell. In addition, the optical anisotropy of the substance is determined.[133] Naturally, our previous note concerning inequality θ_ϵ and θ is still true, and all these methods in fact provide the inclination angle for the principal axis of the dielectric tensor.

Downloaded by [Tomsk State University of Control Systems and Radio] at 12:54 19 February 2013

6.5. Nonlinear optical properties

Ferroelectric liquid crystals are polar, noncentrosymmetric substances for which the expansion of the electric polarization

$$P = \chi_0 + \chi_1 E + \chi_2 E^2 + \chi_3 E^3 + \ldots$$

with a non-zero second order polarizability χ_2 is valid (here, $\chi_0 \equiv P_s$, is the spontaneous polarization, χ_1 is the ordinary linear polarizability). Therefore, for such substances the most important nonlinear effects are due to the $\chi_2 \neq 0$. One of these effects is the optical second harmonic generation. In the experiment an intensive light wave of fundamental frequency ω is directed at the sample and the light with double frequency $\omega' = 2\omega$ is detected. The amplitude of the field at 2ω is proportional to the squared amplitude of the exciting beam

$$E(2\omega) \propto \chi_2 E^2(\omega)$$

and the corresponding light intensities are

$$\sqrt{I(2\omega)} \propto \chi_2 I(\omega)$$

For the first time, the second harmonic generation in ferroelectric liquid crystals was observed on unoriented samples of DOBAMBC.[195] The utilization of oriented samples and a specific temperature dependence of the tilt angle θ allows the second harmonic to be observed in a phase-matched regime.[196,197] The latter is achieved by a change in the refractive index for an extraordinary wave with increasing θ (and, therefore, θ_ϵ) under cooling the sample, Fig. 52. The value for the nonlinear polarizability χ_2 correlates with the magnitude of the spontaneous polarization. Unfortunately, in materials studied until now χ_2 is small. The reason is the small value of the order parameter for short molecular axes which is responsible for ferroelectricity ($\langle\cos\psi\rangle \lesssim 0.1$).[114]

VII. ELECTRO-OPTICAL EFFECTS

In this chapter we discuss experimental data on electro-optical effects in ferroelectric liquid crystals and compare them, where it possible, with theory. For the sake of completeness we begin the discussion with the properties of the achiral smectic C phase.

Downloaded by [Tomsk State University of Control Systems and Radio] at 12:54 19 February 2013

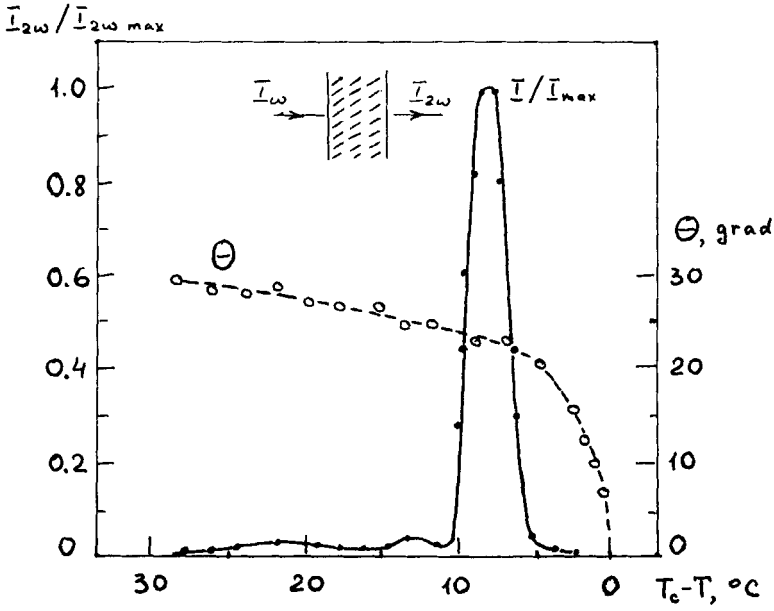

FIGURE 52 The intensity of the phase-matched optical second harmonic generation in DOBAMBC achieved by the temperature tuning of the angle θ (from Ref. 196).

7.1. The Fredericks transition in a smectic C

In contrast to smectics A where a change in orientation of the director must be accompanied by a distortion of the smectic layers, the application of an external (d.c. or a.c.) electric field to the smectic C phase results in the orientation of the director either in the field direction or perpendicular to it in accordance with the sign of the dielectric anisotropy ϵ_a. In this case, the director is switched from an initial to a final state along the surface of a cone with the angle 2θ at its apex, where θ is the tilt angle of the director with respect to the smectic normal (to the first approximation θ is considered to be independent of field and, in addition, for the sake of simplicity we assume $\theta \approx \theta_\epsilon$).

If, for example, $\epsilon > 0$ and in the initial state the director is parallel to the continuing glass plates and perpendicular to the field, then the process of reorientation will have a threshold character in complete analogy to the Fredericks transition in nematics.

The first investigation of the Fredericks effect in a smectic C was made by Pelzl.[194,198] The corresponding geometry is shown in Fig.

Downloaded by [Tomsk State University of Control Systems and Radio] at 12:54 19 February 2013

53. Under action of a field applied across transparent electrodes the director in the bulk of the sample changes its direction from $\mathbf{n}_0$ to $\mathbf{n}_E$ in order to decrease the field term $\epsilon_a E^2$ in the free energy. The only difference from the case of nematics is the fact that all positions of the director are limited by the cone surface. From optical measurements of birefringence or dichroism accompanying the switching of the director one can calculate the angle 2θ at the apex of the cone and, for known value of ϵ_a, evaluate an effective elastic modulus defining the threshold voltage for this effect.[198]

It should be noted that this type of director switching is also important for ferroelectric smectics C* when the value of the spontaneous polarization is small and ϵ_a is high, that is, the inequality $\epsilon_a E^2 > P_s E$ is obeyed.

7.2. The chiral smectic C* phase in a weak electric field

It is convinient to discuss the field behaviour of a chiral smectic C separately for three different cases. For a weak field, $E << E_c$ where E_c is a critical field for helix unwinding the helical structure is only slightly distorted and using such a technique one may study the dynamics of a nearly undistorted helix. The case $E \approx E_c$ corresponds to the process of helix unwinding. For $E > E_c$ the interaction of the external field with the vector of the spontaneous polarization results

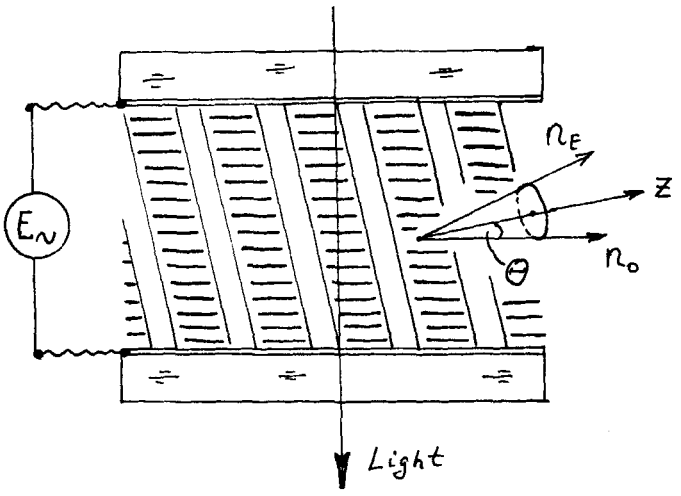

FIGURE 53 The geometry for observation of the Fredericks transition in smectic C.

Downloaded by [Tomsk State University of Control Systems and Radio] at 12:54 19 February 2013

in the field switching of the director accompanied by a change in birefringence.

Let us consider the case of a weak field. The two experimental geometries often used for a study of the linear electro-optical effect in smectic C* are shown in Fig. 50. In the geometry of Fig. 50(a) at zero field, under a polarizing microscope one can observe a conoscopic figure in the form of the Maltese cross. When applying a weak field along the X-axis the center of the figure is shifted perpendicular to the field in the Y-direction. The reason is a field-induced optical biaxiality. The shift of the cross depends linearly upon the field and the direction of the shift (say $+Y$) is inverted (to $-Y$) when the polarity of the field is changed. This effect has already been demonstrated in the original paper of Meyer and others.[1] From the shift of the cross one may calculate the average value for the azimuthal angle $\langle\varphi(z)\rangle$, see eqn. (35) of Chapter II, and, knowing the value of the spontaneous polarization find the elastic modulus K°. Such an attempt was made in Ref. 199. In the same paper an estimate was made of the twist-viscosity coefficient γ_1 for a ferroelectric mixture consisting of an achiral matrix (4-n-nonyloxy-4′-n-hexylphenyl benzoate) doped with a chiral additive.

The geometry for the electro-optical measurement shown in Fig. 50(b) is used more often. In such an experiment one may observe a change in the helical pitch either directly under a microscope or using the diffraction of laser light by the helical structure. A light beam is directed at the cell along the X-axis. In particular, such a geometry was used in paper Ref. 32 where an attempt was made to evaluate the flexo-and piezo-contributions to the total value of the spontaneous polarization of the undistorted helical structure.

The idea of the latter experiment is as follows. Since in eqn. (34) for the angle $\theta(z)$ the piezo-(μ_p) and the flexo ($\delta\mu_f q_0$) contributions are included with different signs we could hope to find a certain compensation point for an electro-optical response when varying the composition of a mixture of right and left ferroelectric liquid crystals. Indeed, a minimum has been observed in the dependence of the light modulation depth upon the composition of a mixture of DOBAMBC and HOBACPC, Fig. 54(a). The curves were obtained for two different frequencies, 40 Hz and 10kHz, which correspond to two different conditions, $\omega = 2\pi f << \tau_s^{-1}$ and $\omega > \tau_s^{-1}$. Here $\tau_s = \gamma_1/Kq_0^2$ is a characteristic time for relaxation of the helix which corresponds to the frequency dispersion of the electro-optical response. For pure DOBAMBC this dispersion is shown in Fig. 54(b).

Downloaded by [Tomsk State University of Control Systems and Radio] at 12:54 19 February 2013

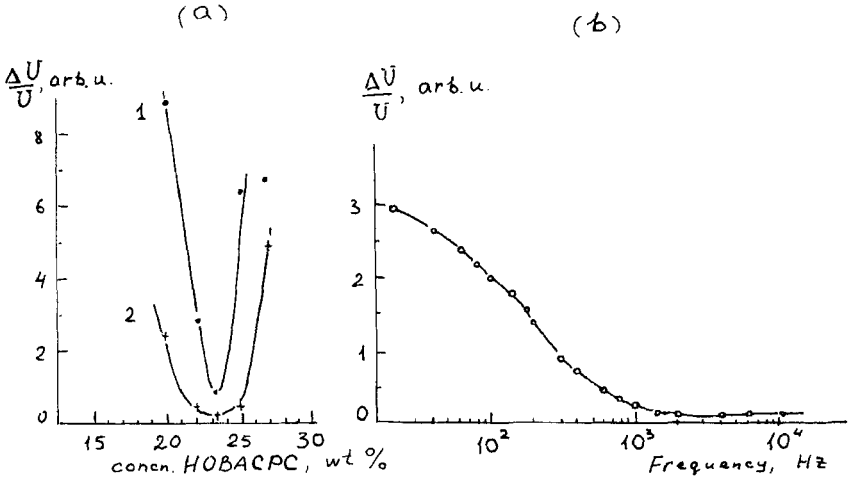

FIGURE 54 The depth of the electro-optical modulation as a function of the composition of a mixture (a), and of the frequency (b) according to Ref. 32. (a) A mixture of DOBAMBC and HOBACPC; (curve 1—frequency 40 Hz, voltage 5V; curve 2—frequency 10 kHz, voltage 15V). (b) DOBAMBC, $T_{CA} - T = 2°C$.

From these experimental data the flexo- and piezo-coefficients were calculated in paper Ref. 33, based on eqns (34, 35).

7.3. The helix unwinding

With increasing electric field applied perpendicular to the helical axis the spiral structure loses its stability.

In the limit of strong field, the director is oriented along the field direction and the structure becomes uniform. The threshold field for helix unwinding E_c is defined by eqn. (33) which was derived neglecting both the dielectric anisotropy ϵ_a and the field dependence of the tilt angle, $\theta = \theta_0$. The field dependence of the helical pitch[24]

$$h\,(\mathrm{E}) = \frac{h_o}{\pi^2} F_1\,(\pi,\mathrm{K})\; F_2\,(\pi,\mathrm{K}) \tag{129}$$

includes the field implicitly through the constant $0 \leqslant \mathrm{K} \leqslant 1$ according to the equation[185]

$$\left(\frac{\chi_\theta \mu_p E}{\mathrm{K}\theta_o}\right)^{1/2} = \frac{\pi^2 \mathrm{K}}{h_o} \Big/ F_2\,(\pi\mathrm{K}) \tag{130}$$

Downloaded by [Tomsk State University of Control Systems and Radio] at 12:54 19 February 2013

Downloaded by [Tomsk State University of Control Systems and Radio] at 12:54 19 February 2013

Here, h_o is the helical pitch at zero field, and

$$F_1(\pi,K) = \int_0^{\pi} \frac{dt}{(1 - K^2 \sin^2 t)^{1/2}}$$

$$F_2(\pi,K) = \int_0^{\pi} (1 - K^2 \sin^2 t)^{1/2} dt$$

are elliptic integrals of first and second orders, respectively.

The purpose of an experiment is a check on the theoretical model and, if possible, the determination of material parameters such as elastic moduli, piezo- and flexo-coefficients, etc. In addition, the application possibilities of the effect of helix unwinding were analysed in the experiments (controllable light diffraction, electro-optical modulation, etc.).[159]

Despite a variety of experimental works concerning the effect of helix unwinding in chiral smectic C* liquid crystals the simple theoretical model described above has only recently been quantitatively confirmed. First of all, this refers to the value of the threshold field E_c. Experimental data on E_c for DOBAMBC ($E_c \approx 4 \cdot 10^2 - 5 \cdot 10^3\ V \cdot cm^{-1}$ in the temperature range $T_c - T$ between 0.2 and 20 K[11,189,200,201]) agree with the theoretically predicted values. Indeed, for $T_c - T$ = 20 K, $h = 2\pi/q_0 = 4\mu$, $\theta_0 = 0.5$, $K = 10^{-6}$ dyn, $\chi_\perp = 0.2$ and μ_p = 120 CGS units[11] eqn. (33) gives $E_c \approx 3$ CGS units $\approx 10^3 V \cdot cm^{-1}$. In earlier investigations once could not manage to detect the anomaly in the temperature behaviour of E_c due to the non-monotonic temperature dependence of the pitch, Fig. 44. However, Takezoe[163] and Kuczynski[202] did recently observe this anomaly, Fig. 55.

The experimental curve for the field dependence of the pitch of DOBAMBC differs markedly from the earlier analytical result, Fig. 56.[199] This discrepancy appears to be due to neglecting[17,185] the dielectric anisotropy. Numerical calculations of $h(E)$ taking into account ϵ_a, were carried out by Dmitrienko.[203] In a particular case, namely, for $R = P_s^2 h_0^2 / \pi \epsilon_a K = 1$ the latter theory gives the very simple dependence

$$h_E = h_0 \left[1 - \frac{\varepsilon_a E}{4\pi P_s} \right]^{-1/2}$$

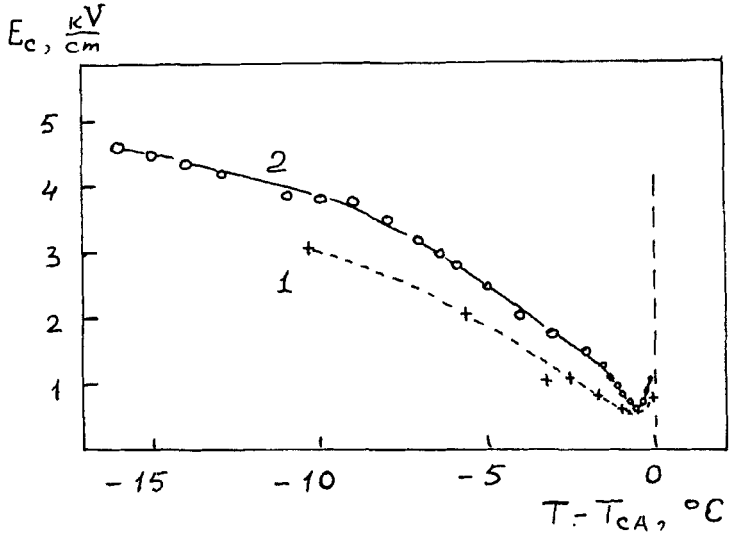

FIGURE 55 Temperature dependence of the threshold field of helix unwinding for DOBAMBC. Curve 1—from Ref. 12, cell thickness 100μ; curve 2—from Ref. 165, thickness 120 μm.

For DOBAMBC P_s = 9 CGS u., h_o = $2 \cdot 10^{-4}$ cm, ϵ_a = 2.4 and R = 1 for the very reasonable value of K = $3 \cdot 10^{-7}$ dyn. The corresponding theoretical curve is given in Fig. 56. It may be seen that the experimental curves lie between the two theoretical ones, that is, in general, the theory agrees with experiment.

The interaction of a liquid crystal with the limiting solid boundaries plays an important role in experiments with helix unwinding. For instance, the critical field depends considerably on the cell thickness. The picture becomes even more complicated in the vicinity of the smectic A–smectic C* phase transition. In fact, such a situation is typical of the experiments with DOBAMBC and other ferroelectrics studied until now. First, a field blurs the phase transition, Fig. 12 and, second, it influences the tilt angle θ for a given temperature difference $T_c - T$ (an electro-clinic effect). The corresponding corrections should be taken into account in any strict future theory.

The role of the solid boundaries in the unwinding process manifests itself by the fact that the helical pitch increases with increasing field in a non-monotonic way. This problem was investigated in detail[182] using an analysis of the corresponding optical pattern with respect to the wave vectors (the technique included a polarizing microscope

Downloaded by [Tomsk State University of Control Systems and Radio] at 12:54 19 February 2013

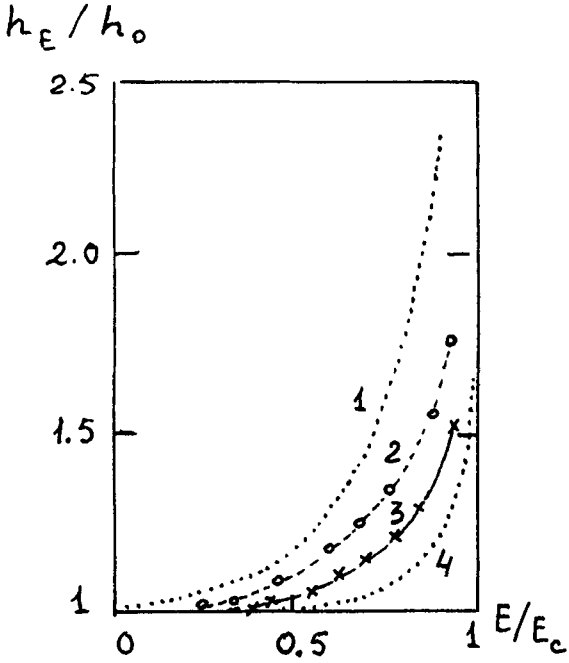

FIGURE 56 The helical pitch as a function of the external field. Curve 1—theory of Ref. 17 for $\varepsilon_a = 0$; curve 4—theory of Ref. 203 for $\varepsilon_a = 2.4$ and R = 1; curve 2—experimental data from Ref. 165, for $T_c - T = 0.7$ K; curve 3—experimental data from Ref. 165 for $T_c - T = 1.7$ K.

with a video camera and a microprocessor). It was shown, that the process of helix unwinding in a sample of DOBAMBC with thickness 60μ proceeds more or less in accordance with theory only for temperatures close ($T_c - T \approx 1$–2 K) to the C* – A transition. In this case, a discrete line in the power spectrum of the scattered light is monotonically shifted to smaller wave vectors with increasing field. When the difference $T_c - T$ is larger (say, 10 K) an increase in the field results not only in the shift of the line but also in its broadening and even in the appearance of new lines in the power spectrum. This means a distortion of the uniform system of linear domains shown in Fig. 51. For still lower temperatures ($T_c - T \approx 25$ K) an external field ($E = 3.3$ kV·cm^{-1}, cell thickness 6μ) converts an initial system of equidistant linear domains into a set of groups of closely located lines with large distances between groups.[204] The increase in viscosity with decreasing temperature appears to harden the process of unwinding which is surely accompanied by the motion of disclinations.

Downloaded by [Tomsk State University of Control Systems and Radio] at 12:54 19 February 2013

According to the Glogarova model,[26] the disclination lines exist near the upper and the lower solid boundaries of a layer of a ferroelectric liquid crystal, Fig. 57(a). With increasing field the upper and lower rows of disclination approach each other, Fig. 57(b) and then form pairs, i.e., π-disclinations, Fig. 57(c). Further increase in the field results in the broadening of the domains with a homogeneous

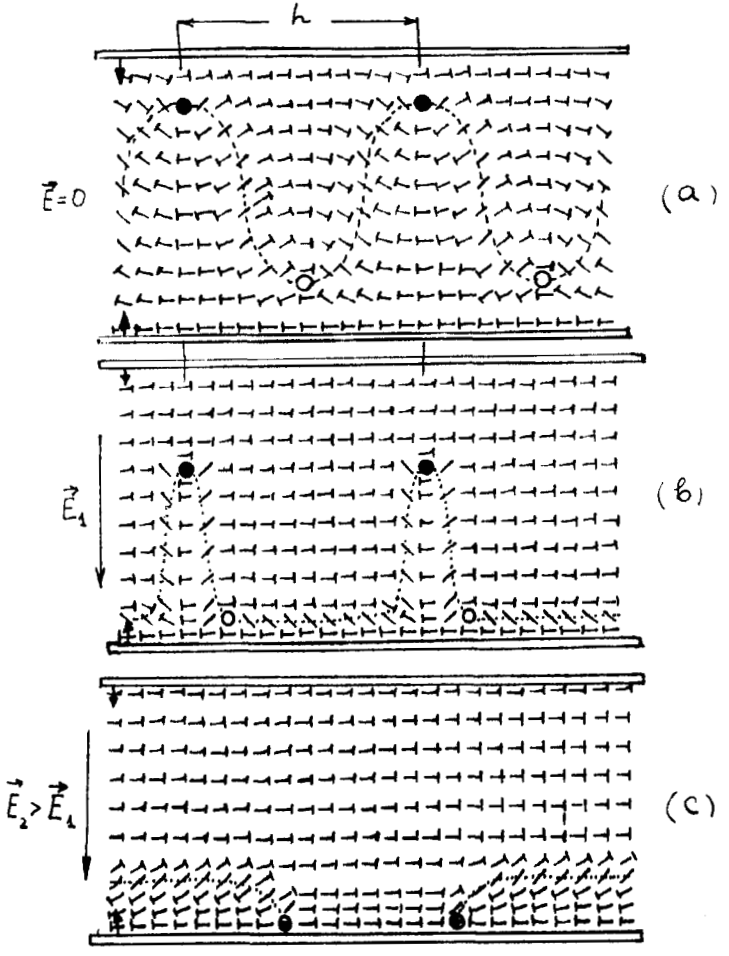

FIGURE 57 The Glogarova model[26] for unwinding the planar helical structure in an electric field. The boundary conditions are symmetrical. Symbols ● and ○ are cross sections of ± 2 disclinations.

Downloaded by [Tomsk State University of Control Systems and Radio] at 12:54 19 February 2013

orientation of the director at the cost of the areas with the opposite orientation. Eventually the uniform structure is achieved. The first critical field E_1 corresponds to the formation of π-disclinations and the second critical field E_2 is associated with the formation of the uniform structure. For DOBAMBC the situation is especially complicated as $E_1 \approx E_2$.

The model[26] explains a lot of optical observations and can be a basis for the quantitative measurements of the material parameters.

The dynamics of helix unwinding was investigated theoretically and experimentally in Ref 205. Experimental results were compared with a numerical solution of the equation

$$K\,\theta_0 \frac{d^2\varphi}{dz^2} - \gamma_1\,\theta_0 \frac{d\varphi}{dt} + \chi\,\mu_p E \sin\varphi = 0$$

which is written for an infinite sample and θ_0 = const. For a small distortion of the helical structure in a weak field its relaxation is described by the time $\tau_s^0 = \gamma_1/Kq_0^2$ (§ 2.4). However, a decrease in a wave vector with increasing field results, in general, in an increase of the relaxation time. At the point $E = E_c$ the relaxation time $\tau_s(E_c)$ becomes infinite, i.e. the ratio $\tau_s(E)/\tau_s^0$ tends to zero, see Inset to Fig. 58. The effect of a strong ($E > E_c$) field on the unwound structure is reduced to switching the director from one position to the other after a change in the sign of the field. In the latter case, the experiment[205] shows the linear field dependence of the inverse time of switching τ_s^{-1}, Fig. 58.

The recent studies[206,207] of the dynamics of helix unwinding in the smectic C* phase point, however, to a more complicated nature of this phenomenon. For example, the fast photography of the process carried out with a pulse lamp (DOBAMBC, cell thickness 100μ[206]) shows that the distance between parallel strips of the domains does not increase smoothly, but instead, separate lines disappear during the transient regime. It looks as if the field pushed some defects (dechiralization lines) out of the sample. These results confirm the Glogarova model, shown in Fig. 57. The important role of structural defects, namely, walls deviding spatial areas with opposite directions of the spontaneous polarization was also emphasized in Ref. 131. Moreover, the walls should remain even in the strong field limit when the helix is unwound. In this case, the speed of switching the director in an a.c. field is limited by the motion of the walls and the switching

Downloaded by [Tomsk State University of Control Systems and Radio] at 12:54 19 February 2013

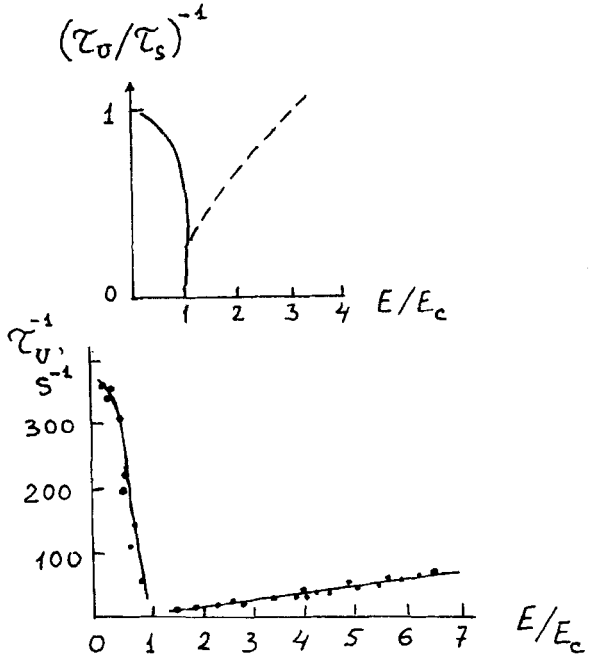

FIGURE 58 Response time for the helical structure of DOBAMBC as a function of the strength of the field in the form of a single pulse. Upper: theoretical curve $\tau_s = \gamma_1/Kq_o^2$. Lower: experiment with a cell of thickness 100 μm (from Ref. 205).

time is proportional to the square root of the external voltage. The experiment carried out on thin (~ 10μ) samples of DOBAMBC[131] appears to confirm this root dependence. Therefore, for thin and thick (Fig. 58) samples the data are controversial and the whole problem requires new investigations.

7.4. Switching the director in a strong field

The linear electro-optical effect is the most remarkable property of liquid crystalline ferroelectrics and is the basis for their practical applications. The first observation of the effect was already made in the pioneering work[1] where a linear field-induced shift of a conoscopic figure was detected for a homeotropic layer of DOBAMBC. The same effect may be used for light modulation by a sequence of voltage pulses with changing polarity. In the latter case, as it was shown in

Downloaded by [Tomsk State University of Control Systems and Radio] at 12:54 19 February 2013

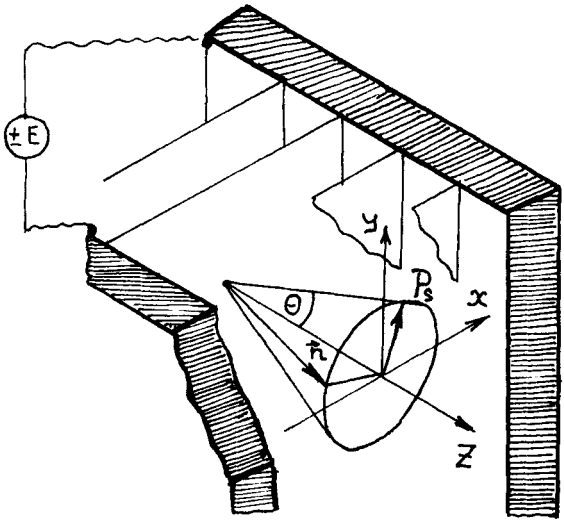

FIGURE 59 Switching the director by the interaction of the field $\pm E_x$ with the spontaneous polarization P_s.

Ref. 185, a ferroelectric liquid crystal has three stable states corresponding to positive, zero, and negative voltages.

The experiment[185] was performed in the following way. The initial structure was helical with the spiral axis lying in the plane of the cell. The helix was unwound in a sufficiently strong field. The homogeneous, optically uniaxial layer was obtained with the direction of the director determined by the field polarity ($+\theta$ or $-\theta$ with respect to a certain mean position). A change in the field polarity switches the director by the angle 2θ. A number of different ways for optical modulation were realized for various polarization directions of the incident light (a He-Ne laser) and the position of the analyser.

In the first experiments[185] a full cycle of 100% optical switching comprised 500 μS (DOMBAMBC, $E = 6 \cdot 10^3$ V·cm^{-1}, cell thickness $\approx 100\mu$) and the inverse time τ_s^{-1} linearly increased with the voltage exceding the threshold for helix unwinding, Fig. 58.[205] Clark and Lagerwall[5,208] improved considerably the fastness of switching using very thin (microns) liquid crystal layers. In the latter case, the helix is unwound by surface forces even at a zero field. The initial direction of the director is preset by rubbing glass surfaces, e.g. along the z-axis, Fig. 60. A light shift of the glasses along the y-axis[186] forces the smectic layers to align perpendicular to the plane of the glasses. In

Downloaded by [Tomsk State University of Control Systems and Radio] at 12:54 19 February 2013

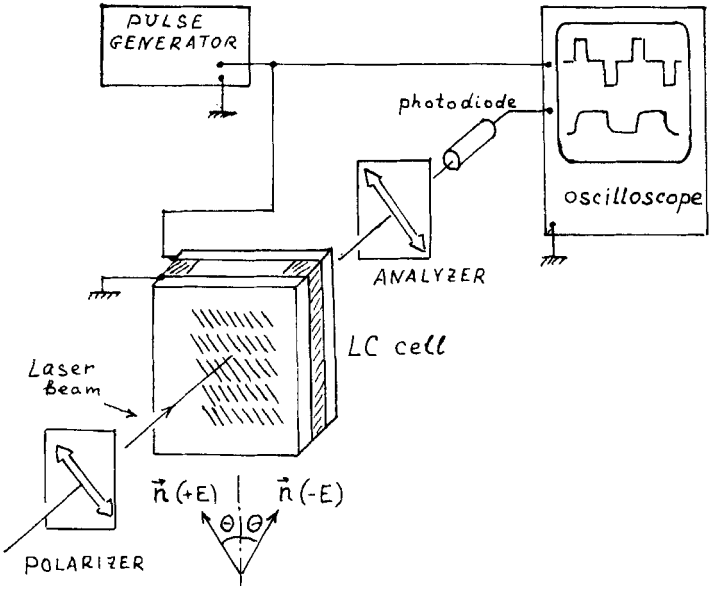

FIGURE 60 Electrooptical arrangement for the observation of the director switching in ferroelectric liquid crystals.

this case, the angle, θ_o between the director and the normal to the smectic layers remains constant.

An applied field interacts with the spotaneous polarization vector and tends to orient $P_s \parallel E$. The reorientation of P_s is accompanied by the turn of the director $\bar{n}$ which remains at the conical surface with the apex angle $2\,\theta$ as discussed above, Fig. 60. The turn of the director means the turn of the optical axis by the angle, say $+\,\theta_o$, from its initial orientation along the z-axis. The change in the field polarity results in the same turn of the director but in the opposite direction and the optical axis turns by the angle $-\,\theta_o$. Thus, switching the optical axis by the angle $2\,\theta_o$ after a change in the field polarity allows the 100% light modulation to be obtained for a proper set of a polarizer and an analyser (remember, that $\theta_o = \theta_\epsilon$ is assumed), Fig. 60.

The switching time may be estimated by the formula

$$\tau \simeq \frac{\gamma_1}{P_s E}$$

Downloaded by [Tomsk State University of Control Systems and Radio] at 12:54 19 February 2013

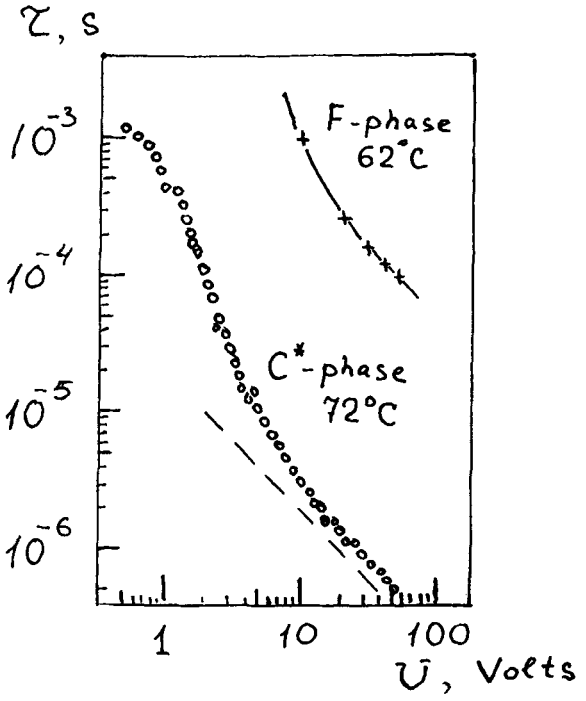

FIGURE 61 Switching time VS applied voltage for different ferroelectric phases of HOBACPC.

which agrees qualitatively with experiment. In Fig. 61 the curve τ (E) for a layer (thickness = 1,5μ) of HOBACPC was reproduced from the original paper.[208] Short times of the order of 0.5μS were obtained at strong field ($E \approx 3 \cdot 10^5$ V·cm^{-1}). This figure agrees qualitatively with an extrapolation from reference[185] where the field was 50 times less (the difference in the P_s values for DOBAMBC and HOBACPC should also be taken into account).

For mixtures having the smectic C* phase at lowered temperatures the switching times increase for an increase in the viscosity coefficient γ_1.[209,210] At room temperature the switching times lie in the millisecond range. Strictly speaking, there are two twist-viscosity coefficients corresponding to changes in the tilt (θ) and the azimuthal (φ) angles of the director. Fortunately, the γ_1^{φ} coefficient which defines the electrooptical behaviour of ferroelectric liquid crystals is one or two order of magnitude smaller than γ_1^{θ} [226] and this fact accounts for

Downloaded by [Tomsk State University of Control Systems and Radio] at 12:54 19 February 2013

the faster switching of smectic C* as compared to nematics at nearly the same values of $\epsilon_a E^2$ and $P_s E$.

The director switching process does not envelope simultaneously a whole sample. Domains where the polarization follows the new field direction are generated in the form of separate islands surrounded by the domain walls. The thickness of the wall is of the order of the coherence length $\xi = (K/P_s E)^{1/2}$.[211] The area of the islands increases during a transient process and the velocity of the wall is proportional to the field strength and is markedly different for the direction along ($\nu_{\parallel}$) and transverse ($\nu_{\perp}$) to the smectic layers, $\nu_{\parallel} \approx 2\nu_{\perp}$[212]. The linear dependence $\nu \propto E$ obtained in Refs. 212 and 211 using a stroboscopic technique for very thin ($\sim 1\mu$) layers does not agree with the square root dependence $\nu \propto E^{1/2}$ obtained in Ref. 131 for rather thick (10μ) layers of DOBAMBC where the helical structure is still preserved. The intensive light scattering by the domain walls, which accompanies switching the director, may be used for manufacturing electro-optical devices with response times in the microsecond range and with no polaroids.

The detailed investigations of the switching process in the smectic C* phase were recently carried out for DOBAMBC and HOBACPC.[68,213] The latter paper contains useful data on various material parameters for HOBACPC which is a classical ferroelectric liquid crystal with a high value of the spontaneous polarization. A field parallel to the plane of a liquid crystal layer also causes the director switching accompanied by an appearance of interference colours. Such an effect was recently studied in Ref. 214.

In addition to the smectic C* phase the optical switching effect is also observed in other, low temperature phases. However, in this case the switching times are considerably longer. This is seen, e.g. in Fig. 61 where the upper curve (62° C) is referred to the smectic I* phase of HOBACPC studied in more detail in Ref. 208.

According to Refs. 137 and 215 the low temperature phases I*, X* and others are truely bistable, i.e., have two or more stable states analogous to those of solid ferroelectrics. The electric field can switch a liquid crystal from one state to the other. In the case of the smectic C* phase, the true bistability could probably be obtained only for specific boundary conditions caused by the polar interaction of the spontaneous polarization with the solid surfaces.[216]

In conclusion of this chapter, it should be noted that a strong electric field interacts not only with the spontaneous polarization but can give rise to an ordinary quadratic orientational effect,[217] electrohydrodynamic instabilities[218] and various modulated structures.[219]

Downloaded by [Tomsk State University of Control Systems and Radio] at 12:54 19 February 2013

Downloaded by [Tomsk State University of Control Systems and Radio] at 12:54 19 February 2013

VIII. POSSIBILITIES FOR THE PRACTICAL APPLICATION OF FERROELECTRIC LIQUID CRYSTALS

From the practical point of view the electrooptical properties of the smectic C* phase are the most important. In comparison with conventional nematics, smectics C* provide an improved speed of response and bistable switching which allows one to display the information in the field-off state. It is accepted[186] that smectics C* could be switched even in a submicrosecond range. With decreasing temperature a strong increase in spontaneous polarization somewhat compensates for an increase in viscosity γ_1 and, hence, the speed of response ($\tau \approx \gamma_1/P_sE$) becomes worse not to such an extent as is typical of nematic mixtures ($\tau \approx \gamma_1/\epsilon_a E^2$) where the value of the dielectric anisotropy quickly reaches saturation. Besides, the twist viscosity coefficient γ_1^{φ} itself is less than the value obtained by an extrapolation of the "nematic" value of γ_1 into the temperature range of the smectic C* phase.[226]

High speed of response opens up strong possibilities for utilization of ferroelectric liquid crystals in various light controlling devices such as optical shutters and modulators, controllable transparencies in optical processing systems, matrix displays, flat TV screens and large information pannels.[220] One of the first practical realizations is a linear modulating array for the xerox system.[221] A wide distribution of ferroelectric liquid crystals is still delayed by an absence of the necessary spectrum of substances with a wide temperature range and high spontaneous polarization. In addition, the technique for preparing optically homogeneous samples is still weakly developed.

The phase transition between a twisted smectic C* and a homogeneous smectic A, in fact, does not reveal a latent heat. It opens up the possibility to use smectic C* as visualizers of the heat radiation. This principle is the basis for recording information by a laser beam[223,222] which is of interest for manufacturing some auxiliary computer devices, e.g., graph plotters. The shift of the phase transition temperature with impurity concentration can be used for the detection of radiolysis products and for constructing detectors of ionizing radiation.

The utilization of ferroelectric liquid crystals in piezo- and pyroelectric elements, that is in the traditional sphere of application of solid ferroelectrics, is also interesting as a liquid crystalline (i.e., in fact, liquid) medium allows the sufficiently bulky devices of an arbitrary form to be constructed. However, in this respect the most important substances are the ferroelectric liquid crystalline polymers

which allow one to prepare solid films with pyro- and piezo-electric properties.[139] In addition, there exists the possibility to build composite materials based on polymeric (non ferroelectric) liquid crystals with solid ferroelectric inclusions.[46]

Further investigations are necessary of the non-linear optical properties[224] of ferroelectric liquid crystals. Apart from the giantic orientational non-linearity characteristic of centrosymmetric phases, these substances reveal optical second harmonic generation and other effects caused by a lack of an inversion center. A remarkable feature of liquid crystalline materials (as compared to crystals) is an enhanced optical strength.

Downloaded by [Tomsk State University of Control Systems and Radio] at 12:54 19 February 2013

REFERENCES

1. R. B. Meyer, L. Liebert, L. Strzelecki and P. Keller, *J. Physique, Lett.* **36**, L-69 (1975).
2. I. E. Dzyaloshinskii, *Zh. Eksp. Teor. Fiz.*, **46**, 1420 (1964).
3. R. B. Meyer, *Mol. Cryst. Liq. Cryst.*, **40**, 33 (1977).
4. P. Pieranski, E. Guyon and P. Keller, *J. Physique*, **36**, 1005 (1975).
5. N. A. Clark and S. T. Lagerwall, *Appl. Phys. Lett.*, **36**, 899 (1980).
6. B. I. Ostrovskii, A. Z. Rabinovich, A. S. Sonin, B. A. Strukov and N. I. Chernova. *Pis'ma v Zh. Eksp. Teor. Fiz.*, **25**, 80 (1977).
7. L. J. Yu, H. Lee, C. S. Bak and M. M. Labes, *Phys. Rev. Lett.*, **36**, 388 (1976).
8. L. A. Beresnev, L. M. Blinov and Z. M. Elashvili, *Pis'ma v Zh. Eksp. Teor. Fiz.*, **4**, 225 (1978).
9. S. Garoff and R. B. Meyer, *Phys. Rev. Lett.*, **38**, 848 (1977).
10. Ph. Martinot-Lagarde, *J. Physique Coll.*, **37**, C3-129 (1976).
11. B. I. Ostrovskii, A. Z. Rabinovich, A. S. Sonin and B. A. Strukov, *Zh. Eksp. Teor. Fiz.*, **74**, 1748 (1978).
12. H. Takezoe, K. Kondo, K. Miyasato, S. Abe, T. Tsuchiya, A. Fukuda and E. Kuze, *Ferroelectrics*, **58**, 55 (1984).
13. C. Y. Young, R. Pindak, N. A. Clark and R. B. Meyer, *Phys. Rev. Lett.*, **40**, 773 (1978).
14. S. A. Pikin, "Structurnyie Prevrascheniya v Zhydkih Kristallaňh" (Nauka, Moscow, 1981) (in Russian).
15. S. A. Pikin and V. L. Indenbom, *Uspekhi Fiz. Nauk.*, **125**, 251 (1978).
16. H. De Vries, *Acta Cryst.*, **4**, 219 (1951).
17. P. G. de Gennes, "The Physics of Liquid Crystals" (Claredon Press, Oxford, 1974).
18. I. Dahl and S. T. Lagerwall, *Ferroelectrics*, **58**, 215 (1984).
19. A. Saupe, *Mol. Cryst. Liq. Cryst.*, **7**, 59 (1969).
20. Orsay Group on Liquid Crystals, *Solid State Comm.*, **9**, 653 (1971).
21. M. A. Osipov, S. A. Pikin, *Zh. Eksp. Theor. Fiz.*, **82**, 774 (1982).
22. A. Levstik, B. Žekš, C. Filipič, R. Blinc and I. Levstik, *Ferroelectrics*, **58**, 33 (1984).
23. E. P. Pozhidayev, L. A. Beresnev, L. M. Blinov and S. A. Pikin, *Pis'ma v Zh. Eksp. Teor. Fiz.*, **37**, 9 (1983).
24. P. G. De Gennes, *Solid State Comm.*, **6**, 163 (1968).

25. B. I. Ostrovskii, S. A. Pikin and V. G. Chigrinov, *Zh. Eksp. Teor. Fiz.*, **77**, 1631 (1979).
26. M. Glogarova, J. Fousek, L. Lejček and J. Pavel, *Ferroelectrics*, **58**, 161 (1984).
27. R. Blinc, *Phys. Stat. Sol.*, **B70**, K 29 (1975).
28. R. Blinc, *Ferroelectrics*, **14**, 603 (1976).
29. R. Blinc, *Ferroelectrics*, **16**, 33 (1977).
30. R. Blinc, B. Žekš, *Phys. Rev.*, **A18**, 740 (1978).
31. G. Durand and Ph. Martinot-Lagarde, *Ferroelectrics*, **24**, 89 (1980).
32. L. A. Beresnev, V. A. Baikalov and L. M. Blinov, *Ferroelectrics*, **58**, 245 (1984).
33. V. G. Chigrinov, V. A. Baikalov, E. P. Pozhidayev, L. M. Blinov, L. A. Beresnev and A. I. Allagulov, *Zh. Eksp. Teor. Fiz.*, **88**, 2015 (1985).
34. L. Musevič, B. Žekš, R. Blinc, Th. Rasing and P. Wyder, *Phys. Rev. Lett.*, **48**, 192 (1982).
35. A. Michelson, L. Benguigui and D. Cabib, *Phys. Rev.*, **A16**, 394 (1977).
36. A. Michelson and D. Cabib, *J. Physique Lett.*, **38**, L-321 (1977).
37. S. A. Pikin and K. Yoshino, *Jap. J. Appl. Phys.*, **20**, L-557 (1981).
38. L. Lejček, *Ferroelectrics*, **58**, 139 (1984).
39. Ph. Martinot-Lagarde, R. Duke and G. Durand, *Mol. Cryst. Liq. Cryst.*, **75**, 249 (1981).
40. M. A. Handschy and N. A. Clark, *Ferroelectrics*, **59**, 69 (1984).
41. J. M. Kosterlitz and D. Thouless, *J. Phys.*, **C6**, 1181 (1973).
42. D. R. Nelson and R. A. Pelcovits, *Phys. Rev.*, **B16**, 2191 (1977).
43. R. A. Pelcovits and B. I. Halperin, *Phys. Rev.* **B19**, 4614 (1979).
44. A. Z. Patashinskii and V. L. Pokrovskii, "Fluktuatsionnaya Teoriya Fazovyh Perehodov," (Nauka, Moscow, 1982) (in Russian).
45. S. Heinekamp, R. A. Pelcovits, E. Fontes, E. Yi. Chen, R. Pindak and R. B. Meyer, *Phys. Rev. Lett.*, **52**, 1017 (1984).
46. E. M. Terentjev and S. A. Pikin, *Ferroelectrics*, **59**, 11 (1984).
47. K. Yoshino, M. Ozaki, S. Kishio, T. Sakurai, N. Mikami, R. Higuchi and M. Honma, *11th Int. Liq. Cryst. Conf.*, Berkeley (USA), 1986, Abstracts, FE-01.
48. Ch. Bahr and G. Heppke. ibid., FE-8.
49. C. Salleneuve, Nguyen Huu Tinh and C. Destrade. ibid., 0-016-FE.
50. A. Alstermark and B. Otterholm. ibid., 0-031-FE.
51. W. Kuszyński, S. T. Lagerwall, K. Sharp, B. Stebler and J. Wahl, *ibid.*, 0-036-FE.
52. H. A. Razavi, D. M. Walba, D. S. Parma, N. A. Clark and M. D. Wand, *ibid.*, 0-038-FE.
53. "Ferroelectric Liquid Crystals and intermediates" from Displaytech, Inc., Catalog W7, W37, W81, W82.
54. R. T. Vohra, D. M. Walba, D. S. Parmar and N. A. Clark., *11th Int. Liq. Cryst. Conf.*, Berkeley (USA), 1986, Abstracts, 0-039-FE.
55. V. M. Kaganer and S. A. Pikin, *Kristallografiya*, **31**, 640 (1986).
56. K. Yoshino, T. Uemoto and Y. Inuishi, *Jap. J. Appl. Phys.*, **16**, 571 (1977).
57. J. Hoffmann, W. Kuczyński and Y. Malecki, *Mol. Cryst. Liq. Cryst.*, **44**, 287 (1978).
58. L. M. Blinov, L. A. Beresnev, N. M. Shtykov and Z. M. Elashvili, *J. Physique Coll.*, **40**, C3-269 (1979).
59. L. Petit, P. Pieranski and E. Guyon, *C. R. Acad. Sci. Paris*, **B284**, 535 (1977).
60. C. Rosenblat, R. Pindak, N. A. Clark and R. B. Meyer, *Phys. Rev. Lett.*, **12**, 1220 (1979).
61. C. B. Sauyer and C. H. Tower, *Phys. Rev.*, **35**, 269 (1930).
62. H. Diamant, K. Drenk and R. Pepinsky, *Rev. Sci. Instr.*, **28**, 30 (1957).
63. J. Pavel, M. Glogarova, D. Demus, A. Mädicke and G. Pelzl, *Cryst. Res. and Techn.*, **18**, 915 (1983).
64. K. Sharp, T. Dahl, S. T. Lagerwall and B. Stebler, Preprint (*Mol. Cryst. Liq. Cryst.*—in press).

Downloaded by [Tomsk State University of Control Systems and Radio] at 12:54 19 February 2013

65. Ph. Martinot-Lagarde, *J. Physique Lett.*, **38**, L-17 (1977).
66. K. Miyasato, S. Abe, H. Takezoe, A. Fukuda and E. Kuze, *Jap. J. Appl. Phys.*, **22**, L-661 (1983).
67. T. Urabe, K. Yoshino and Y. Inuishi, *Tech. Repts. Osaka Univ.*, **33**, 81 (1983).
68. J. Wahl and S. C. Jain, *Ferroelectrics*, **59**, 181 (1984).
69. B. I. Ostrovskii, A. Z. Rabinovich, A. S. Sonin, E. L. Sorkin, B. A. Strukov and S. A. Taraskin, *Ferroelectrics*, **24**, 309 (1980).
70. W. Kuszynski and H. Stegemeyer, *Chem. Phys. Lett.*, **70**, 123 (1980).
71. L. A. Beresnev, L. M. Blinov and E. B. Sokolova, *Pis' ma v Zh. Eksp. Teor. Fiz.*, **28**, 340 (1978).
72. E. P. Pozhidayev, L. M. Blinov, L. A. Beresnev and V. V. Belyayev, *Mol. Cryst. Liq. Cryst.*, **124**, 359 (1985).
73. N. Maruyama, *Ferroelectrics*, **58**, 187 (1984).
74. A. Buka and L. Bata, *Mol. Cryst. Liq. Cryst. Lett.*, **49**, 159 (1979).
75. L. Bata and A. Buka, *Mol. Cryst. Liq. Cryst.*, **63**, 307 (1981).
76. R. Blinc, *Ann. Phys.*, **3**, 189 (1978).
77. J. Hoffmann and W. Kuszynski, *Ferroelectrics Letters*, **4**, 89 (1985).
78. D. S. Parmar and Ph. Martinot-Lagarde, *Ann. Phys.*, **3**, 275 (1978).
79. S. Garoff and R. B. Meyer, *Phys. Rev. A*, **18**, 2739 (1978).
80. S. Garoff and R. B. Meyer, *Phys. Rev. A*, **19**, 338 (1979).
81. a) M. Delaye, *Ann. Phys.*, **3**, 387 (1978); b) M. Delaye, *J. Physique*, **40**, C3-350 (1979); c) M. Delaye and P. Keller, *Phys. Rev. Lett.*, **37**, 1065 (1976).
82. R. Bartolino, J. Doucet and G. Durand, *Ann. Phys.*, **33**, 389 (1978).
83. T. Carlsson and J. Dahl, *Mol. Cryst. Liq. Cryst.*, **95**, 373 (1983).
84. C. C. Huang and J. M. Viner, *Phys. Rev. A.*, **25**, 3385 (1982).
85. Ph. Martinot-Lagarde and G. Durand, *J. Physique*, **42**, 269 (1981).
86. L. Benguigui, *J. Physique*, **43**, 915 (1982).
87. K. Yoshino, T. Uemoto and Y. Inuishi, *Jap. J. Appl. Phys.*, **18**, 1261 (1979).
88. B. Žekš, A. Levstik and R. Blinc, *J. Physique*, **40**, C3-409 (1979).
89. A. Levstik, B. Žekš, I. Levstik, R. Blinc and C. Filipič, *J. Phusique*, **40**, C3-303 (1979).
90. K. Yoshino, M. Ozaki, H. Agawa and Y. Shigeno, *Ferroelectrics*, **58**, 283 (1984).
91. B. Otterholm, C. Alstermark, A. Dahlgren, K. Flatischler and S. T. Lagerwall, *11th Int. Conf. on Liquid Crystals*, Berkeley (USA), 1986, Abstracts, 0-033-FE.
92. I. Muševič, B. Žekš, R. Blinc, Th. Rasing and P. Wyder, *Phys. Stat. Sol.* (b), **119**, 727 (1983).
93. E. P. Pozhidayev, L. A. Beresnev and L. M. Blinov, *5th All-Union Conf. on Liquid Crystals*, Ivanovo, 1985, Abstracts, v. 1, No. 2, p. 176.
94. V. L. Indenbom, S. A. Pikin and E. B. Loginov, *Kristallografiya*, **21**, 1093 (1976).
95. L. A. Beresnev and L. M. Blinov, *Zh. Vsesoyuzn. Chimicheskogo Obsh. im D. I. Mendeleyeva*, **28**, 149 (1983).
96. P. Keller, L. Liebert and L. Strzelecki, *J. Physique*, **37**, C-3-27 (1976).
97. T. Uemoto, K. Yoshino and U. Inuishi, *Mol. Cryst. Liq. Cryst.*, **67**, 137 (1981).
98. K. Yoshino, T. Uemoto, K. G. Balakrishnan, S. Yanagida and Y. Inuishi, in: "Proceedings of the 1st Meeting on Ferroelectric Materials and Their Applications," Kyoto, 1977, L-1, p. 115–120.
99. L. A. Beresnev, *Doct. Diss.*, Moscow, 1979.
100. M. Imasaki, T. Fujimoto, T. Nishichara, T. Yoshioka and Y. Narushige, *Jap. J. Appl. Phys.*, **21**, 1100 (1982).
101. P. Keller, S. Juge, L. Liebert and L. Strzelecki, *C. R. Acad. Sci. Paris*, **C-282**, 639 (1976).
102. L. A. Beresnev, L. M. Blinov and G. V. Purvanetskas, *Pis'ma v Zh. Eksp. Teor. Fiz.*, **31**, 37 (1980).
103. A. Hallsby, M. Nilsson and B. Otterholm, *Mol. Cryst. Liq. Cryst.*, **82** (Lett.), 61 (1982).

Downloaded by [Tomsk State University of Control Systems and Radio] at 12:54 19 February 2013

104. T. M. Leslie, *Ferroelectrics*, **58**, 9 (1984).
105. K. Yoshino, M. Ozaki, T. Sakurai, K. Sakamoto and M. Honma, *Jap. J. Appl. Phys.*, **23**, L175 (1984).
106. T. Sakurai, K. Sakamoto, M. Honma, K. Yoshino and M. Ozaki, *Ferroelectrics*, **58**, 21 (1984).
107. P. Keller, *Mol. Cryst. Liq. Cryst.*, **102** (Lett.), 295 (1984).
108. M. V. Loseva, B. I. Ostrovskii, A. Z. Rabinovich, A. S. Sonin and N. I. Chernova, *Fiz. Tverd. Tela*, **22**, 938 (1980).
109. J. Billard, *Ferroelectrics*, **58**, 81 (1984).
110. K. Furukawa, K. Terashima, M. Ichihashi, H. Inoue, S. Saito and T. Inukai, *6th Liq. Cryst. Conf. Soc. Count.*, Halle (GDR), 1985, Abstracts, A37.
111. P. Keller, *Ferroelectrics*, **58**, 3 (1984).
112. M. F. Bone, D. Coates and A. B. Davey, *Mol. Cryst. Liq. Cryst.*, **102** (Lett.), 331 (1984).
113. J. L. Alabart, M. Marcos, E. Melendez and J. L. Serrano, *Ferroelectrics*, **58**, 37 (1984).
114. M. Luzar, V. Rutar, J. Seliger and R. Blinc, *Ferroelectrics*, **58**, 115 (1984).
115. L. M. Blinov and L. A. Beresnev, *Usp. Fiz. Nauk*, **143**, 391 (1984).
116. L. A. Beresnev and L. M. Blinov, *Ferroelectrics*, **33**, 129 (1981).
117. L. A. Beresnev, L. M. Blinov, V. A. Baikalov, E. P. Pozhidayev, G. V. Purvanetskas and A. I. Pavluchenko, *Mol. Cryst. Liq. Cryst.*, **89**, 27 (1982).
118. L. A. Beresnev, E. P. Pozhidayev, L. M. Blinov, A. I. Pavluchenko and N. B. Etingen, *Pis'ma v Zh. Eksp. Teor. Fiz.*, **35**, 430 (1982).
119. D. Demus, H. Demus and H. Zaschke, "Flussige Kristalle in Tabelen," VEB Deutscher Verlag, Leipzig, 1974.
120. G. S. Chilaya and L. N. Lisetskii, *Usp. Fiz. Nauk*, **134**, 279 (1981).
121. M. A. Osipov, *Ferroelectrics*, **58**, 305 (1984).
122. M. A. Osipov and S. A. Pikin, *Mol. Cryst. Liq. Cryst.*, **103**, 57 (1983).
123. H. Matsumura, *Mol. Cryst. Liq. Cryst., Lett.*, **49**, L-105 (1978).
124. M. Imasaki, S. Kai, Y. Narushige and T. Fujimoto, *Ferroelectrics*, **58**, 47 (1984).
125. V. G. Ivkov, and G. N. Berestovskii, "Dinamicheskaya struktura lipidnogo bisloya," Moscow, Nauka, 1981.
126. A. A. Shaginyan, V. A. Zakaryan, A. A. Sanasaryan and M. H. Minasyants, *5th Liq. Cryst. Conf. Soc. Countries*, Odessa (USSR), 1983, Abstracts, v. 2, p. 190.
127. M. Brunet and U. Williams, *Ann. Phys*, **3**, 237 (1978).
128. M. Glogarova and J. Pavel, *J. Physique*, **45**, 143 (1984).
129. L. A. Beresnev, V. A. Baikalov, L. M. Blinov, E. P. Pozhidayev and G. V. Purvanetskas, *Pis'ma v Zh. Eksp. Teor. Fiz.*, **33**, 553 (1981).
130. R. Duke, G. Durand and Ph. Martinot-Lagarde, *6th Int. Liq. Cryst. Conf.*, Kent State University, 1976.
131. P. E. Cladis, H. R. Brand and P. L. Finn, *Phys. Rev. A*, **28**, 512 (1983).
132. L. A. Beresnev, E. P. Pozhidayev and L. M. Blinov, *Ferroelectrics*, **59**, 1 (1984).
133. V. A. Baikalov, L. A. Beresnev and L. M. Blinov, *Mol. Cryst. Liq. Cryst.*, **127**, 97 (1985).
134. L. A. Beresnev, L. M. Blinov, V. A. Baikalov and E. P. Pozhidayev, *9th Int. Liq. Cryst. Conf.*, Bangalore (India), 1982, Abstracts, p. 209.
135. S. B. Lang. *Ferroelectrics*, **34**, 3 (1981).
136. J. Doucet, P. Keller, A. M. Levelut and P. Porquet, *J. Physique*, **39**, 548 (1978).
137. H. R. Brand and P. E. Cladis, *J. Physique* (Lett.), **45**, L-217 (1984).
138. M. V. Kozlovskii, S. G. Kononov and L. A. Beresnev, *5th All-Union Liq. Cryst. Conf.*, Ivanovo (USSR), 1985, Abstracts, E-45.
139. V. P. Shibayev, M. V. Kozlovskii, L. A. Beresnev, L. M. Blinov and N. A. Platé, *Polymer Bulletin*, **12**, 299 (1984).
140. S. G. Galaktionov, *Asimmetriya biologicheskih molekul*, Minsk, Vysheishaya Shkola, 1978.

Downloaded by [Tomsk State University of Control Systems and Radio] at 12:54 19 February 2013

141. V. A. Kizel', *Usp. Fiz. Nauk*, **131**, 209 (1980).
142. H. Athenstaedt, H. Claussen, and D. Schaper, *Ferroelectrics*, **39**, 1243 (1981).
143. L. A. Beresnev, L. M. Blinov and E. I. Kovshev, *Dokl. Akad. Nauk SSSR*, **265**, 210 (1982).
144. M. Hentschel and R. Hosemann, *Mol. Cryst. Liq. Cryst.*, **94**, 291 (1983).
145. J. W. Doane, R. S. Parker, B. Cvikl, J. L. Johbson and D. L. Fishel, *Phys. Rev. Lett.*, **28**, 1894 (1972).
146. J. Seliger, V. Zagar and R. Blinc, *Phys. Rev. A*, **17**, 1149 (1978).
147. M. A. Osipov and S. A. Pikin, *Sov. Phys. JETP*, **53**, 1245 (1981).
148. W. J. A. Goosens, *Mol. Cryst. Liq. Cryst.*, **12**, 237 (1971).
149. H. Kimura, M. Hosino and H. Nakano, *J. Physique*, **40**, C3-174 (1979).
150. B. W. Van der Meer, G. Vertogen, A. J. Dekker and J. G. Ypma, *J. Chem. Phys.*, **65**, 3935 (1976).
151. B. W. Van der Meer and G. Vertogen, in: "The Molecular Physics of Liquid Crystals," ed. by G. R. Luckhurst and G. W. Gray, Academic Press, 1979.
152. A. I. Derzhanski and A. G. Petrov, *Mol. Cryst. Liq. Cryst.*, **89**, 339 (1982).
153. B. W. Van der Meer and G. Vertogen, *Z. Naturforsch.* **34a**, 1359 (1979).
154. M. A. Cotter, *Mol. Cryst. Liq. Cryst.*, **97**, 29 (1983).
155. W. M. Gelbart, *J. Phys. Chem.*, **86**, 4288 (1982).
156. J. P. Straley, *Phys. Rev. A*, **14**, 1835 (1976).
157. J. Mahanty and B. W. Ninham, "Dispersion forces"—London, New York, San-Francisco, Acad. Press, 1976.
158. A. Z. Rabinovich, A. S. Sonin, T. N. Anisimova, M. V. Loseva and N. I. Chernova, *Pis'ma v Zh. Tehn. Fiz.*, **6**, 44 (1980).
159. B. I. Ostrovskii and V. G. Chigrinov, *Kristallografiya*, **25**, 560 (1980).
160. T. Uemoto, K. Yoshino and Y. Inuishi, *Jap. J. Appl. Phys.*, **19**, 1467 (1980).
161. R. B. Meyer, *Phys. Rev. Lett.*, **22**, 918 (1969).
162. G. W. Gray and D. G. McDonnel, *Mol. Cryst. Liq. Cryst.*, **37**, 189 (1976).
163. H. Takezoe, K. Kondo, A. Fukuda and E. Kuze, *Jap. J. Appl. Phys.*, **21**, L-627 (1982).
164. K. Kondo, H. Takezoe, A. Fukuda and E. Kuze, *Jap. J. Appl. Phys.*, **21**, 224 (1982).
165. S. A. Rozanski, *Phys. Stat. Sol.(a)*, **79**, 309 (1983).
166. I. Musevic, B. Žekš, R. Blinc, L. Jansen, A. Seppen and P. Wyder. *Ferroelectrics*, **58**, 71 (1984).
167. M. Yamashita and H. Kimura, *J. Phys. Soc. Jpn.*, **52**, 33 (1983).
168. T. R. Taylor, J. L. Fergason and S. L. Aurora, *Phys. Rev. Lett.*, **25**, 722 (1970).
169. I. S. Zheludev, "Simmetriya i eyo prilozheniya," Moscow, Atom'izdat, 1976.
170. V. A. Belyakov and A. S. Sonin, "Optika holestericheskih zhidkih kristallov," Moscow, Nauka, 1982.
171. D. Berreman, *Mol. Cryst. Liq. Cryst.*, **38**, 633 (1977).
172. Yu. I. Sirotin and M. P. Shaskol'skaya, "Osnovy kristallofiziki," Moscow, Nauka, 1982.
173. T. E. Lockhart, E. Gelerinter and M. E. Neubert, *Phys. Rev. A*, **25**, 2262 (1985).
174. M. A. Osipov, *Fiz. Tverdogo Tela*, **27**, 1651 (1985).
175. M. Born and E. Wolf, Principles of Optics. Pergamon Press, Oxford, 1968.
176. S. M. Osadchii, D. G. Hoshtariya, A. G. Chanishvili and G. S. Chilaya, *5th All-,Union Liq. Cryst. Conf.*, Ivanovo, 1985, Abstracts, v. 1, part 1, A-40.
177. H. Takezoe, K. Furuhata, T. Nakagiri, A. Fukuda and E. Kuze, *Jap. J. Appl. Phys.*, **17**, 1219 (1978).
178. D. F. Aliev, M. A. Aslanov and A. H. Zeinally, Izv.VUZ'ov, Ser. Fizika, N°8, 114 (1982).
179. G. S. Chilaya, S. N. Aronishidze and M. N. Kushnirenko, *4th Liq. Cryst. Conf. Soc. Count.*, Tbilisi (USSR), 1981, Pros., **1**, 382.
180. K. Hori, *Mol. Cryst. Liq. Cryst.* (Lett.), **82**, 13 (1982).
181. S. M. Osadchii, *Kristallografiya*, **28**, 758 (1983).

Downloaded by [Tomsk State University of Control Systems and Radio] at 12:54 19 February 2013

182. S. Kai, Y. Narushige, K. Nishida and M. Imasaki, *Jap. J. Appl. Phys.*, (22, L-236 (1983).
183. K. Yoshino, K. G. Balakrishnan, T. Uemoto, Y. Iwasaki and Y. Inuishi, *Jap. J. Appl. Phys.*, **17**, 597 (1978).
184. J. S. Patel, T. M. Leslie and J. W. Godby, *Ferroelectrics*, **59**, 137 (1984).
185. B. I. Ostrovskii, A. Z. Rabinovich, A. S. Sonin and B. A. Strukov, *Fiz. Tverdogo Tela*, **21**, 917 (1979).
186. N. A. Clark, M. A. Handschy and S. T. Lagerwall, *Mol. Cryst. Liq. Cryst.*, **94**, 213 (1983).
187. A. Jakly, L. Bata, A. Buka, N. Eber and I. Janossy, *J. Physique Lett.*, **46**, L759 (1985).
188. K. Kondo, F. Kobayashi, H. Takezoe, A. Fukuda and E. Kuze, *Jap. J. Appl. Phys.*, **19**, 2293 (1980).
189. D. S. Parmar, K. K. Raina and J. Shankar, *Mol. Cryst. Liq. Cryst.*, **103**, 77 (1983).
190. K. Ishikawa, K. Hashimoto, H. Takezoe, A. Fukuda and E. Kuze, *Jap. J. Appl. Phys.*, **23**, L211 (1984).
191. K. Kondo, H. Takezoe, A. Fukuda, E. Kuze, K. Flatischler and K. Skarp, *Jap. J. Appl. Phys.*, **22**, L294 (1983).
192. Y. Galerne, *Phys. Rev. A*, **24**, 2284 (1981).
193. Y. Galerne, S. Lagerwall and I. W. Smith, *Opt. Comm.*, **19**, 147 (1976).
194. G. Pelzl, P. Kolbe, U. Preukschas, S. Diele and D. Demus, *Mol. Cryst. Liq. Cryst.*, **53**, 167 (1979).
195. A. N. Vtúrin, V. R. Ermakov, B. I. Ostrovskii and V. F. Shabanov, *Kristallografiya*, **26**, 546 (1981).
196. M. I. Barnik, L. M. Blinov and N. M. Shtykov, *Sov. Zh. Eksp. Teor. Fiz.*, **86**, 1681 (1984).
197. M. I. Barnik, L. M. Blinov, N. M. Shtykov and L. A. Beresnev, *Mol. Cryst. Liq. Cryst.*, **124**, 379 (1985).
198. P. Schiller and G. Pelzl, *Cryst. Res. Technol.*, **18**, 923 (1983).
199. W. Kuszynski, *Ber. Bunsenges. Phys. Chem.*, **85**, 234 (1981).
200. S. Kai, M. Takata and K. Hirakawa, *Jap. J. Appl. Phys.*, **22**, 938 (1983).
201. K. Kondo, Y. Sato, H. Takezoe, A. Fukuda and E. Kuze, *Jap. J. Appl. Phys.*, **20**, L871 (1981).
202. S. A. Rozanski and W. Kuszynski, *Chem. Phys. Lett.*, **105**, 104 (1984).
203. V. E. Dmitrienko and V. A. Belyakov, *Sov. Zh. Eksp. Teor. Fiz.*, **78**, 1568 (1980).
204. K. Yoshino, Y. Iwasaki, T. Uemoto and Y. Inuishi, *Jap. J. Appl. Phys.*, **18**, Suppl. 18-1, 427 (1979).
205. B. I. Ostrovskii, A. Z. Rabinovich and V. G. Chigrinov, in: "Adv. in Liq. Cryst. Res. and Application," ed. L. Bata, Pergamon Press-Akad, Kiado, Budapest, 1980, p. 469.
206. H. Orihara and Y. Ishibashi, *Ferroelectrics*, **58**, 179 (1984).
207. S. Kai, J. Narushige and R. Fujimoto, *Ferroelectrics*, **58**, 255 (1984).
208. N. A. Clark and S. T. Lagerwall, in: "Recent Developments in Condensed Matter Physics," v. 4, ed. J. I. Devreese, L. F. Lemmens, V. E. Van Doren, and J. Van Royen, Plenum Publ. 1981, p. 309.
209. L. A. Beresnev, V. A. Baikalov and L. M. Blinov, *Zh. Tekhn. Fiz.*, **52**, 2109 (1982).
210. J. P. Le Pesant, J. N. Perbet, B. Mourey, M. Hareng, G. Decobert and J. C. Dubois, *10th Inst. Liq. Cryst. Conf.*, York, 1984, Abstracts, G6.
211. M. A. Handschy and N. A. Clark, *Appl. Phys. Lett.*, **41**, 39 (1982).
212. H. Orihara and Y. Ushibashi, *Jap. J. Appl. Phys.*, **23**, 1274 (1984).
213. K. Yoshino, T. Urabe and Y. Inuishi, *Techn. Repts. of Osaka Univ.*, **33**, 289 (1983).
214. W. Kuszynski and J. Hoffmann, *Ferroelectrics*, **59**, 117 (1984).

Downloaded by [Tomsk State University of Control Systems and Radio] at 12:54 19 February 2013

215. J. W. Goodby, J. S. Patel and T. M. Leslie, *Ferroelectrics*, **59**, 121 (1984).
216. M. A. Handschy, N. A. Clark and S. T. Lagerwall, *Phys. Rev. Lett.*, **51**, 471 (1983).
217. D. F. Aliev, M. A. Aslanov, M. V. Loseva and N. I. Chernova, *Fiz. Tverdogo Tela*, **24**, 3179 (1982).
218. D. F. Aliev, A. H. Zeinally and N. I. Chernova, *Kristallografiya*, **26**, 863 (1981).
219. N. A. Clark, *Appl. Phys. Lett.*, **35**, 688 (1979).
220. S. T. Lagerwall, *6th Liq. Cryst. Conf. Soc. Count.*, Halle (GDR), 1985.
221. N. A. Clark, S. T. Lagerwall and J. Wahl, 4th display research conference, Paris, 1984, Proc., p. 73.
222. A. N. Nesrullaev, A. Z. Rabinovich and A. S. Sonin, *Zh. Tekhn. Fiz.*, **50**, 2468 (1980).
223. A. N. Nesrullaev, A. Z. Rabinovich, A. S. Sonin and E. B. Shelepin, *Kvant. elektronika*, **7**, 2578 (1981).
224. S. M. Arakelyan and Yu. S. Chilingaryan, "Nelineinaya optika zhidkih kristallov," Moscow, Nauka, 1984.
225. K. Eidman, D. M. Walba, D. S. Parar and N. A. Clark, *11th Int. Liq. Cryst. Conf.*, Berkeley (USA), 1986, Abstracts, 0-040-FE.
226. L. M. Blinov, L. A. Beresnev, E. P. Pozhidayev, V. A. Baikalov and M. I. Barnik, *Liquid Crystals*, **2**, 121 (1987).

Downloaded by [Tomsk State University of Control Systems and Radio] at 12:54 19 February 2013